**Paper 08GM0203**

**IEEE POWER ENGINEERING SOCIETY**
**ENERGY DEVELOPMENT AND POWER GENERATION COMMITTEE**

# International Practices for Methods and Techniques for Energy Loss Minimization Worldwide

**T. J. Hammons, L. L Lai, K P Wong**

***Working Group on International Practices in Distributed Generation***[1]

**2008 IEEE PES General Meeting, July 20-24 2008, Pittsburgh, PA, USA**
**Thursday, July 24 2008, 9:00 a.m~1:00 p.m (Any Unforeseen Change to be Notified in Preliminary/Final Program and by Letter)**

**Sponsored by: International Practices for Energy Development and Power Generation**

Chairs: T. J. Hammons, University of Glasgow, Scotland, UK
L. L Lai, City University London, UK
K P Wong, Hong Kong Polytechnic University, Hong Kong

**Track: New Technologies**

## INTRODUCTION

Energy is being transmitted over greater distances. The further energy is transferred, the harder it is to maintain constant voltage on the transmission system and the higher the losses. Delivering energy over greater distances requires greater reactive support and could lead to voltage instability. It is necessary to look into ways of assessing the extent of the energy losses and discuss developing technologies that can reduce the loss and improve energy efficiency.

The objectives of this panel are to share experience and knowledge in:

- Developing technologies to reduce energy losses in power generation, transmission and distribution and electric power conversion systems
- Reducing energy consumption in the residential and commercial sectors
- Employing information technology systems to increase the efficiency of energy used in processes and buildings; and
- New techniques and algorithms for loss assessment and control.

Through case studies, worked examples and open discussions, delegates will have the opportunity examine energy loss reduction in all areas of energy use (utility, industrial, commercial, and residential).

Areas of opportunity include:

- Automatic generation control
- Load management
- Flexibility AC Transmission Systems in reducing Energy Loss

[1] Document prepared and edited by T J Hammons

- Co-generation Operation and Scheduling
- End-user distribution systems
- Energy pricing
- Others.

The Panelists and Titles of their Presentations are:

1, Yoci Rosales. Hernandez and Takashi Hiyama, Department. of Electrical & Computer Engineering. Kumamoto University, Kumamoto, Japan. Distance Measure based Rules for Voltage Regulation with Loss Reduction (Invited Panel Presentation Summary 08GM01659)
2. Loi Lei Lai, City University London, UK. A Review on Energy Loss Development (Invited Panel Presentation Summary 08GM1419)
3. Takayuki Tanabe, and Toshihisa Funabashi (Meidensha Corporation, Japan), Koichi Nara (Fukushima National College of Technology, Japan), Yuji Mishima (Hakodate National College of Technology, Japan) and Ryuichi Yokoyama (Waseda University, Japan). A Loss Minimum Re-configuration Algorithm of Distribution Systems under Three-phase Unbalanced Condition (Invited Panel Presentation Summary 08GM0363).
4. Junichi Arai and Seiji Fujino (Kogakuin University, Japan), Hideaki Tanaka, (The Federation of Electric Power Companies, Japan), and Ryuichi Yokoyama (Waseda University, Tokyo, Japan). Coordinated Control for Isolated Distribution Networks Supplied by Inverter Power Sources (Invited Panel Presentation Summary 08GM0360)
5. Yosuke Nakanishi (Fuji Electric Systems Company Ltd.), Hiromitsu Ota (Fuji Electric Systems Co., Ltd.), Ryuichi Yokoyama (Waseda University), Kiyoshi Yoshida (The Kansai Electric Power Co., Inc.) and Katsuhiko Kouchi (The Kansai Electric Power Co., Inc.), Japan.. Centralized Control of Clustered PV Generations for Loss Minimization and Power Quality (Invited Panel Presentation Summary 08GM0744).
6. Xiao-Ping Zhang, Professor and Director, Institute for Energy Research and Policy, The University of Birmingham, UK. Energy Loss Minimization of Electricity Networks with Renewable Generation using FACTS (Invited Panel Presentation Summary 08GM0037)
7. Jizhong Zhu, Davis Hwang, and Ali Sadjadpour, AREVA T&D Inc., Redmond, WA, USA. Loss Reduction From use of New SVC Model (Invited Panel Presentation Summary 08GM0402)
8. Invited Discussers

Each Panelist will speak for approximately 30 minutes. Each presentation will be discussed immediately following the respective presentation. There will be a further opportunity for discussion of the presentations following the final presentation.

The Panel Session has been organized by Loi Lei Lai (Professor, City University London, UK), Kit Po Wong (Professor, Hong Kong Polytechnic University, Hong Kong) and Tom Hammons (Chair of International Practices for Energy Development and Power Generation IEEE, University of Glasgow, UK).

Loi Lei. Lai, Kit Po Wong and Tom Hammons will moderate the Panel Session.

**PANELISTS**

1. Yoci Rosales. Hernandez
Professor Takashi Hiyama
Dept. of Electrical & Computer Eng.
Kumamoto University
2-39-1 Kurokami
Kumamoto 860-8555,
Japan
E-mail: hiyama@cs.kumamoto-u.ac.jp

E-mail: yoelcuba@st.eecs.kumamoto-u.ac.jp
Tel: +81-96-342 3614
Fax: +81-96-342 3630

2. Loi Lei Lai
Energy Systems Group
School of Engineering and Mathematical Sciences
City University
London, EC1V 0HB
UK
E-mail: l.l.lai@city.ac.uk
Tel: +44 20 7040 3889
Fax: +44 20 7040 8568

3. Takayuki Tanabe
Meidensha Corporation
Think Park Tower
2-1-1 Ohsaki
Shinagawa-ku,
Tokyo 141-6029
Japan
E-mail: tanabe-t@mb.meidensha.co.jp
Tel: +81-3-6420-7214
Fax: +81-3-5745-3042

Dr. Toshihisa Funabashi
Meidensha Corporation
Think Park Tower
2-1-1 Ohsaki,
Shinagawa-ku
Tokyo 141-6029
Japan
E-mail: funabashi-t@mb.meidensha.co.jp
Tel: +81-3-6420-7208

4. Junichi Arai
Professor
Department of Electrical Engineering
KOGAKUIN UNIVERSITY
1-24-2, Nishi-Shinjuku, Shinjuku-ku,
Tokyo 163-8677
Japan
E-mail: arai@cc.kogakuin.ac.jp
Tel:+81-3-3340-2996
Fax:+81-3-3348-3486

Seiji Fujino
Department of Electrical Engineering
Kogakuin University
Japan
E-mail: cm06033@ns.kogakuin.ac.jp

Hideaki Tanaka
The Federation of Electric Power Companies
Japan
E-mail: tanakahd@fepc.or.jp

Ryuichi Yokoyama
Graduate School of Environment and Energy Engineering,
Waseda University
Japan
E-mail: yokoyama-ryuichi@waseda.jp

5. Yosuke Nakanishi

Yosuke Nakanishi
General Manager
Power System Analysis Gr.
R&D Management Office
Technology Development Group
Fuji Electric Systems Co., Ltd.
1, Fuji-machi
Hino-city
Tokyo 191-8502
Japan
E-mail nakanishi-yosuke@fesys.co.jp
Tel: +81-42-586-8875
Fax: +81-42-585-6035

Hiromitsu Ota
Assistant Manager
Fuji Electric Systems Co., Ltd.
1, Fuji-machi
Hino-city
Tokyo 191-8502
Japan
E-mail: oota-hiromitsu@fesys.co.jp
Tel: +81-42-586-8875
Fax: +81-42-585-6035

Ryuichi Yokoyama
Professor
Graduate School of Environment and Energy Engineering
Waseda University
1-1-7, Nishi-Waseda Shinjyuku-ku
Tokyo 169-0051
Japan
E-mail: yokoyama-ryuichi@waseda.jp
Tel: +81-3-5935-6684
Fax: +81-3-5935-6684

Kiyoshi Yoshida
General Manager
The Kansai Electric Power Co., Inc.
6-16, 3-Chome,
Nakanoshima
Kita-ku
Osaka, 530-8270
Japan
E-mail: yoshida.kiyoshi@e2.kepco.co.jp
Tel: +81-6-6441-8821
Fax: +81-6-6446-3203

Katsuhiko Kouchi
Project Manager
The Kansai Electric Power Co., Inc.
11-20 Nakoji, 3-Chome
Amagasaki
Hyogo, 661-0974
Japan
E-mail: kouchi.katsuhiko@b5.kepco.co.jp
Tel: +81-6-6494-9701

Fax: +81-6-6494-9703

6. Professor Xiao-Ping Zhang
Director, Institute for Energy Research and Policy
The University of Birmingham
School of Engineering
Electronic, Electrical and Computer Engineering
Edgbaston
Birmingham
B15 2TT
UK
E-mail: X.P.Zhang@bham.ac.uk
Tel: ( 44) (0) 121 414 4166
Fax: ( 44) (0) 121 414 4291

7. Dr Jizhong Zhu
AREVA T&D Inc.
10865 Willows Road NE
Redmond, WA 98052
USA
Tel: (425) 250-2622
Fax: (425)250-1400
E-mail: jizhong.zhu@areva-td.com
Tel.: +1 425 250 2622
Fax: +1 425 250 1400

Dr Davis Hwang
AREVA T&D Inc.
10865 Willows Road. NE
E-mail: davis.hwang@areva-td.com
Tel.: +1 425 250 2614
Fax: +1 425 250 1400

Ali Sadjadpour
Network Manager
AREVA T&D Inc.
10865 Willows Road. NE
Redmond, WA 98052, USA
E-mail: ali.sadjadpour@areva-td.com
Tel.: +1 425 250 2615
Fax: +1 425 250 1400

## PANEL SESSION CHAIRS

Thomas James Hammons
Chair International Practices for Energy Development and Power Generation
Glasgow University
11C Winton Drive
Glasgow G12 0PZ
UK
E-mail: T.Hammons@ieee.org
Tel: +44 141 339 7770

Loi Lei Lai
Energy Systems Group
School of Engineering and Mathematical Sciences
City University
London, EC1V 0HB
UK
E-mail: l.l.lai@city.ac.uk
Tel: +44 20 7040 3889
Fax: +44 20 7040 8568

Kit Po Wong
Chair Professor of Electrical Engineering
Department of Electrical Engineering
The Hong Kong Polytechnic University
Hung Hom
Kowloon
Hong Kong
E-mail: eekpwong@polyu.edu.hk
Tel: +852 2766-6168
Fax: +852 2330-1544

## BIOGRAPHIES

**Thomas James Hammons** (F'96) received the degree of ACGI from City and Guilds College, London, U.K. and the B.Sc. degree in Engineering (1st Class Honors), and the DIC, and Ph.D. degrees from Imperial College, London University.

He is a member of the teaching faculty of the Faculty of Engineering, University of Glasgow, Scotland, U.K. Prior to this he was employed as an Engineer in the Systems Engineering Department of Associated Electrical Industries, Manchester, UK. He was Professor of Electrical and Computer Engineering at McMaster University,Hamilton, Ontario, Canada in 1978-1979. He was a Visiting Professor at the Silesian Polytechnic University, Poland in 1978, a Visiting Professor at the Czechoslovakian Academy of Sciences, Prague in 1982, 1985 and 1988, and a Visiting Professor at the Polytechnic University of Grenoble, France in 1984. He is the author/co-author of over 350 scientific articles and papers on electrical power engineering. He has lectured extensively in North America, Africa, Asia, and both in Eastern and Western Europe.

Dr Hammons is Chair of International Practices for Energy Development and Power Generation of IEEE, and Past Chair of United Kingdom and Republic of Ireland (UKRI) Section IEEE. He received the IEEE Power Engineering Society 2003 Outstanding Large Chapter Award as Chair of the United Kingdom and Republic of Ireland Section Power Engineering Chapter (1994~2003) in 2004; and the IEEE Power Engineering Society Energy Development and Power Generation Award in Recognition of Distinguished Service to the Committee in 1996. He also received two higher honorary Doctorates in Engineering. He is a Founder Member of the International Universities Power Engineering Conference (UPEC) (Convener 1967). He is currently Permanent Secretary of UPEC. He is a registered European Engineer in the Federation of National Engineering Associations in Europe.

**Loi Lei Lai** (SM'92, F'2007) received the B.Sc. (First Class Honors) and the Ph.D. degrees from the University of Aston in Birmingham, UK. He also gained his D.Sc. from City University London. Currently he is Professor and Head of Energy Systems Group at City University, London, UK. He is a Visiting Professor at Southeast University, Nanjing, China and also a Guest Professor at Fudan University, Shanghai, China. He has authored/co-authored over 200 technical papers. In 1998, he also wrote a book entitled Intelligent System Applications in Power Engineering Evolutionary Programming and Neural Networks. Recently, he edited a book entitled Power System Restructuring and Deregulation Trading, Performance and Information Technology. In 1995, he received a high-quality paper prize from the International Association of Desalination, USA. Among his professional activities are his contributions to the organization of several international conferences in power engineering and evolutionary computing, and he was the Conference Chairman of the IEEE/IEE International Conference on Power Utility Deregulation,

Restructuring and Power Technologies 2000. Dr. Lai is a Corporate Member of the IEE. He was awarded the IEEE Third Millennium Medal, 2000 IEEE Power Engineering Society UKRI Chapter Outstanding Engineer Award, and 2003 IEEE Power Engineering Society Outstanding Large Chapter Award.

**Kit Po Wong** (M'87-SM'90-F'02) obtained M.Sc and Ph.D. degrees from the University of Manchester, Institute of Science and Technology, UK in 1972 and 1974, respectively. Prof. Wong was awarded a higher doctorate DEng degree by UMIST in 2001. Prof. Wong is currently Chair Professor of Department of Electrical Engineering, Hong Kong Polytechnic University. He was Guest Professor of Tsinghua University, Beijing China, and is Guest Professor of Southeast University, Nanjing China. Prof. Wong was Professor of University of Western Australia. During that period, he received three Sir John Madsen Medals (1981, 1982 and 1988) from the Institute of Engineers Australia, the 1999 Outstanding Engineer Award from the IEEE Power Chapter Western Australia and the 2000 IEEE Third Millennium Award. Prof. Wong has published numerous research papers in power systems and on the applications of artificial intelligence and evolutionary computation to power system planning and operations. His current research interests include evolutionary optimization in power, power market analysis, power system planning and operation in the deregulated environment, and power quality. Prof. Wong has served as Editor-in-Chief for IEE Proceedings Generation, Transmission and Distribution. He was the conference chairman of IEEE/CSEE PowerCon2000. He is a Fellow of IEEE, IET, HKIE and IEAust.

Received February 19 2008
Paper 08GM1659

# 1. Distance Measure Based Rules for Voltage Regulation with Loss Reduction

Yoci Rosales. Hernandez, Department. of Electrical & Computer Engineering., Kumamoto University, Kumamoto, Japan
Takashi Hiyama, Department. of Electrical & Computer Engineering., Kumamoto University, Kumamoto, Japan

***Abstract*--** This paper presents a rule-based method to control the voltage in a power transmission network. Shunt capacitors and transformers with a tap changer installed in the system are selected by the proposed method as control devices. For each bus under voltage violation, the most effective control device is selected by using the minimum electric distance criteria. In order to demonstrate the efficiency of the method, several simulations are performed using an IEEE 30-bus network as a model system. The distance measure method is compared with another classic voltage regulation method and the results obtained indicate the advantages of the proposed method.
***Index Terms*—**Knowledge based systems, Losses, Voltage Control.

## 1. INTRODUCTION

The new concepts regarding the operation of a modern distribution network demand a high performance of operation parameters of the system and consequently require more effective control strategies. Voltage deviation control is one of the strategies extensively investigated and still is an important problem to solve in any distribution power system. Voltage control algorithms may be classified into two kinds of algorithms: rule-based and network model-based. The rule-based algorithms use rules that control switched capacitors and transformer tap changers based on real-time measurements and past experiences. The network model-based systems use distribution network topology, impedance, real-time measurements and statistical information to establish the current states of the system. It then applies optimization techniques to get the best possible solution.

Within the network models-based systems there are many different approaches. In reference [1] a simulated annealing technique for global optimal solution is presented. The authors propose a knowledge-based expert system, which detects buses with maximum voltage deviations and operates the nearest and available transformer control unit to correct the problem. Then, a simulated annealing algorithm is utilized to reach optimum capacitors manipulation as a final solution.

The paper presents a very good result related to power loss reductions but does not guarantee an economic use of manipulations on transformers operations. Restriction of number of switching operation gets more importance in [2]. Here, dynamic programming and fuzzy logic algorithms are combined to control voltages and reduce power losses. The problem is decomposed into two sub-problems: sub-problem 1 at substation level to control load tap changers (LTC); and capacitor banks and sub-problem 2 on feeder level to control the capacitor banks installed there. Dynamic programming is used in sub-problem 1 and fuzzy logic is adopted for the second sub-problem. Simulation results show an excellent performance of the proposed approach. Genetic algorithm is another technique used to control voltage and reactive power in the system. The approach in [3] combines the benefits of a linearized system model and a genetic algorithm (GA).

Whenever a voltage correction is demanded an initial calculation of a sensitivity matrix is done in order to identify an initial population for the GA. Then the GA finds a proper set of

control actions to execute. The method offers good solutions for the voltage/reactive power problem and also reduces the number of actions over the control devices. In reference [4] a method based on artificial neural network is used to find the suitable capacitor-switching regime for every load state.

The main objective is to reduce power losses and the only constraint considered is bus voltage. The advantage of this method is on the small calculation time. But, on a real application it could be difficult because the system requires new training sessions every time any small change on the network topology is done. The method presented in this paper is a rule based system, and is a new approach for a centralized control of voltage as a support tool for decision-making. When the system lacks automatic function control the task has to be performed manually by the supervisor in the dispatch center. Due to the complexity of a modern power system and the severe consequences to the economy of power failures, reliable algorithms have to be part of the daily support tools in a dispatch center.

This research was motivated by the necessity to design a simple and effective support algorithm for the voltage control process. The algorithm is based on the identification of a bus under the worst voltage violations and the respective nearest bus where a voltage control device is installed. A control device setting is changed in order to improve the voltage situation of the bus under violation. A 30-bus network was used as a study case. Some classic control elements such as transformers with tap changers, shunt capacitor banks, synchronous condensers and generators were modeled. The important details regarding the study case system, the proposed method and a search algorithm are explained in section 2-4. Simulation results for the 30-bus system under different load stages are discussed in Section 5.

## 2. STUDY CASE SYSTEM

The modeled system is an IEEE 30-bus scheme. The system bus data is given in Table 1, and Fig. 1 shows the single line diagram. Shunt capacitor banks are located at bus 10 and 24. Bank capacitor found at node 10 contains up to 10 units with a reactive power capacity of 1.9 Mvar for each unit. In the case of bus 24, banks have been installed up to 3 units per 0.8 Mvar. The tap changer settings ranges are modeled from -0.1 to 0.1 with a step of 0.01 per unit. Four synchronous condensers are also considered at buses 5, 8, 11 and 13.

TABLE I

BUS DATA OF THE STUDY CASE SYSTEM

| Name | Type | V(p.u) | Pg(p.u) | Qg(p.u) | Pd(p.u) | Qd(p.u) |
|---|---|---|---|---|---|---|
| 1 | S | 0.97 | | | 0.0 | 0.0 |
| 2 | PV | 0.97 | 0.4 | | 0.217 | 0.127 |
| 3 | PQ | | 0.0 | 0.0 | 0.024 | 0.012 |
| 4 | PQ | | 0.0 | 0.0 | 0.076 | 0.016 |
| 5 | PV | 0.97 | 0.0 | | 0.942 | 0.19 |
| 6 | PQ | | 0.0 | 0.0 | 0.0 | 0.0 |
| 7 | PQ | | 0.0 | 0.0 | 0.228 | 0.109 |
| 8 | PV | 0.97 | 0.0 | | 0.3 | 0.0 |
| 9 | PQ | | 0.0 | 0.0 | 0.0 | 0.0 |
| 10 | PQ | | 0.0 | 0.0 | 0.058 | 0.02 |
| 11 | PV | 0.97 | 0.0 | | 0.0 | 0.0 |
| 12 | PQ | | 0.0 | 0.0 | 0.112 | 0.075 |
| 13 | PV | 0.97 | 0.0 | | 0.0 | 0.0 |
| 14 | PQ | | 0.0 | 0.0 | 0.062 | 0.016 |
| 15 | PQ | | 0.0 | 0.0 | 0.082 | 0.025 |
| 16 | PQ | | 0.0 | 0.0 | 0.035 | 0.018 |
| 17 | PQ | | 0.0 | 0.0 | 0.09 | 0.058 |
| 18 | PQ | | 0.0 | 0.0 | 0.032 | 0.009 |
| 19 | PQ | | 0.0 | 0.0 | 0.095 | 0.034 |
| 20 | PQ | | 0.0 | 0.0 | 0.022 | 0.007 |
| 21 | PQ | | 0.0 | 0.0 | 0.175 | 0.112 |
| 22 | PQ | | 0.0 | 0.0 | 0.0 | 0.0 |
| 23 | PQ | | 0.0 | 0.0 | 0.032 | 0.016 |
| 24 | PQ | | 0.0 | 0.0 | 0.087 | 0.067 |
| 25 | PQ | | 0.0 | 0.0 | 0.0 | 0.0 |
| 26 | PQ | | 0.0 | 0.0 | 0.035 | 0.023 |
| 27 | PQ | | 0.0 | 0.0 | 0.0 | 0.0 |
| 28 | PQ | | 0.0 | 0.0 | 0.0 | 0.0 |
| 29 | PQ | | 0.0 | 0.0 | 0.024 | 0.009 |
| 30 | PQ | | 0.0 | 0.0 | 0.106 | 0.019 |

## 3. PROPOSED METHOD

Usually the system is exposed to overload and under-load conditions within a 24 hours interval. The voltage limits are violated in several buses, as a natural response of the network. A safe voltage operation range is considered from 0.95 to 1.05 per unit. A rule-based method is proposed in order to bring the system to a normal point of operation. The details of the rules are presented in Table 2. The ranking list order is based on the electrical distance criteria between every voltage control device and the target bus. Once the nearest voltage control device is selected, the device setting modifications have to be executed using a minimum variation steps in order to avoid unnecessary control actions.

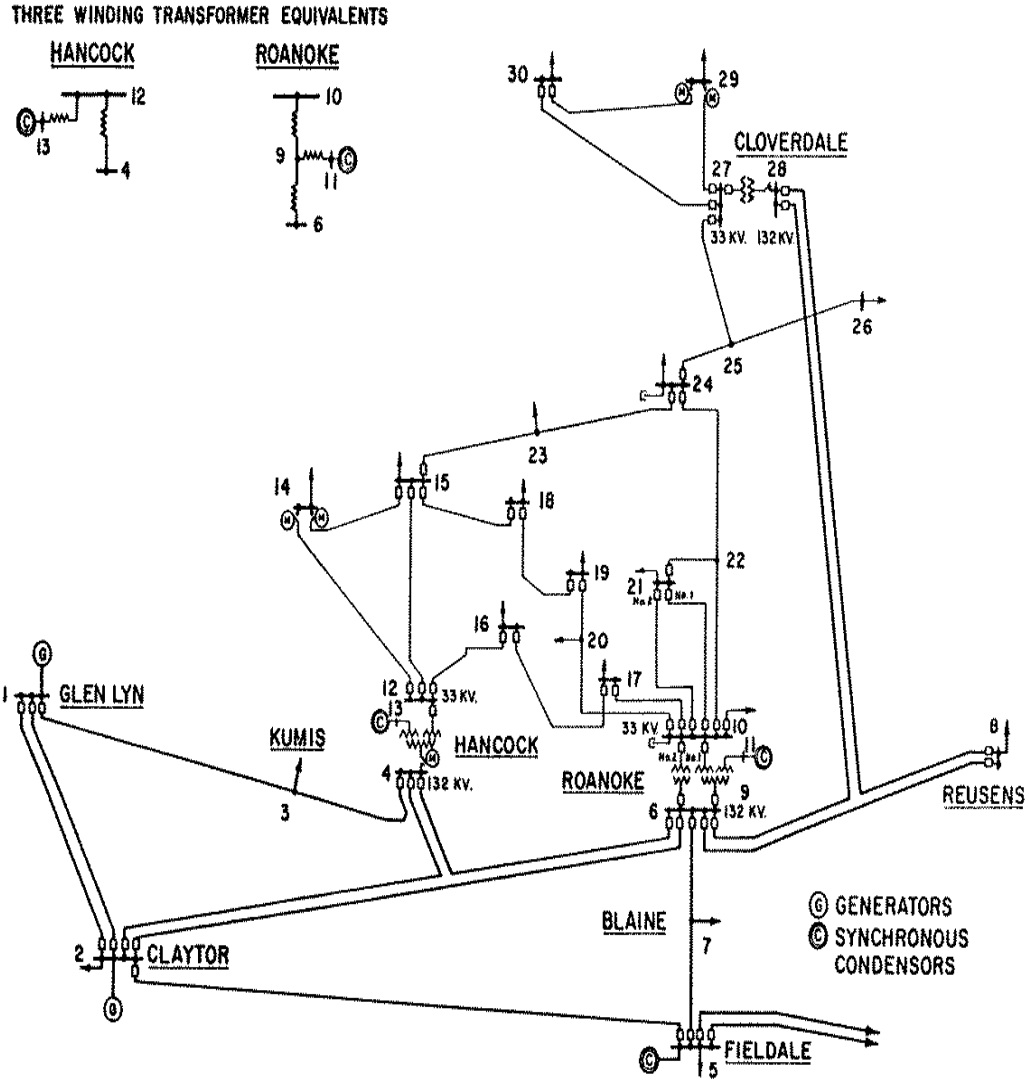


Fig. 1. IEEE 30 bus scheme.

TABLE II
BUS DATA OF THE STUDY CASE SYSTEM

**Step1:** Perform the power flow calculation. If there is any violation of voltage then move to step 2. If not then move to step 4.

**Step2:** Identification of the bus under the worst voltage condition as target bus. Creation of a ranking list of voltage control devices.

**Step3:** Identification of the device located at the first position of the ranking as optimal control device. If is not available, due to settings reaching upper/lower limits, then the device in the next ranking position is selected as the optimal control device. If is available, then perform setting modifications at the optimal control device. Return to step 1. If there is not any more control action possible and the target bus remains as same bus, then move to step 4.

**Step4:** The calculation is stopped.

## 4. DISTANCE MEASURE ALGORITHM

The shortest route from the bus under worst voltage condition to a corresponding control device location is calculated by using Dijkstra's algorithm [5]. Basic operation of this algorithm is edge

relaxation. In this case, the edges are the electrical distance Lij of the transmission line between buses i and j. The electrical distance is defined in (1)

.

$$L_{ij} = \sqrt{R_{ij}^2 + X_{ij}^2} \qquad (1)$$

Once the minimum paths are found, a ranking of distance measure is established in order to develop a decision strategy to solve the problem of voltage violation.

## 5. SIMULATION RESULTS

Several simulations were been made under different load conditions in order to compare the performances of the voltage local control and the proposed method. The execution of unnecessary control actions is an important point to consider in the new proposal. Therefore, only strictly necessaries operation actions for each device are allowed. A control effort index CEI is defined to count the number of control actions involved in every simulation. The CEI mathematical definition is presented below.

$$CEI = \sum_{i=1}^{n} \left| setting_i^{s} - setting_i^{(s-1)} \right| \qquad (2)$$

Where *s* describes the control action stage and *n* is the number of control devices. This section is structured into two parts. First, an analysis and comparison of the system's responses under the action of three control strategies: A local control at the transformer units, a random selection of control devices and finally the distance measure rule-based method. Second part illustrates the performance of the new proposed method under a load variation within an interval of 24 hours.

### *5.1 Voltage local control, a random selection of control devices and the new proposal voltage control: A comparison.*

Voltage local control is a classic method based on a local way of monitoring and operating each control device. It means that at every node, where a control device is installed, a local and independent control strategy is followed, and control actions are executed exclusively where problems of voltages appear. Fig. 2 illustrates an initial voltage profile of the network under a hypothetical load scenario that is considered as maximum load scenario. The voltage profile shows several nodes violating the minimum voltage limit. Buses that are under violation and where a control device is installed are marked with a circle. In this initial condition only transformer operations are available because all capacitor banks are already connected. Table 3 shows the positions of transformer taps at the initial conditions, the two sub-solutions and the final solution. The final solution is reached when the four buses pointed in Fig. 2 are out of violation zone. The final solution, as shown in Fig. 3, does not solve the problem of voltage at other nodes except at those where control devices are installed.

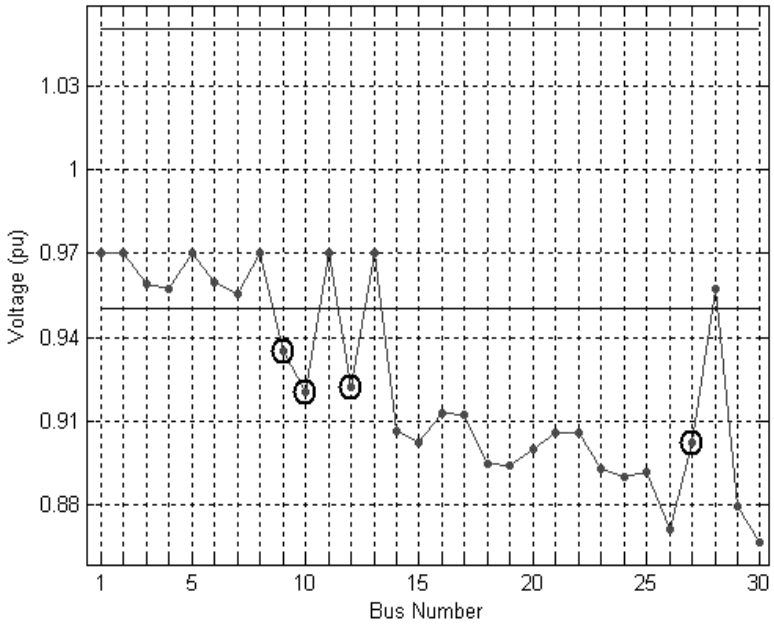


Fig. 2. Voltage profile of the network obtained for initial conditions.

TABLE III

OPERATION OF THE CONTROL DEVICES USING THE VOLTAGE LOCAL CONTROL METHOD

| | Bus Number | | Tap(p.u) | | | |
|---|---|---|---|---|---|---|
| Name | Sending | Receiving | Initial | 1 | 2 | Final |
| T1 | 6 | 9 | 0.97 | **1.00** | 1.00 | **1.04** |
| T2 | 6 | 10 | 0.96 | **0.99** | **1.01** | **1.02** |
| T3 | 11 | 9 | 1.00 | 1.00 | 1.00 | 1.00 |
| T4 | 9 | 10 | 1.00 | 1.00 | **0.91** | 0.91 |
| T5 | 4 | 12 | 0.93 | 0.93 | 0.93 | 0.93 |
| T6 | 13 | 12 | 1.00 | **1.03** | **1.05** | **1.06** |
| T7 | 28 | 27 | 0.96 | **1.00** | **1.02** | **1.04** |
| CEI | | | 0.00 | 0.13 | 0.15 | 0.08 |
| Total CEI | | | 0.36 | | | |

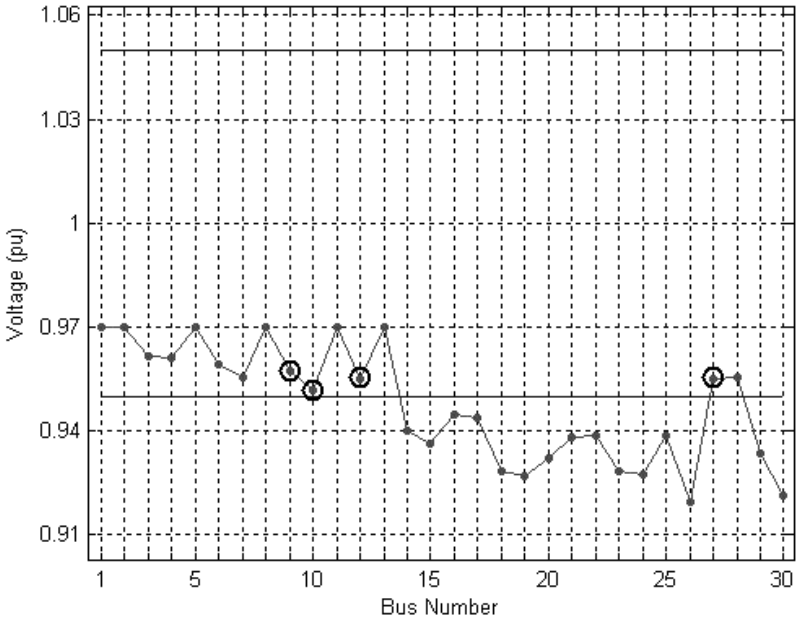


Fig. 3. Voltage profile of the network obtained after execution of voltage local control.

If an attempt to solve the voltage situation were made by without using any rules, by a random selection of control devices, a resulting voltage profile would be like the one in Fig. 4. All voltages are in the non-violating voltage zone, but as Table 4 illustrates, the amount of control actions is too large. As the CEI is larger the expectation life of control devices is smaller.

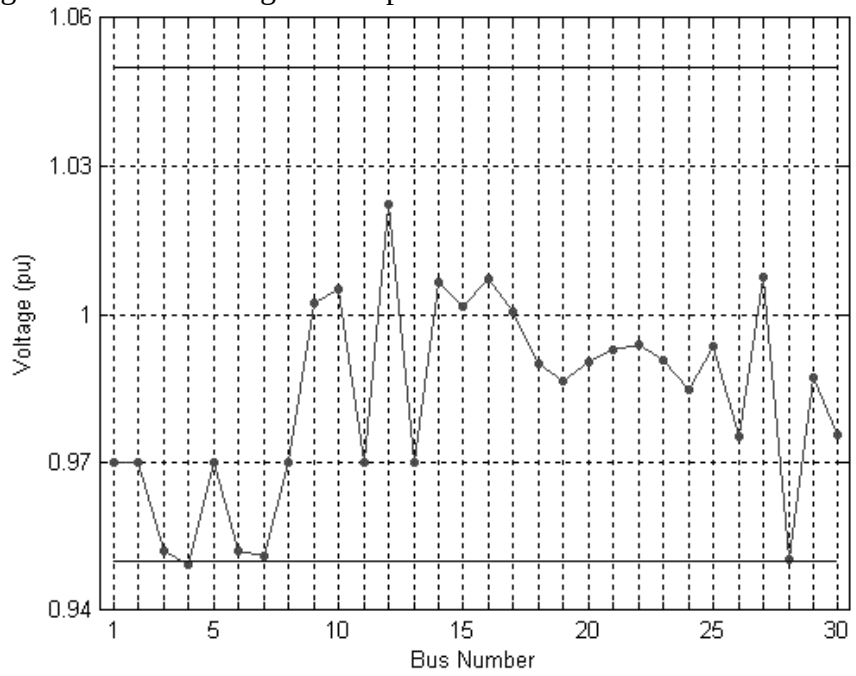


Fig. 4. Voltage profile of the network obtained after execution of random device selection.

TABLE IV
OPERATION OF THE CONTROL DEVICES USING A RANDOM SELECTION OF CONTROL DEVICES

| | Bus Number | | Tap(p.u) | | | |
|---|---|---|---|---|---|---|
| Name | Sending | Receiving | Initial | 1 | 2 | Final |
| T1 | 6 | 9 | 0.97 | **1.06** | 1.06 | **1.09** |
| T2 | 6 | 10 | 0.96 | 0.96 | **1.0** | **1.1** |
| T3 | 11 | 9 | 1.00 | 1.00 | 1.00 | 1.00 |
| T4 | 9 | 10 | 1.00 | **1.05** | 1.05 | **1.0** |
| T5 | 4 | 12 | 0.93 | 0.93 | 0.93 | **1.07** |
| T6 | 13 | 12 | 1.00 | 1.00 | **1.1** | 1.1 |
| T7 | 28 | 27 | 0.96 | **1.05** | 1.05 | **1.1** |
| CEI | | | 0.00 | 0.23 | 0.14 | 0.37 |
| Total CEI | | | 0.74 | | | |

In the case of the rule-based method proposed more buses could participate on the voltage control operation, even if voltages at those nodes are in non-violation voltage zone. Initial condition is the same as showed in Fig. 2. Worst voltage is located at node 30 and transformer T7 is the best control device to solve the problem. Tap position in transformer 7 was moved from 0.96 to 1.00 and the voltage problem in node 30 was solved. Then bus 19 appeared as the worst bus and the most effective device control was transformer 2. The process was repeated many times until final solution was reached. Table 5 shows initial conditions of tap positions, two sub-solutions and the final solution. In Fig. 5, 6 and 7 voltage profile for the two sub-solutions and the final result are presented respectively.

Is important to note that the difference between total CEI of the new method proposed and

classic method is small. Using the new method, just 5 additional control actions were necessary to put all bus voltages in the non-violating zone.

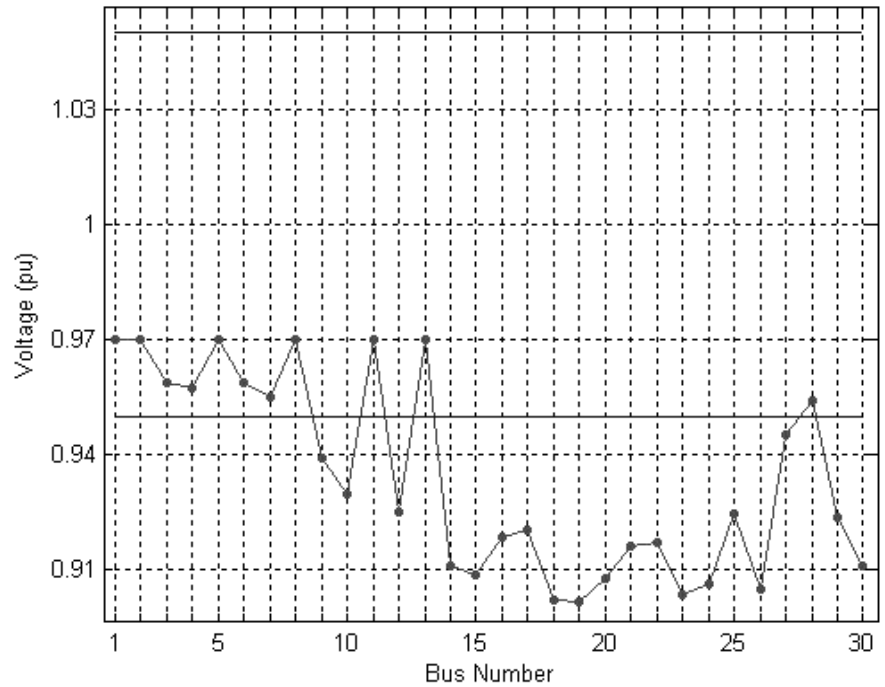


Fig. 5. Voltage profile of the network obtained from sub-solution 1.

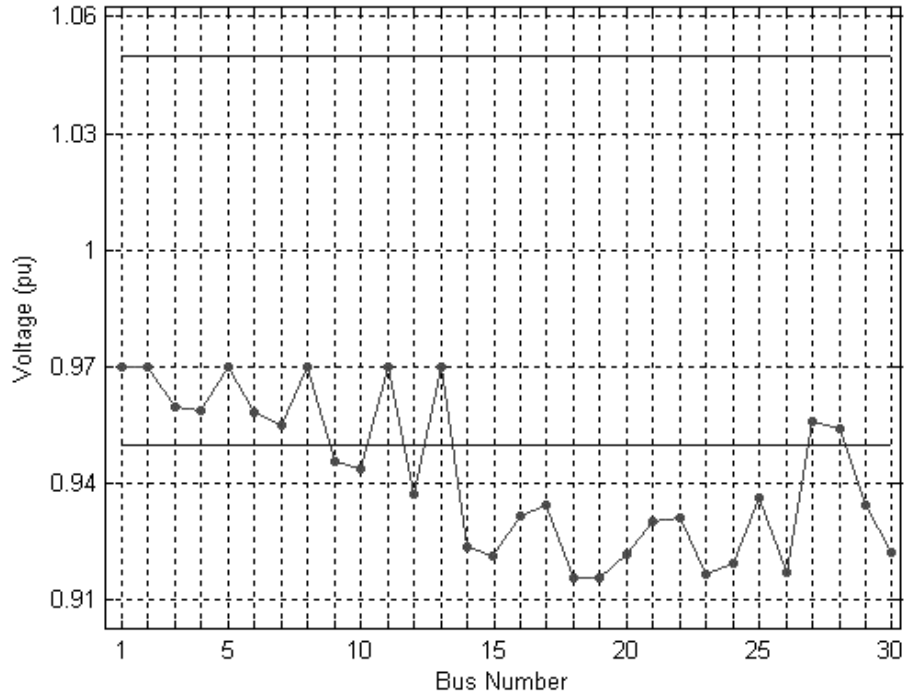


Fig. 6. Voltage profile of the network obtained from sub-solution 2.

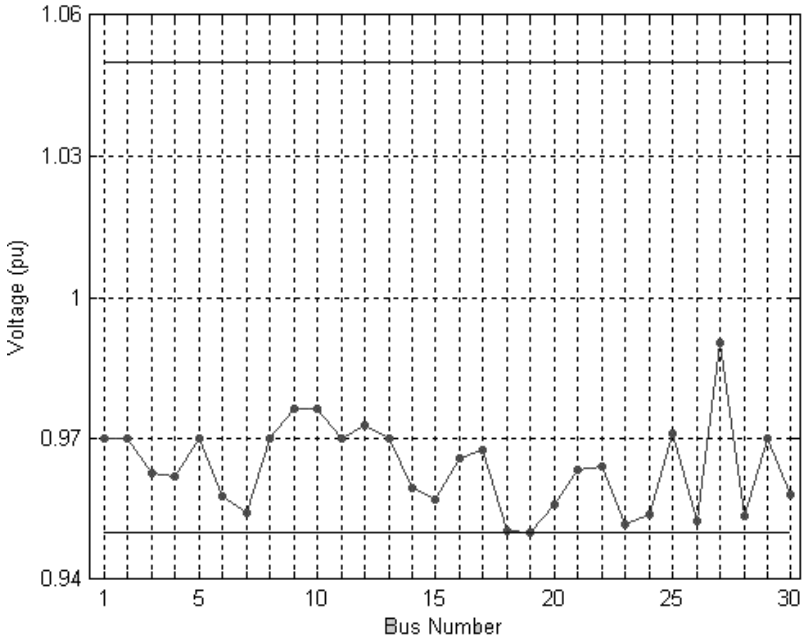


Fig. 7. Voltage profile of the network obtained from the final solution.

TABLE V
OPERATION OF THE CONTROL DEVICES USING THE DISTANCE MEASURE METHOD

| | Bus Number | | Tap(p.u) | | | |
|---|---|---|---|---|---|---|
| **Name** | **Sending** | **Receiving** | **Initial** | **1** | **2** | **Final** |
| T1 | 6 | 9 | 0.97 | 0.97 | 0.97 | **1.03** |
| T2 | 6 | 10 | 0.96 | **0.99** | **1.06** | **1.1** |
| T3 | 11 | 9 | 1.00 | 1.00 | 1.00 | 1.00 |
| T4 | 9 | 10 | 1.00 | 1.00 | 1.00 | 1.00 |
| T5 | 4 | 12 | 0.93 | 0.93 | 0.93 | 0.93 |
| T6 | 13 | 12 | 1.00 | 1.00 | **1.02** | **1.09** |
| T7 | 28 | 27 | 0.96 | **1.04** | **1.05** | **1.09** |
| CEI | | | 0.00 | 0.11 | 0.10 | 0.21 |
| Total CEI | | | 0.42 | | | |

Although, in this research power loss reduction was not the main objective, it was also monitored and studied. This new control method brings the system to a very flat voltage scenario that is a very important condition to achieve power loss reductions. Fig. 8 illustrates how the power losses are reducing gradually in each sub-solution obtained by the method proposed. The final solution gives a 0.67 % of power loss reduction.

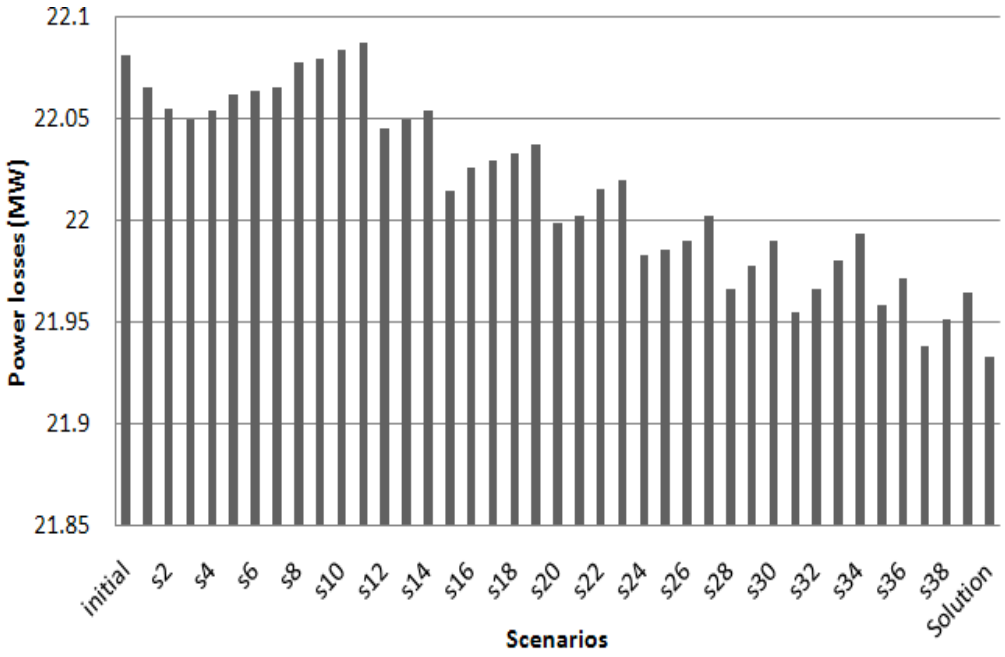


Fig. 8. Power losses in each control scenario.

### *5.2 Performance of the new method applied for a load variation within an interval of 24 hours.*

It is well known that power demand in a real system is changing continually during a day, and consequently state variables are varying as well. For this typical behavior, it is necessary to study and prove the effectiveness of the new control method proposed. Load variation was modeled as a coincident load variation in time. Fig. 9 shows the percentage of the rate load at every bus and the voltage at 6 buses after application of distance measure method.

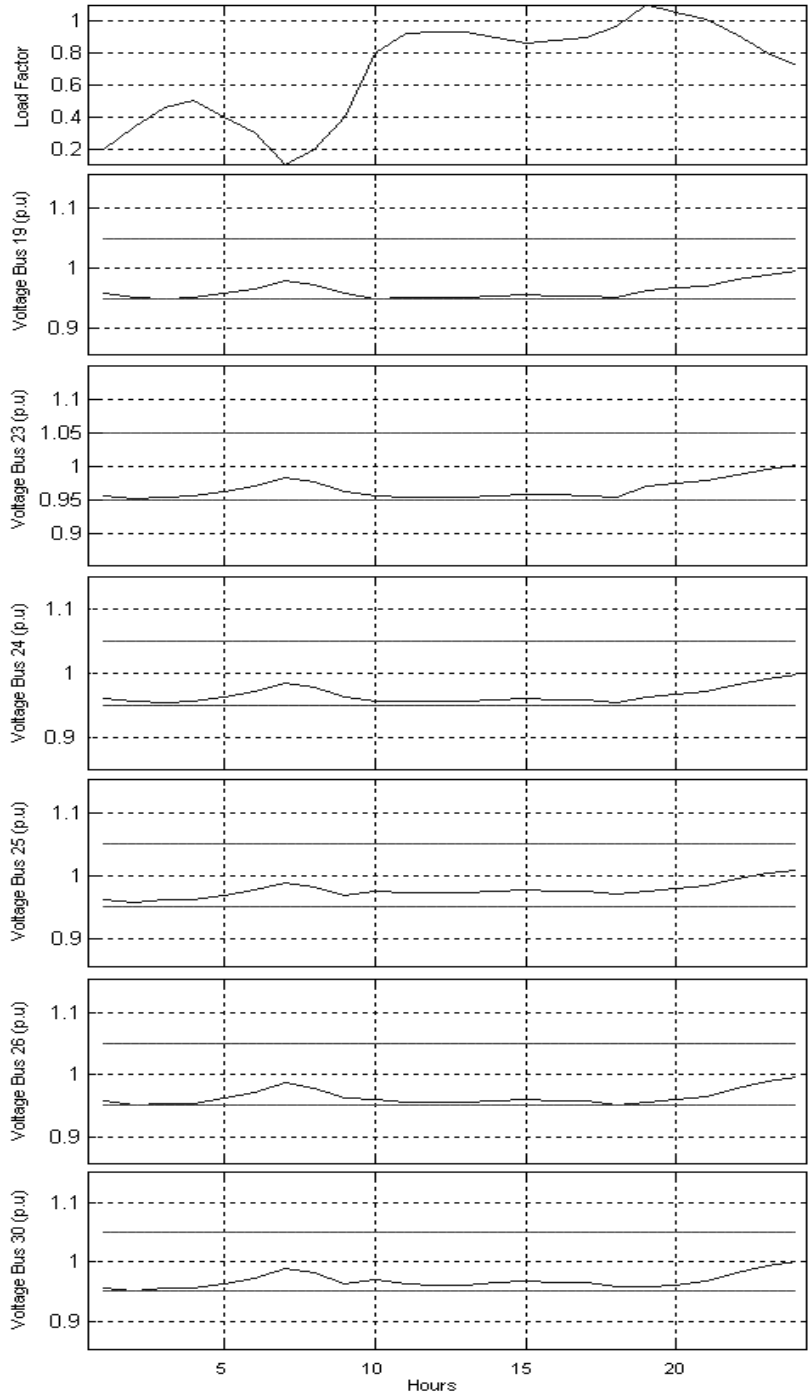


Fig. 9. Voltage at buses 19, 23, 24, 25, 26 and 30 after the application of distance measure method for a load variation of 24 hours.

Besides the buses presented in Fig. 9, the rest of them are kept within the non-violating voltage zone. Variations of transformer taps are illustrated in Fig. 10. In the case of manipulation of capacitor banks, none of them were executed because all banks were connected at initial condition and the voltage violations that appeared were only under-voltage type.

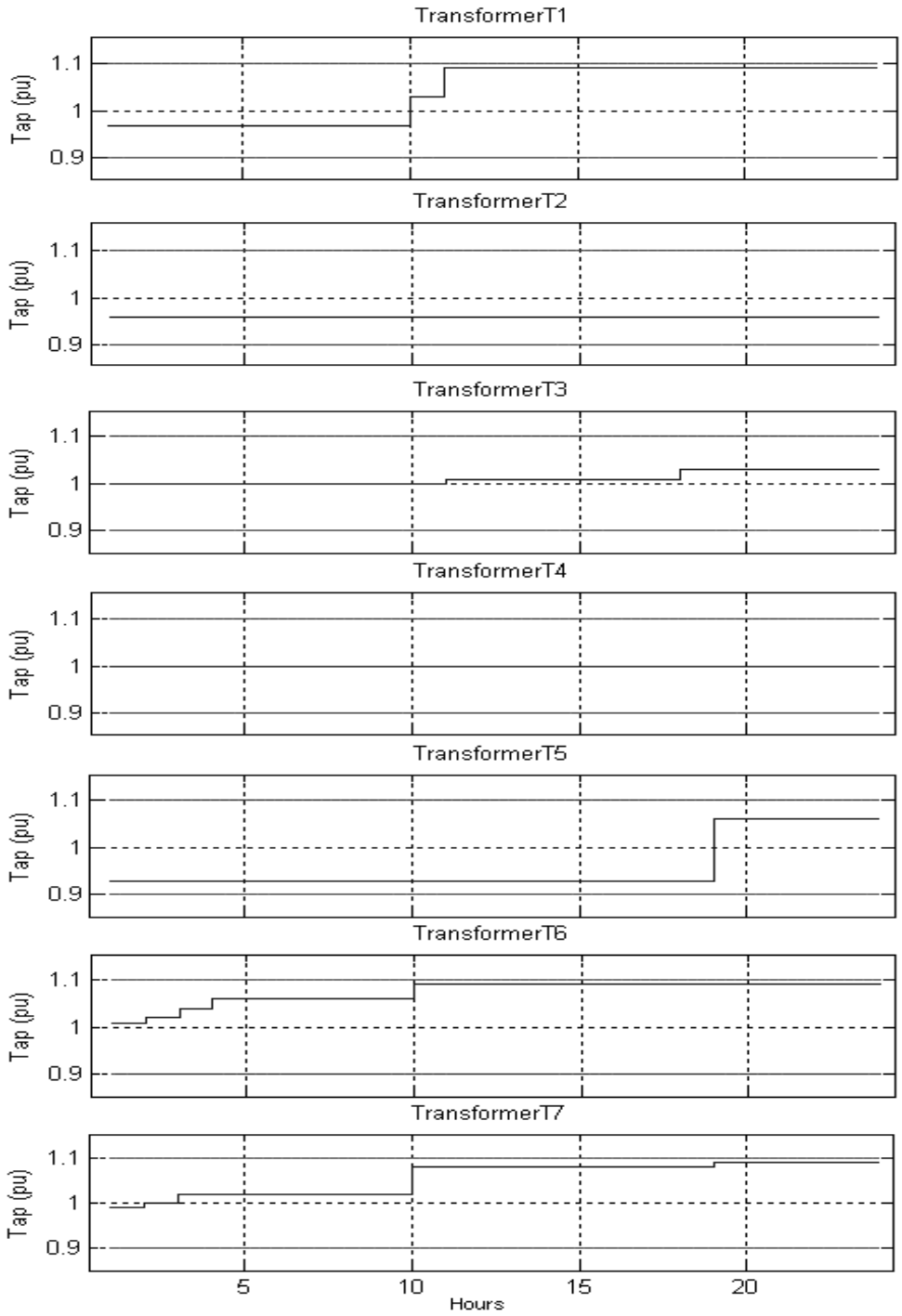


Fig. 10. Position of taps in every transformer after the application of distance measure method for a load variation of 24 hours.

## 6. CONCLUSIONS

In this paper a Rule-based method was presented for regulate voltage deviations and to reduce power losses of a transmission system. The control method is based on simple rules. These rules permit to find the most effective control device available to solve any voltage violation on the system. Thus, control actions were executed under the principle of minimum operations of control devices. Several simulations were done to compare a local voltage control strategy with the new method and the results proved that:

1) The new method achieves the goal where the classic fails.

2) Difference between number of control actions of classic method and distance method is very small.

Another result worth mentioning is that: The rule-based method reduces power losses of the system under maximum load condition. Such result brings technical improvement and also economical benefits to utility companies.

Finally, the new control method was tested under a load variation interval of 24 hours and the system response was quite good. Voltages at all buses were maintained out the voltage violation zone.

## 7. REFERENCES


[1] T. Ananthapadmanabha, "Knowledge-based expert system for optimal reactive power control in distribution system," *International Journal of Electrical Power and Energy Systems*, vol. 18, pp. 27-31, January 1996.

[2] Yutian Liu, Peng Zhanga and Xizhao Qiu, "Optimal volt/var control in distribution systems," *International Journal of Electrical Power and Energy Systems*, vol. 24, pp. 271-276, May 2002.

[3] Yair Malachi and Sigmond Singer, "A genetic algorithm for the corrective control of voltage and reactive power," *IEEE Trans. Power Syst.*, vol. 21, pp. 295-300, Feb 2006.

[4] Biswarup Das, Pradeep Kumar Verma, "Artificial neural network-based optimal capacitor switching in a distribution system," *Electric Power System Research*, vol. 60, pp. 55 - 62, June 2001.

[5] H. I. Hagenaars, J. Imura, and H. Nijneijer, " Approximate continuos-time optimal control in obstacule avoidance by time/space descrifization of non-convex state constraints," in *Proc. 2004 IEEE Conference on Control Applications*, pp. 878-883.


## 8. BIOGRAPHIES

**Yoel Rosales Hernandez** was born in Habana Cuba, on April 12, 1977. He received his B.E. and MS. Degrees in Electrical Engineering from Jose Antonio Echeverría Polytechnic University Cuba in 2001 and 2003 respectively. He joined the Jose Antonio Echeverría Polytechnic University from 2001 until 2006. From April 2004 through June 2004 he was at University of Applied Science Giessen-Friedberg in Germany, and was involved with real time monitoring systems research. He is currently a PhD student at Graduated School of Science and Technology in Kumamoto University, Japan. His current interests include intelligent system applications to the operation and control of power system.

**Takashi Hiyama (S.M)** received his B.E., M.S., and PhD degrees all in Electrical Engineering from Kyoto University Japan in 1969, 1971, and 1980, respectively. He joined Kumamoto University in 1971 and has been a Professor from 1989. During the period of June 1985 through September 1986, he was at Clarkson University, and was involved with power system harmonic research.

His current interests include intelligent system applications to electric power systems and the applications of renewable energy power sources to power distribution systems operation, control and management. He is a Senior Member of IEEE, a member of IEE of Japan and Japan Solar Energy Society.

Received 9 February 2008
Paper 08GM1419

# 2. A REVIEW ON ENERGY LOSS DEVELOPMENT

Loi Lei Lai[2], City University London, UK

***Abstract*** – This paper presents a very brief review on the energy loss development so far. There are lots of advancements in terms of generation, distribution, transmission and utilization. Also energy loss could also be reduced through training so the users know the limitation of the devices used.

## 1. INTRODUCTION

Electric power losses due to power generation and delivery are small compared to power requirements for the rest of the electrical system. However, it is essential to encourage improvements in existing technologies that would reduce the existing losses. A good power quality is necessary to get the appropriate results from most end-use energy efficient systems.

## 2. IMPROVEMENTS

### *2.1 Energy Management*

Through improvements to the processes of monitoring and coordinating the generation, transmission, and distribution of energy, opportunities for energy loss reduction may be found in all areas of energy use (utility, industrial, commercial, and residential). Areas of opportunity include, but are not limited to [1,2]:

- Power system data acquisition and control;
- Automatic generation control;
- Load and energy management;
- Distribution generation; and
- Real-time energy pricing.

Other areas include the recovery of energy from exergic or exothermal processes (such as cogeneration or combined heat and power systems) or processes having combustible waste as a byproduct.

IEEE-USA recommends that the U.S. government promote aggressive research, development, commercialization, and utilization of energy efficient technologies and processes. IEEE-USA supports programs that will help to reduce waste and increase the efficient use of energy by [3]:

- Increasing user awareness of economical energy efficient opportunities;
- Providing incentives for capital investment in energy efficient technologies and processes in all sectors;
- Developing technologies to further reduce energy losses in power generation, power delivery and electric power conversion systems;
- Improving direct combustion processes to increase efficiency and reduce pollutants;

[2] L.L. Lai is with the Energy Systems Group, City University, London, United Kingdom
E-MAIL: l.l.lai@city.ac.uk

- Improving and upgrading industrial processes to reduce energy consumption per unit, while optimizing process performance and reducing maintenance costs;
- Reducing energy consumption in the residential and commercial sectors;
- Upgrading transportation systems to lower energy consumption per passenger mile and cargo-ton mile;
- Using communications and information technology systems to reduce the need for traveling;
- Employing information technology systems to increase the efficiency of energy using-processes; and
- Improving energy storage and other demand management techniques.

### *2.2 Renewable Energy*

Biomass power boilers are typically in the 20-50 MW range, compared to coal-fired plants in the 100-1500 MW range. The small capacity plants tend to be lower in efficiency because of economic trade-offs; efficiency-enhancing equipment cannot pay for itself in small plants. Although techniques exist to push biomass steam generation efficiency over 40%, actual plant efficiencies are in the low 20% range.

Co-firing involves substituting biomass for a portion of coal in an existing power plant furnace. It is the most economic near-term option for introducing new biomass power generation. Because much of the existing power plant equipment can be used without major modifications, co-firing is far less expensive than building a new biomass power plant. Compared to the coal it replaces, biomass reduces sulfur dioxide (SO2), nitrogen oxides (NOx), and other air emissions. After "tuning" the boiler for peak performance, there is little or no loss in efficiency from adding biomass. This allows the energy in biomass to be converted to electricity with the high efficiency (in the 33-37% range) of a modern coal-fired power plant.

Biomass gasifiers operate by heating biomass in an environment where the solid biomass breaks down to form a flammable gas. This offers advantages over directly burning the biomass. The biogas can be cleaned and filtered to remove problem chemical compounds. The gas can be used in more efficient power generation systems called combined-cycles, which combine gas turbines and steam turbines to produce electricity. The efficiency of these systems can reach 60%.

Gasification systems will be coupled with fuel cell systems for future applications. Fuel cells convert hydrogen gas to electricity (and heat) using an electro-chemical process. There are very little air emissions and the primary exhaust is water vapor. As the costs of fuel cells and biomass gasifiers come down, these systems will proliferate.

Modular systems employ some of the same technologies mentioned above, but on a smaller scale that is more applicable to villages, farms, and small industry. These systems are now under development and could be most useful in remote areas where biomass is abundant and electricity is scarce. There are many opportunities for these systems in developing countries.

In Oct 2003, a leading electrical manufacture has launched a generator for wind turbines based on permanent magnet technology. Compared to a traditional machine, the generator offers high output relative to the frame size, making for instance a 3.6 MW unit a full frame size smaller [4].

Such a generator could operate in a wide speed range and with efficiency over 98%.
The permanent magnet generator is a synchronous machine where the rotor windings have been replaced with permanent magnets. This eliminates the excitation losses in the rotor, which otherwise typically represent 20 to 30 percent of the total generator losses. The reduced losses also give a lower temperature rise in the generator, which means that a smaller and simpler cooling system can be used.

The temperature reduction in the rotor also reduces the temperature in the bearings, improving reliability by increasing the lifetime of the bearings and the bearing grease. The high

efficiency of the generator means better utilization of the wind energy, producing more electrical power. The reduction in size and weight also makes the construction of the windmill easier as smaller lifting equipment can be used.

Recent developments in permanent magnet generator technology have been made possible by a significant improvement of the magnetic materials during the past decade. A piece of neodymium boron iron (NeFeB) material can have a magnetic force more than 10 times stronger than a traditional ferrite magnet.

### *2.3 Transmission Loss Reduction based on FACTS*

Optimal Power Flow (OPF) is a static non-linear program that intends to schedule the controls of the power system in such a manner that certain objective function like real power loss is optimized with some operating equipment and security requirement, limit constraints forced on the solution. The OPF problem has been solved from different perspectives like studying the effects of load increase/decrease on voltage stability/power flow solvability, generation rescheduling to minimize the cost of power generation, controls like taps, shunts and other modern VAR sources adjustments to minimize real power losses in the system.

With the advent of Flexible AC Transmission Systems (FACTS) technology a new possibility of optimizing the power flow without resorting to generation rescheduling or topology changes has arisen. UPFC the most advanced in the family of these devices can provide a lot of flexibility in OPF by injecting a controlled series and shunt compensation.

Proper coordination of the UPFC with the existing OLTC transformer taps already present in the system will certainly improve the steady state operating limit of any power system. An optimal location and parameters of an UPFC along with values of OLTC taps could be determined to minimize the real power losses of a power network [5].

### *2.4 Real Energy Cost Saving*

In reference [6], it concluded that there are significant opportunities for reducing energy losses and energy demand through the use of improved industrial energy systems. It is over $18 billion in energy expenditures that could potentially be avoided though the energy loss programme. Some of the opportunities represent relatively near-term targets achievable in the next five years (energy system integration). These near-term targets will not require R&D, but might require increased plant awareness, promotion of energy best practices, better justification of energy efficiency projects, new tools and training.

## 3. CONCLUSIONS

A very brief review on energy loss reduction has been presented and there are many developments are happening at present.

## 4. REFERENCES


[1] EIA Renewable Energy Annual 2002.

[2] Loi Lei Lai and Tze Fun Chan, Distributed Generation - Induction and Permanent Magnet Generator, Wiley and IEEE Press, October 2007.

[3] http://www.ieeeusa.org/policy/positions/efficiency.asp

[4] www.abb.co.uk

[5] M. Tripathy, S. Mishra, L L Lai and Q P Zhang, “Transmission loss reduction based on FACTS and bacteria foraging algorithm,” Lecture Notes in Computer Science, Springer-Verlag, 2006.

[6] Technology Road: Energy loss reduction and Recovery in Industrial Energy Systems, Prepared by Energetics, Incorporated for the US Department of Energy, November 2004.

## BIOGRAPHY

**L. L. Lai** (SM'92, F'07) received his B.Sc. (First Class Honors) and Ph.D. degrees from the University of Aston in Birmingham, UK. He was awarded a higher doctorate, D.Sc. by City University London in 2005 and is its honorary graduate. Currently he is Head of Energy Systems Group and Chair Professor of Electrical Engineering at City University, London, UK. He is also a Visiting Professor at Southeast University, Nanjing, China and Guest Professor at Fudan University, Shanghai, China. He has authored/co-authored over 200 technical papers. In 1998, he also wrote a book entitled *Intelligent System Applications in Power Engineering - Evolutionary Programming and Neural Networks*. In 2001, he edited a book entitled *Power System Restructuring and Deregulation - Trading, Performance and Information Technology*. In 1995, he received a high-quality paper prize from the International Association of Desalination, USA. Among his professional activities are his contributions to the organization of several international conferences in power engineering and evolutionary computing; he was the Conference Chairman of the IEEE/IEE International Conference on Power Utility Deregulation, Restructuring and Power Technologies 2000. Presently he is an Officer (Secretary) in the Board of Governors of the IEEE Systems, Man, and Cybernetics Society. Dr. Lai is a Fellow of the IET (UK). He was awarded the IEEE Third Millennium Medal, 2000 IEEE Power Engineering Society UKRI Chapter Outstanding Engineer Award and 2003 IEEE Power Engineering Society Outstanding Large Chapter Award. In June 2006, he was awarded a Prize Paper by IEEE Power Engineering Society Power Generation and Energy Development Committee.

Received 6 February 2008
Paper 08GM0363

# 3. A Loss Minimum Re-configuration Algorithm of Distribution Systems under Three-phase Unbalanced Condition

Takayuki Tanabe, (Meidensha Corporation, Japan)
Toshihisa Funabashi (Meidensha Corporation, Japan)
Koichi Nara (Fukushima National College of Technology, Japan)
Yuji Mishima (Hakodate National College of Technology, Japan)
Ryuichi Yokoyama (Waseda University, Japan

***Abstract*—**Many single phase distributed generators (DGs) - such as solar cells, small scale gas-engine CHP systems, etc. - are being installed in an electric power distribution system in recent years. These distributed generators are not always generating steady power due to the weather conditions or hot-water demand conditions, etc. Therefore, DGs could make "balanced three-phase load" unbalanced. Unexpected load unbalance creates many unpredicted problems in power distribution systems: voltage unbalances, frequency deviations, etc. It is also known that the loss minimum normal open sectionalizing switch positions for three phase unbalanced conditions are not the same as the ones calculated by assuming three-phase balanced. Therefore, a method to find the optimal normal open sectionalizing switch positions that minimize both distribution loss and three phase unbalance is required. The problem is the multi-objective planning problem, and the palate solution must be found. In this paper, a solution algorithm for loss minimum re-configuration is explained and several numerical examples are shown.

***Index Terms***— Distributed generator, Distribution system, Load transfer, Loss minimization, Re-configuration, Three-phase unbalance

## 1. INTRODUCTION

It has been 20 years since Distribution Automation (DA) systems including the optimal load transferring and fault restoration functions began in Japan [1]. Currently, most distribution feeders have been automated, and the aged DA facilities must be replaced. In replacing the system, new concepts must be introduced to the system. Future functions of DA systems have been discussed in reference [2], etc. In a new system being developed in Japan, the small DA systems in business offices are unified and integrated into the ones in the branch of the company, and the supervised area or controlled area of one DA system becomes wider than those of the existing system. A new trend of distribution system is a connection of such distributed generators (DGs) as photovoltaic generations (PVs) and combined heat and power systems (CHPs) using gas engines or fuel cells. The functions to cope with DGs are also installed to the new DA system. Caused by a connection of lots of single phase DGs to the distribution system, three-phase unbalance must be considered to control electric power distribution systems.

An electric power distribution system is normally constructed as so-called "open loop radial distribution system" in many countries. In this system, loops of the distribution network are made open by so-called "sectionalizing switches" and then the system is operated as a radial distribution system. Normal open positions of sectionalizing switches are determined to minimize distribution losses or to balance feeder-loads among distribution feeders by supposing that a section load is three phase balanced in any section. However, the normal open positions of the sectionalizing switches for the unbalanced load condition are normally different from the ones calculated by assuming that loads are three phases balanced. Therefore, we must take unbalancing of loads into consideration, when we determine the normally open positions of

sectionalizing switches where three phase unbalance are significant (caused by installing single phase distributed generators etc.).

Several research results have been published relating to the load conditions where single phase distributed generators are connected [3,4]. Also, varieties of loss minimum re-configuration methods for distribution system have been proposed by many researchers; such as branch exchange, heuristic loop opening, genetic algorithm, Petri-net, simulated annealing, tabu search, and so on. Meta-heuristic methods applied to the distribution systems re-configuration are summarized in reference [5].

From the above background, the authors have developed a new distribution system's re-configuration algorithm for minimizing distribution losses where three phase unbalance is taken into account. The algorithm is based on tabu search and three phases load flow through Gauss-Seidel method, which is implemented for the purpose of analyzing unbalanced three phases power flow.

In this paper, the loss minimum re-configuration problem under three-phase unbalanced condition is defined and formulated in Section 2. In Section 3, a developed new method based on tabu search and three-phase load flow is explained, and the validity of the developed re-configuration algorithm is demonstrated through several numerical examples in Section 4.

## 2. PROBLEM FORMULATION

A loss minimum re-configuration algorithm where three phase unbalance is considered by using three-phase power flow can be formulated as follows.

Objective function is defined as equation (1).

$$Min.\sum_{t}\sum_{j}\sum_{i} Loss_{ijt}\left(x_{ij}{}^{t}\right) + \alpha_1 \sum_{t}\sum_{k} V^{t}_{kunba} + \alpha_2 \sum_{t}\sum_{m} I^{t}_{munba} \tag{1}$$

The first term of the objective function (1) shows the total distribution loss of the whole distribution network for the all time zones under consideration. Second term shows the penalty for the three phases voltage unbalance (the sum of three phase unbalance of all the nodes). Third term represents the penalty for the three phase current unbalance at the roots of feeders (the sum of three phase unbalance of transformer currents). Coefficients $\alpha_1$ and $\alpha_2$ are the penalty cost for the sum of the three phase unbalances for voltage and current respectively. Therefore, to minimize the objective function, both distribution loss and three-phase unbalance of voltage and current are minimized. Weights that determine which factor of the objective function must be minimized most are determined by selecting the values of $\alpha_1$ and $\alpha_2$ according to the planner's decision.

Constraints are defined for (2) line capacity, (3) transformer capacity, (4) upper and lower limits of line-to-line voltages, (5) upper and lower limits of phase voltages, (6) power supply to all the nodes and (7) radial configuration. Three phase power flow through Gauss-Seidel method [6] is employed to calculate the power flow and three phase unbalance of the voltage and current.

## 3. SOLUTION ALGORITHM

The formulated problem is a mixed integer-programming (MIP) problem, and is difficult to solve large-scale problems. Therefore, "Tabu Search" is employed to solve the MIP problem. So as to reduce the number of decision variables, the positions of open sectionalizing switches are memorized and the optimal positions are determined through tabu search. To apply tabu search, constraints (2)-(5) are relaxed to the objective function. Then, the neighborhood solutions are created not to violate constraints (6) and (7). The solution algorithm is shown below.

*(Solution algorithm)*

(Step1) Initial three phases power flow is solved by Gauss-Seidel method.
(Step2) Neighborhood solutions for tabu search are created, and all the neighborhood solutions are evaluated by three phases load flow. If all the neighborhood solutions are evaluated, then go to Step3
(Step3) Move to the best neighborhood solution, and tabu list is updated.
(Step4) If pre-determined iteration number is reached, then quit the algorithm. If not, then go back to Step2, and start the next iteration.

In Step2 of the above algorithm, the neighborhood solutions are created by shifting all the positions of opened sectionalizing switches to the both neighboring positions. Namely, the number of neighborhood solutions is $l \times 2$, if a number of normally open sectionalizing switches are *l*. The neighborhood solutions are created not to violate the constraints (6) and (7). The violations of other constraint equations (2)-(5) are added to the objective function by multiplying the appropriate penalty factors not to violate the constraints. To evaluate the objective function, three phase load flow through Gauss-Seidel method is used [6].

## 4. NUMERICAL EXAMPLES

The solution algorithm is tested with an electric power distribution system model having 103 load sections (total load 18.7[MW]) as shown in Fig. 1. Fig.1 shows the initial state of the normal open positions of sectionalizing switches (section loads and impedances are omitted because of the space of the paper). Fig.2 shows the loss minimum positions for three phase-balanced loads found by applying the algorithm shown in Section III. In Fig.1 and Fig.2, white rectangles with X show the open sectionalizing switches, and black and white rectangles denote closed switches. Dotted circles in Fig.2 indicate the positions of the open sectionalizing switches in the initial state. The total losses for Fig.1 and Fig.2 are shown in Table 1.

For the initial system shown above, 36 single-phase distributed generators (DGs) are connected, and three phase unbalanced conditions are created. Three single phase generators are connected at one location of the distribution line just as one three phase generator. Namely, at the same location of the distribution feeder, three single phase DGs are connected between lines ab, bc and ca. Fig. 3 shows 12 locations where DGs are connected. In Fig.3, black circles show the locations of installed DGs.

For the above distribution system, many cases of calculations are tested. Among them, several cases of the following three calculation cases are shown in this paper.

Case 1: three phases balanced DGs are connected.
Case 2: only two phases of DG among three generate output.
Case 3: three phases unbalance is created randomly.

For the all calculation cases, tabu length is set to10, and 2,000 iterations are calculated. The calculated results, for the total 12MW (1MW for each position) generation and $\alpha_1 = \alpha_2 = 0.001$ are shown in Table 2.

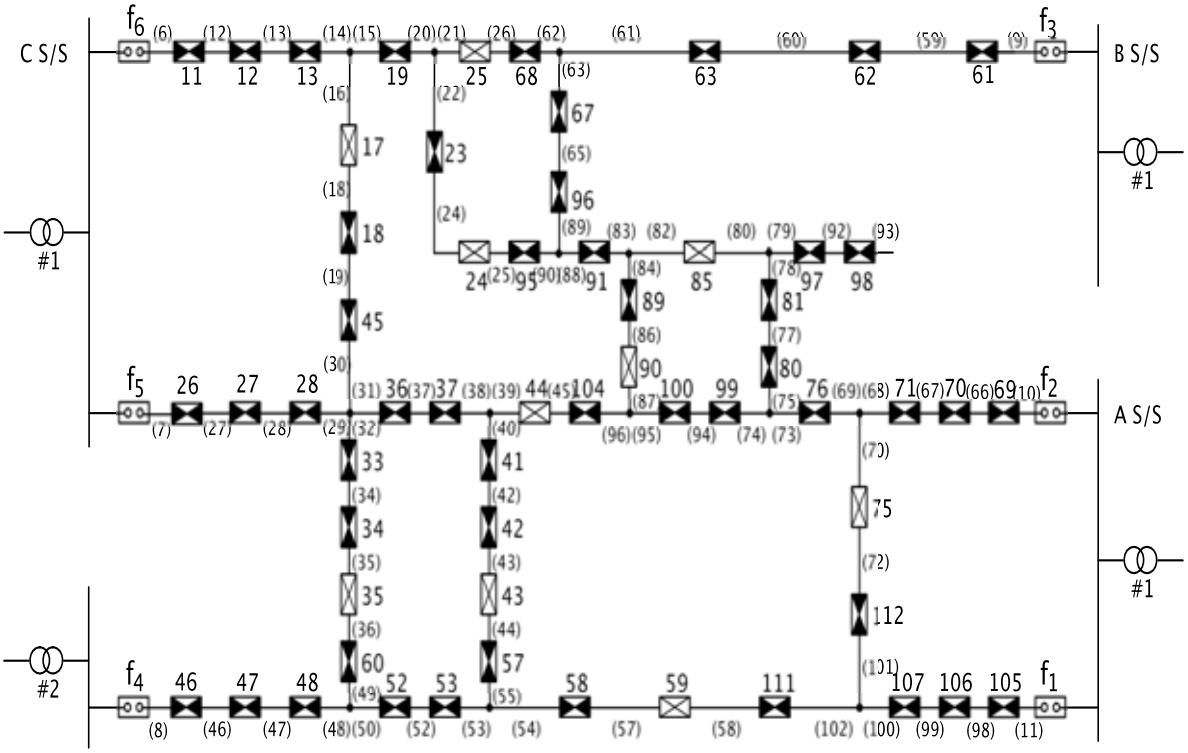


Fig.1 Initial state of example distribution system

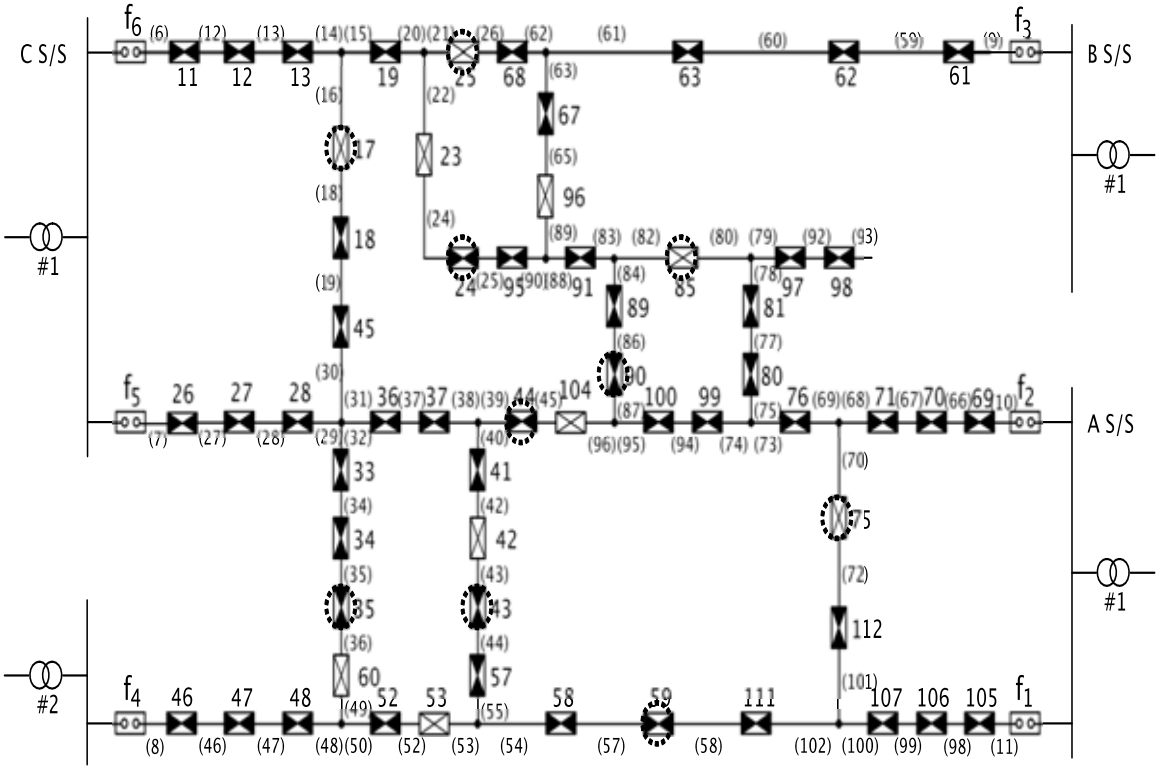


Fig.2 Optimal solution for three phase balanced loads

TABLE 1 LOSSES FOR BALANCED LOAD WITH NO DG

| Initial loss (Fig.1) | Optimal loss (Fig.2) |
|---|---|
| 0.496 [MW] | 0.410 [MW] |

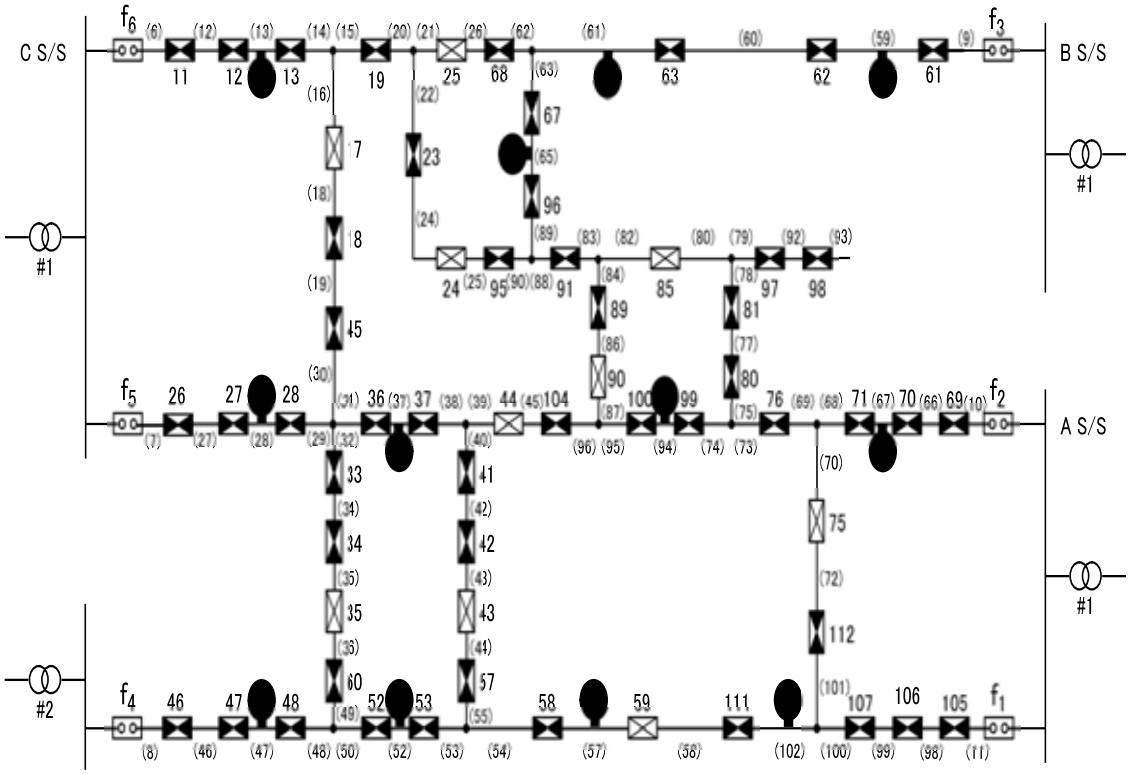


Fig.3 Location of 12 DGs

TABLE 2. CALCULATION RESULTS

| | Case1 | Case2 | Case3 |
|---|---|---|---|
| Objective Function | 0.089 | 0.829 | 0.649 |
| Line loss [MW] | 0.089 | 0.221 | 0.243 |
| Volt. Unbalance[%] | 0.0 | 1.822 | 1.090 |
| Current Unbalance[%] | 0.0 | 105.2 | 73.46 |

For Table 2, minimum distribution loss for $\alpha_1 = \alpha_2 = 0.0$ is 0.203 and 0.227 respectively. That is, three-phase unbalance is mitigated by sacrificing distribution loss for the cases in Table 2. The resulting system configurations for the cases of Table2 are shown in Fig. 4 – Fig.6.

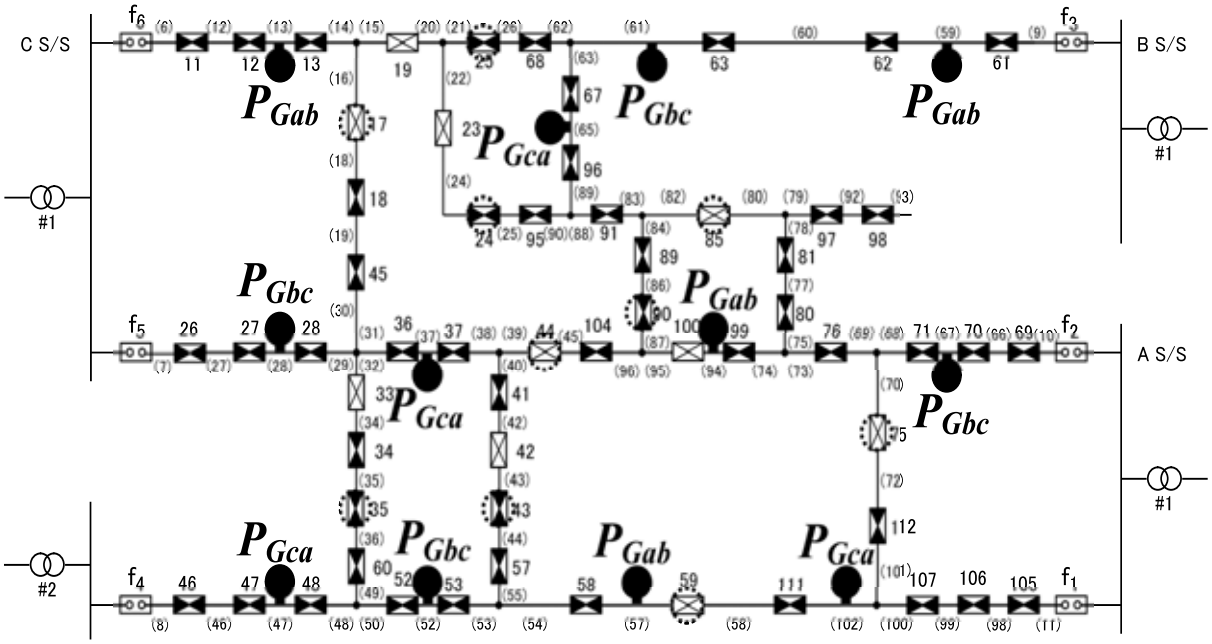


Fig.4. Optimal solution for Case 1

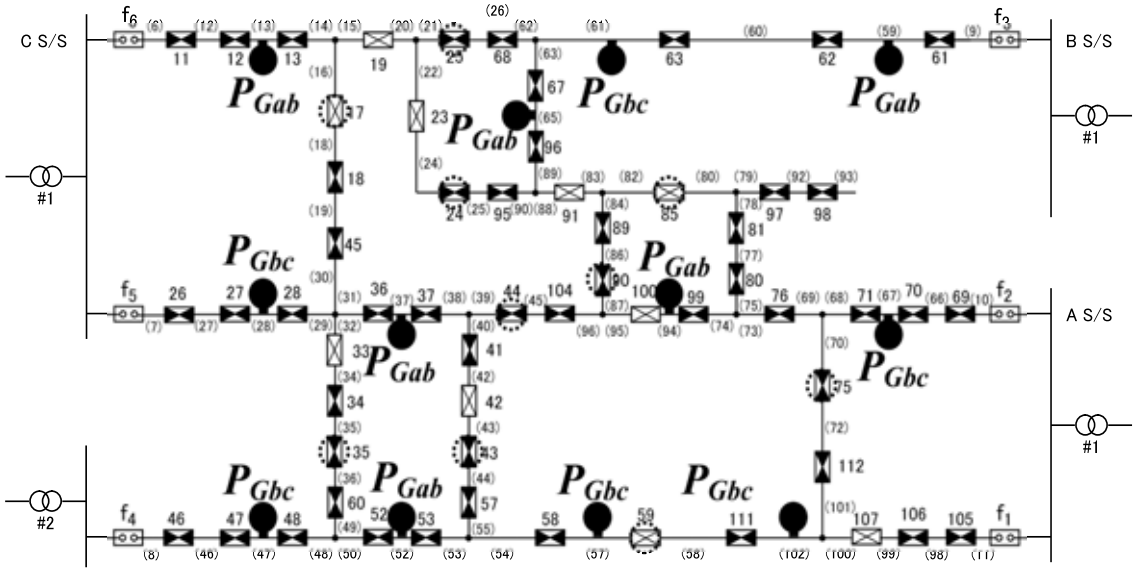


Fig.5. Optimal solution for Case 2

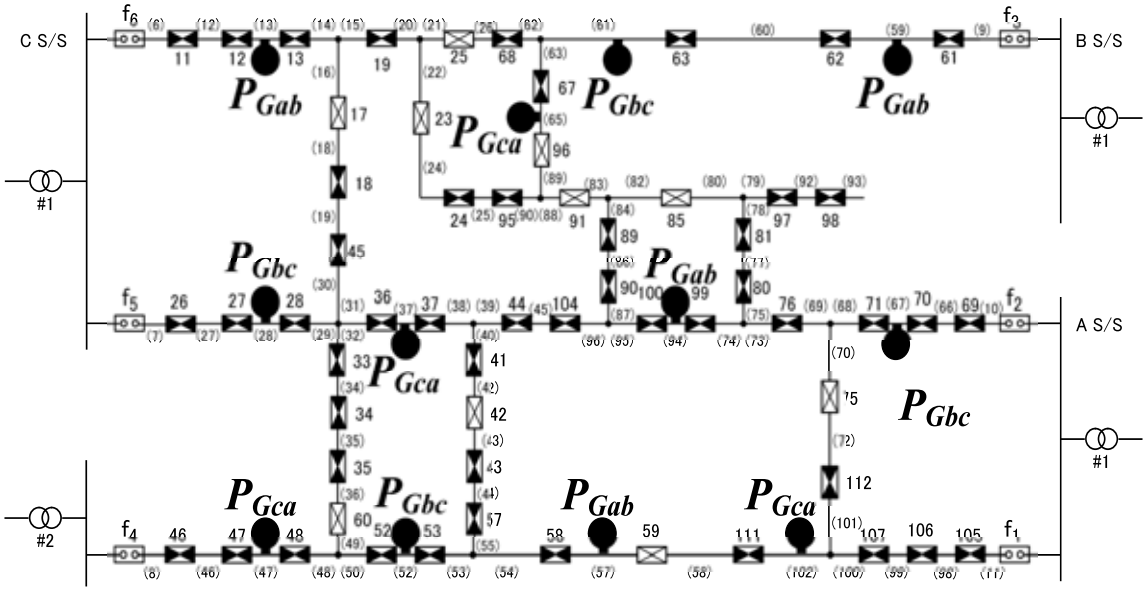


Fig.6. Optimal solution for Case 3

For Case 2, deviations of distribution loss and average transformer current unbalance to DG's capacities are shown in Fig.7 and Fig.8.

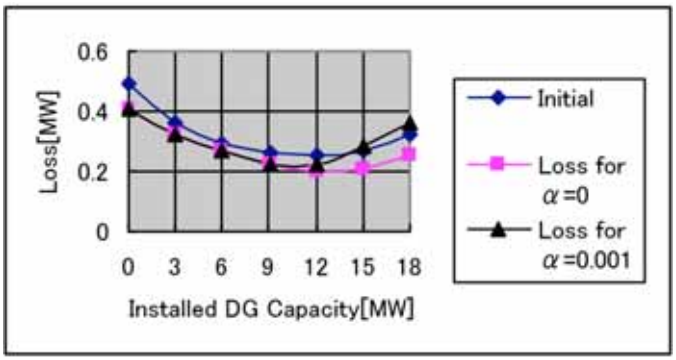


Fig.7. Distribution loss vs. installed DG capacity

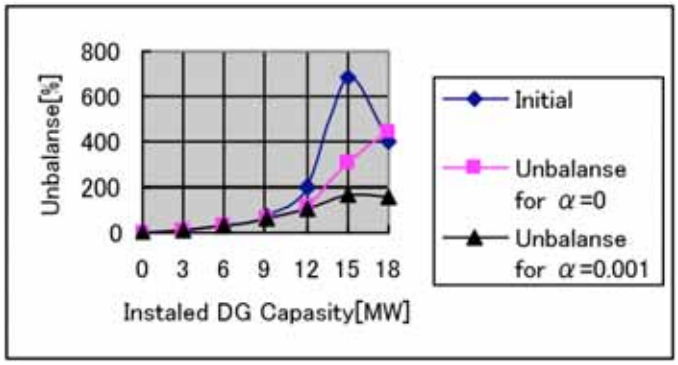


Fig.8. Average Tr. current unbalance vs. DG capacities

From the above results, the following can be estimated.

(1) The normal open sectionalizing switch positions are completely different if the condition of three phases unbalance is different.

(2) Normally, if capacities of DGs increase, distribution loss decreases at first, and then increases again if reverse power flow current increases when three phases balance is guaranteed. However, if three phases unbalance becomes significant, this is not always true.

## 5. CONCLUSION

The solution algorithm is tested using an electric power distribution system model with 103 load sections. By solving many examples, the validity of the solution algorithm is demonstrated. Comparing the calculation results between three phase balanced cases and three phase unbalanced ones, it shows that the normal open positions of the sectionalizing switches for loss minimization are different in most cases. Therefore, for the system where three-phase unbalance is significant, it is desirable to determine the positions of normal open sectionalizing switches by evaluating the losses with three phases power flow. For a future work, how to determine the penalty factors of the three phase unbalance of voltage and current must be evaluated considering the weight balance between loss reduction and unfavorable effects of three phase unbalance.

## 6. REFERENCES


[1] K. Aoki, K. Nara et al., "Totally automated switching operation in distribution system," *IEEE Trans. Power Delivery*, vol. 5, No.1 pp. 514-520, Jan. 1990.

[2] S.S. Venkata et al., "What future distribution engineers need to learn," *IEEE Trans. Power Systems*, vol. 19, No.1 pp. 17-23, Feb. 2004.

[3] *For example*, J.H. Teng C.Y. Chang, "A novel and fast three phase load flow for unbalanced radial distribution systems," *IEEE Trans. Power Systems*, vol. 17, No.4 pp. 1238-1224, Nov. 2002

[4] Y. Hayashi and J. Matsuki, "Loss Minimum Configuration of distribution System Considering N-1 Security of Dispersed Generators," IEEE Trans. Power Systems, Vol.19, No.1, Feb. (2004)

[5] K. Nara and Y.H. Song: “Modern Heuristic Application to Distribution System Optimization”, Proc. of IEEE PES Winter Meeting.2002, NY (2002)

[6] T.Mishima, K.Nara et al. “Three phase power flow for FRIENDS network,” Proc. of IEEE International Symposium on Circuit and Systems, pp.4733-4736, May 20


## BIOGRAPHIES

**Takayuki Tanabe** was born in Shizuoka, Japan, on September 19, 1969. He graduated from the Department of Mechanical System Engineering, Yamanashi University, Japan, in March 1994. He joined Meidensha Corporation in April 1994 and has engaged in research on control system. Currently, he is a Chief Staff of the Power Systems Solution Technology Section, Power Systems Engineering Division. He is a member of the Japan Society of Mechanical Engineers (JSME) and The Society of Instrument and Control Engineers (SICE) of Japan.

**Toshihisa Funabashi** (M'90, SM'96) was born in Aichi, Japan, on March 25,1951. He graduated in March 1975 from the Department of Electrical Engineering, Nagoya University, Japan. He received, in March 2000, a Doctor degree from Doshisha University, Kyoto, Japan. He joined Meidensha Corporation in April 1975 and has engaged in research and development on power system simulations and integration of distributed generation. Currently, he is a Senior Engineer of the Power Systems Solutions Sales and Engineering

Division. Dr. Funabashi is a chartered engineer in UK, a member of IET and the IEE of Japan.

**Koichi Nara** (M'84, SM'06) received B.E., M.E. and D.E. degrees from Hokkaido University Japan, in 1968, 1970 and 1986 respectively. After his industrial and academic experiences at Mitsubishi Electric Co., Kitami Institute of Technology, Hiroshima University and Ibaraki University Japan, he is currently a President of Fukushima National College of Technology, Japan. His research is concentrated in the area of operation and planning of power systems and power distribution systems.

**Yuji Mishima** received his PhD in systems engineering from Hokkaido University Japan, in 1999, and joined the faculty of Engineering, Ibaraki University, Japan as research associate. He is currently an associate professor of the electrical engineering at Hakodate National College of Technology, Japan. His research interests are the optimization of power systems planning and operation.

**Ryuichi Yokoyama** has received the degrees of B.S., M.S., and Ph.D. in electrical engineering from Waseda University, Tokyo, Japan, in 1968, 1970, and 1974 respectively. After working in Mitsubishi Research Institute, since 1978 he has been a professor in the Faculty of Technology of Tokyo Metropolitan University. Since 2007, he is a professor of the Graduate School of Environment and Energy Engineering in Waseda University. His fields of interests include planning, operation, control and optimization of large-scale systems and economic analysis and risk management of deregulated power markets. He is a senior member of IEEE and IEE of Japan,and a member of the Society of Instrument and Control Engineers (SICE) of Japan, and CIGRE.

# 4. Coordinated Control for Isolated Distribution Networks Supplied by Inverter Power Sources

Junichi Arai and Seiji Fujino (Kogakuin University, Japan), Hideaki Tanaka, (The Federation of Electric Power Companies, Japan), and Ryuichi Yokoyama (Waseda University, Tokyo, Japan).

***Abstract*—**New energy generation systems, such as photovoltaic cells or fuel cells are increasing in application on distribution networks. These power sources require an inverter to connect to an ac network. There is the possibility that sub-network containing inverter power sources will be disconnected from the utility system to become isolated networks. This paper focuses on an isolated distribution network supplied by inverter power sources without the use of a synchronous generator, and proposes coordinated control for the inverters. The feature of inverter control is that one inverter has constant frequency characteristics and the other inverters are operated by constant active power control. The coordinated control is demonstrated by digital simulation**.**

***Index Terms*—**control, dc power source, distribution network, efficiency, isolated network, inverter, voltage source converter

## 1. INTRODUCTION

Distributed power sources such as fuel cells and photovoltaic cells have been developed and applied to distributed networks. The application of NAS (sodium-sulfur) battery energy storage systems for load-leveling or stand-by power sources is also increasing. These systems generate dc power, and require inverters for connection to an ac distribution network. An isolated distribution network with power supplied by an inverter power source is examined in this study. No synchronous generator is connected in the network. Such an isolated network could be feasible in a large factory or in a micro grid when it is disconnected from the large utility network. The problem with an isolated network is how to determine frequency and achieve stable operation.

Many studies of control to obtain stable operation of an isolated system have been reported, and they usually contain synchronous generators. Stable operation can be obtained by applying the same active power and frequency (P-f) droop characteristics as a conventional generator [1,2].

Several papers have reported isolated networks fed by inverters excepting synchronous generators [3-5], which also apply P-f or Q-f droop characteristics. This means that the frequency changes depending on the power level.

As mentioned in [3], such isolated networks do not have a conventional power-frequency relationship, due to the absence of a synchronous generator. The inverter is able to generate ac voltage with a specified frequency. If the inverter operates with constant frequency instead of droop characteristics, then good power quality is supplied with respect to frequency. Therefore, in this study, we have focused on an isolated distribution network with constant frequency operation. A conventional uninterrupted power source (UPS) has a similar configuration; however, only one control signal is distributed to all parallel inverters in the UPS. This is the same condition as in a single inverter, and therefore no problems arise.

In this paper, a new control strategy for inverters in an isolated distribution network without a synchronous generator is proposed, and stable operation of the network is demonstrated by

digital simulation.

## 2. NETWORK MODEL AND CONSTANT FREQUENCY OPERATION

### *2.1 Simple network model*

The simple network model is shown in Fig. 1, in which two inverters, INV-A and INV-B, and one load are connected through an ac bus. INV-A and INV-B represent the power source, which consists of a dc power source as a battery storage system or a fuel cell, a chopper, an inverter, and transformer, as shown in Fig. 2. The characteristics of the power source are determined by the characteristics of inverter control.

INV-A is assumed to be a battery energy storage system, such as a NAS battery system, with no charge and discharge restrictions. INV-B is assumed to be a fuel cell with restrictions, i.e. constant power operation is desired, rapid power change is suppressed, there is a minimum power output, and high efficiency operation range for output level. Ideal chopper operation is assumed, then a constant dc voltage source with a resistor in series is applied on the dc side of the inverter. A full bridge voltage source inverter (VSC) with six arms is assumed.

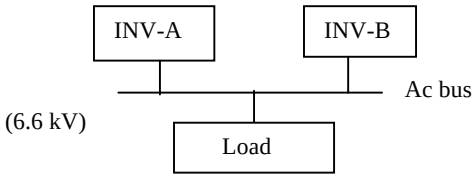


Fig. 1. Isolated distribution network model.

In Fig. 1, the capacity of INV-A is supposed as 200 kW, and the capacity of INV-B is treated as a parameter for determining the limit of stable operation. INV-A has constant frequency characteristics and INV-B has constant active power (P) and constant reactive power (Q) operation.

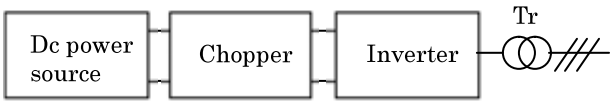


Fig. 2. Internal configuration of INV.

### *2.2 Control of inverter*

The control block for INV-A is shown in Fig. 3. Fo is the reference frequency, i.e. 50 Hz. An integrator is applied to obtain the phase angle ($\theta$) of the ac voltage generated by the inverter. Ac voltage control is applied to obtain the ac voltage amplitude (A). Vac is the detected ac voltage at the ac bus and is subtracted from the reference voltage (Vref =1 pu), and sent to the PI-control with Kpv=0.5 and Kiv=50. Three phase ac voltage signals of the desired output voltages are calculated from the angle and the amplitude as $Va = A\sin(\theta)$, $Vb = A\sin(\theta - 2\pi/3)$, $Vc = A\sin(\theta - 4\pi/3)$. The pulse width modulation (PWM) block generates six on/off pulses for the arm of the inverter.

INV-B has constant P and Q control; the control block is shown in Fig. 4. This configuration of control is general and is applied to many VSC inverters. The P and Q control adopt PI-control with Kpp=Kpq=0.7 and Kip=Kiq=28. The phase angle of the ac voltage is detected by a phase locked loop (PLL) using the d-q axes decomposition method. The outputs of the P control and Q control are sent to the current controller with the feedback signals of the inverter currents, Iac.

The Vd and Vq signals obtained are used to calculate the three phase ac voltage signals followed by PWM logic.

INV-A operates with constant frequency and voltage control, while INV-B operates with P-control and Q-control. The problem is whether the large capacity of INV-B compared to INV-A can allow stable operation.

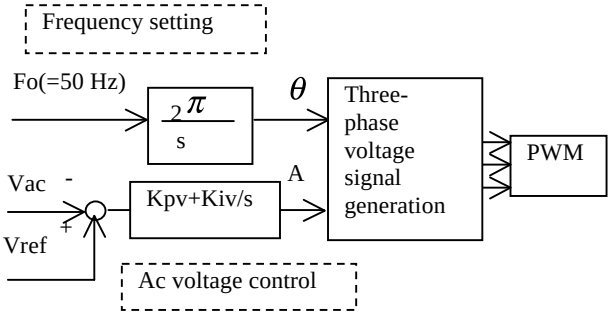


Fig. 3. Control block for INV-A.

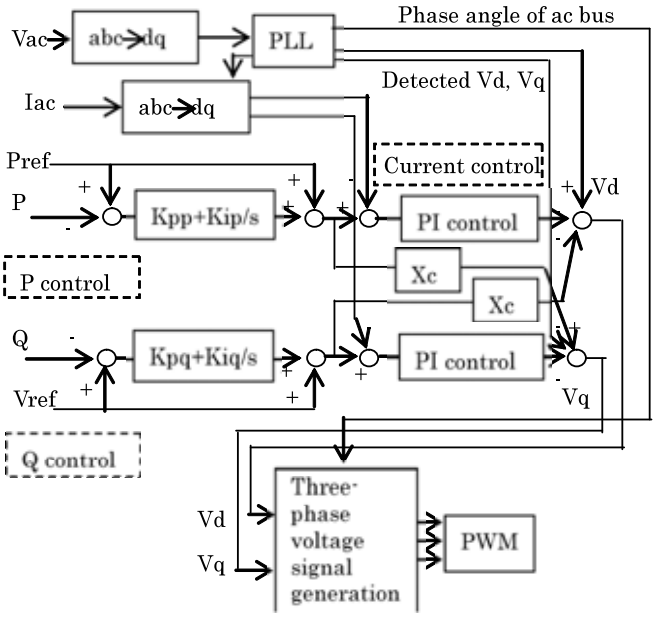


Fig. 4. Control block for INV-B.

The Electro Magnetic Transients Program-Alternative Transients Program (EMTP-ATP) [6] carries out the simulation for Fig. 1. An infinite bus, not shown in Fig. 1, is connected at the start of the simulation to obtain normal inverter operation and then disconnected to obtain operation of the isolated ac network supplied by the inverter power sources. The load is represented by a constant impedance model with a R-L load of pf=0.95; a compensation capacitor is connected to achieve pf=1.0 as the total load.

### *2.3 Stable Operation*

The capacity of INV-A is fixed as 200 kW, and the capacity of INV-B is started from 200 kW (as the same capacity) and increased. The case study results are shown in Table 1.

TABLE 1.
CAPACITY OF INVERTERS AND OPERATION RESULTS

| | CAPACITY (kW) | | |
|---|---|---|---|
| CASE | INV-A | INV-B | RESULTS |
| 1 | 200 | 800 | Stable |
| 2 | 200 | 1000 | Stable (Fig. 5) |
| 3 | 200 | 2000 | Stable (Fig. 6) |

Fig. 5 shows the simulation results of Case-2, where (a) are the active and reactive power of INV-A and INV-B, (b) is the rms ac voltage, and (c) are the three phase voltage waves between 1.30 s and 1.50 s. The initial operating points are Pa=0 kW and Qa=0 kVAr for INV-A, and Pb=1000 kW and Qb=0 kVAr for INV-B. An additional load of 100 kW is switched on at 1.2 s. The frequency of the network is determined by INV-A and the ac voltage is controlled by INV-A. INV-B maintains Pb and Qb. The power of the additional load is supplied from INV-A and stable operation is obtained.

Fig. 6 gives the results of Case-3. A stable system is still observed, but time is required to dampen the power swing. This result indicates that even if the capacity of INV-B is ten times that of the INV-A, stable operation can be obtained.

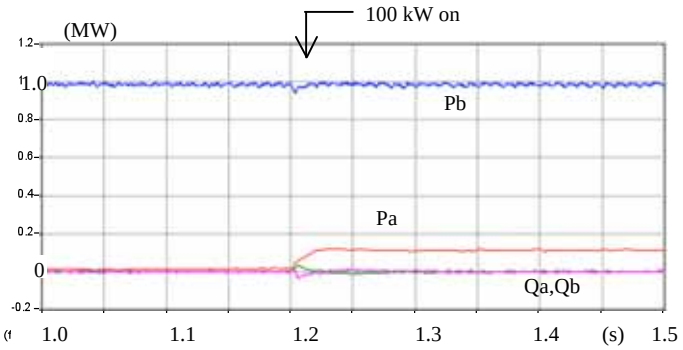


(a) Active and reactive power of INV-A and INV-B.

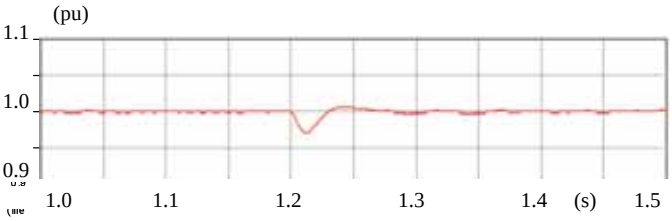


(b) Ac voltage.

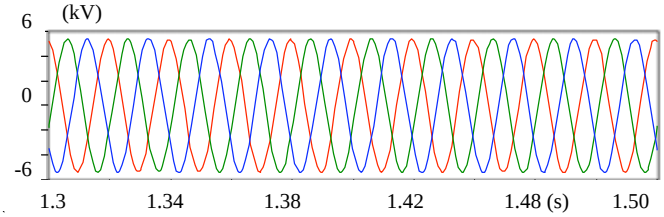


(c) Three phase voltage.

Fig. 5. Simulation results for Case 2.

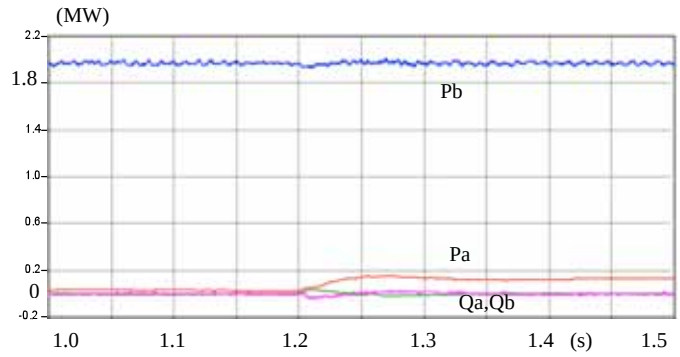


(a) Active and reactive power of INV-A and INV-B.

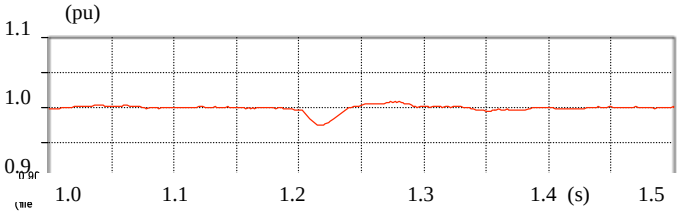


(b) Ac voltage.

Fig. 6. Simulation results for Case 3.

Many induction motors are usually included in loads; therefore, a part of the constant impedance load of Case-2 was replaced by an induction motor with a capacity of 200 kW. The same stable operation was obtained. The induction motor operates with slip, and when the shaft load torque is increased the slip is increased, and it reaches another operating point. The induction motor does not determine frequency. Similar results were reported in [7], where the combination of an inverter with constant frequency and an induction generator representing wind power was studied and stable operation was obtained.

## 3. COORDINATED CONTROL

### *3.1 Distribution network model*

An extension of the isolated distribution network model is shown in Fig. 7. INV-A with constant frequency operation is the same as before, and two P-Q control type inverters, indicated by INV-B1 and INV-B2, are assumed. The capacity and ratings of the network components are shown in Table 2.

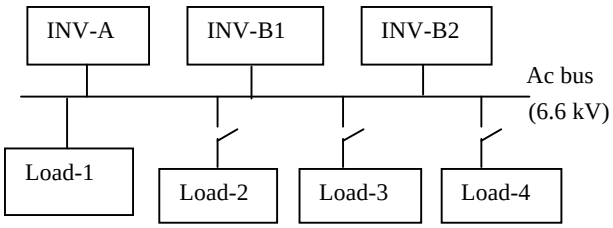


Fig. 7. Distribution network model.

TABLE 2.
EQUIPMENT RATINGS

| Equipment | Rating | Characteristics |
|---|---|---|
| INV-A | 200 kW | F-constant, V-control |
| INV-B1 | 400 kW | P-Q control } Total 1000 kW |
| INV-B2 | 600 kW | P-Q control |
| Load-1 | 700 kW | Base load |
| Load-2 | 50 kW | For step load change |
| Load-3 | 50 kW | For step load change |
| Load-4 | 100 kW | For step load change |

The total capacity of INV-B1 and INV-B2 is five times that of INV-A, which corresponds to the ratio of Case-2.

### *3.2 Proposed control*

Fig. 8 shows the proposed frequency characteristic settings for INV-A. When the output of INV-A exceeds +0.8 pu and +0.9 pu (discharge operation), the frequency is set to 49.5 Hz and 49.0 Hz, respectively, as shown in Fig. 8. This is the countermeasure against system collapse when the output of INV-A exceeds its maximum limit. The values of 0.8 pu or 49.5 Hz are one example for study, and they will be modified to smaller values for application. When the output of INV-A exceeds -0.8 pu and -0.9 pu (charge operation), the frequency is set to 50.5 Hz and 51.0 Hz, respectively. The frequency is used as a signal between the inverters for output power distribution.

When the frequency monitored in INV-B1 and INV-B2 exceeds a preset value, the active power references (Pref) of INV-B1 and INV-B2 are modified to return the frequency back to Fo. This can be realized using the control shown in Fig. 9. The preset value of DF is selected as DF=0.25 Hz which is lower than the first stage frequency change of 0.5 Hz in Fig. 8. In Fig. 9, when the detected frequency error (Fdet-Fo) exceeds +/-0.25 Hz, the error signal is integrated and modifies Pref to New-Pref.

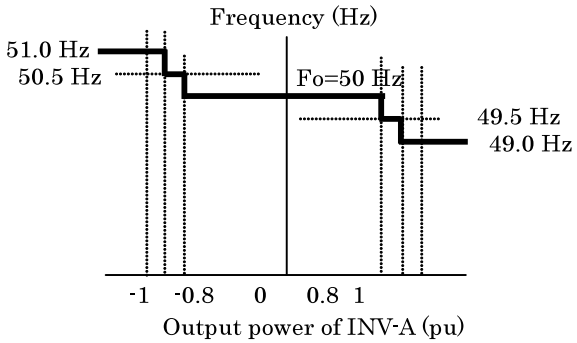


Fig. 8. Frequency vs. power characteristics.

If the same value of DF is applied to both INV-B1 and INV-B2, they change their output simultaneously. If different DF is applied, then the priority of INV-B1 and INV-B2 can be assigned.

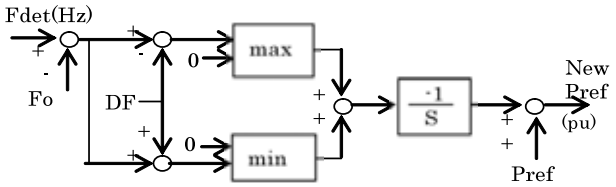


Fig. 9. Additional control block for INV-B1 and INV-B2.

### *3.3 Simulation results*

Simulation results of the discharge and charge operations in INV-A are shown in Figs. 10 and 11, respectively.

In Fig. 10, the initial operating points are Pa=150 kW, Qa=0 kVAr, Pb1=200 kW, Qb1=0 kVAr, Pb2=300 kW and Qb2=0 kVAr. When Load-2 (50 kW) is switched on, Pa exceeds 0.8 pu, and the frequency becomes 49.5 Hz. Pb1 and Pb2 are increased and Pa is reduced, and the frequency is returned to 50 Hz. The same operations are obtained for the switching on of Load-3 (50 kW). At the time of switching on Load-4 (100 kW), the frequency reaches 49.0 Hz due to the large load increase.

In Fig. 11, INV-A is initially in the charging operation of 130 kW, and Load-2, Load-3 and Load-4 are switched off step by step. The frequency reaches 50.5 Hz and 51.0 Hz temporarily. The power output limit of 100 kW in INV-B1 is assumed in this case, so that the output of INV-B1 maintains 100 kW after Load-4 is switched off and a larger output reduction is observed in INV-B2.

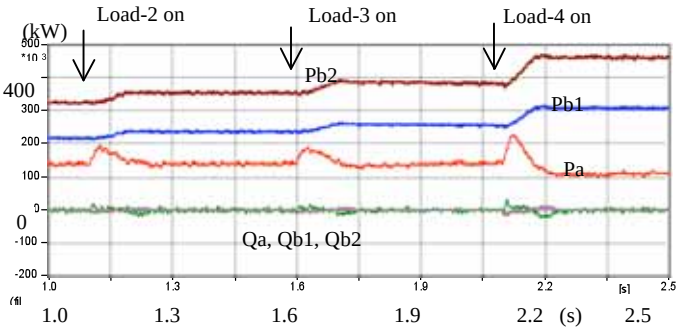


(a) Active and reactive power.

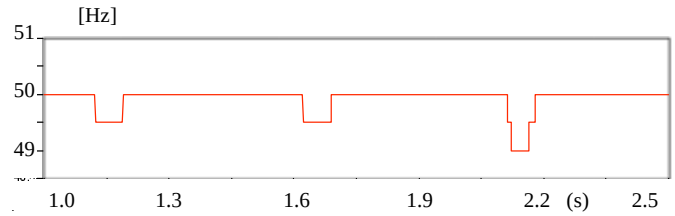


(b) Ac system frequency.

Fig. 10. Results of discharge operation with INV-A and DF=0.25 Hz for both INV-B1 and INV-B2.

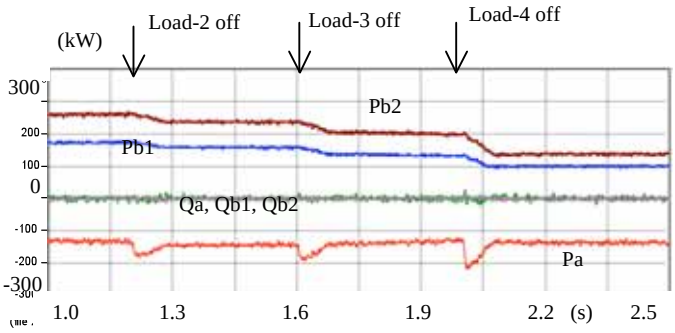


(a) Active and reactive power.

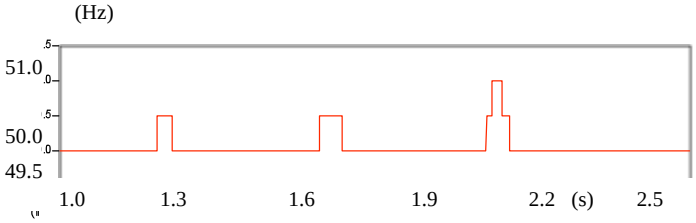


(b) Ac system frequency.

Fig. 11. Results of charge operation with INV-A and DF=0.25 Hz for both INV-B1 and INV-B2.

*Priority of power sources for efficient operation*

Each power source has different characteristics. For example, the NAS battery system accepts quick power charge and discharge, whereas some fuel cells require constant power operation or slow power change. In addition, there are sources that have high efficiency operation bands and require operation in that particular band. It is possible to achieve a suitable combination of operation between these sources by selecting different DF values among the different types of INV-B sources. Fig. 12 shows results for the case with DF=0.25 Hz for INV-B1 and DF=0.75 Hz for INV-B2; the output power of INV-B2 changes after INV-B1 reaches its upper limit.

The change in the frequency slope, similar to droop characteristics can be applied for over +/-0.8 pu, instead of a step as shown in Fig. 8.

These simulation results show the possibility for stable operation of a network consisting of all inverter type power sources.

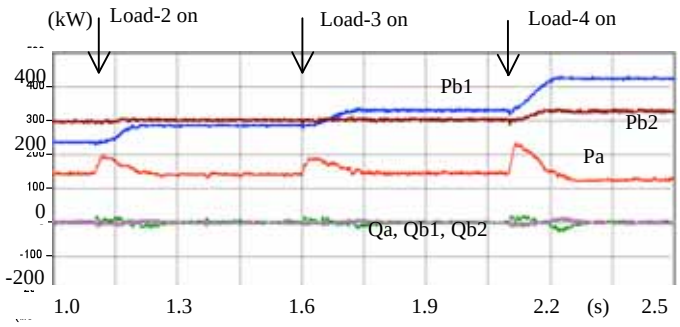


(a) Active and reactive power.

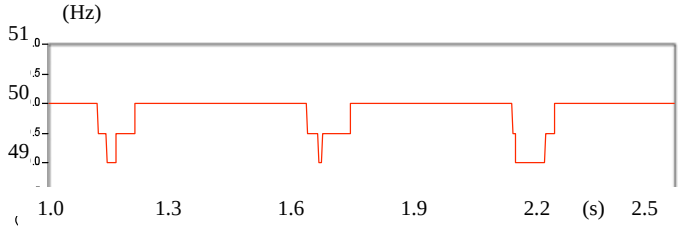


(b) Ac system frequency.

Fig. 12 Results of discharge operation with INV-A and DF=0.25 Hz for INV-B1 and DF=0.75 Hz for INV-B2.

## 4. CONSIDERATION FOR DISTRIBUTION NETWORKS

The control proposed in this paper has many restrictions when compared to a conventional ac system, and it also has many requirements. The following items should be considered for realizing this type of isolated distribution network.

*1) Operation at system fault*

The inverter model used here has no protection logic [8], and a fault study was not carried out in this study. When a fault is applied, large fault current will flow. Most inverter control reduces the inverter's generated voltage to suppress inverter current, so that the inverter will be protected from large current due to faults. Otherwise it is considered that in case of a large system fault, inverters should be blocked and restarted again.

*2) Inrush currents of transformers*

When a transformer is energized, inrush current flows. If the inrush current is larger than the current capacity of the inverter, the inverter will be blocked. In a test system [9] a soft start of an inverter with a pre-connected distribution transformer is applied. If the capacity of the transformer is small, the inrush current will be acceptable and no countermeasures are required. However, if the capacity of the transformer is large, then it will be feasible to apply a circuit breaker with resister insertion for suppression of the inrush current.

*3) Inrush current of shunt capacitor*

When a capacitor is connected to ac bus, inrush current flows during one cycle. The same

consideration should be discussed. If the capacity is large, this inrush current can be suppressed by application of series reactors or by phase control switching.

*4) Connection to synchronous generators*

The proposed system does not take into account synchronous generator connection. If a synchronous generator is connected, another inverter control is required, such as a control with droop characteristic, as for the synchronous generator.

*5) Connection to a large ac system*

This isolated system must be able to connect to a large ac utility system. When an isolated system is connected to a utility system [10], the control of INV-A should be changed from a constant frequency setting to constant active power control, as is used for INV-B. Signals representing connection to a large ac system will be required for change of the control.

## 5. CONCLUSION

A distribution network fed by inverter power sources was examined, and a new control method was proposed. The network loads are supplied by inverter power sources and non-interconnection to a normal ac system is assumed. Simulation results indicate that stable operation can be obtained and constant frequency network can be realized. This system becomes a local network with higher power quality of constant frequency and with well-controlled voltage amplitude. When the output of the inverter that determines frequency reaches the upper limit, then power distribution among the inverters is available. Furthermore, the desired output power operation can be selected and this allows efficient operation among various dc power sources.

However there are many restrictions in this combination of controls, the proposed system will be more applicable to the power source of a large factory or local distribution network.

## 6. REFERENCES


[1]. Lopes, J. A. P., Moreira, C. L., Madureira, A. G., “Defining control strategies for MicroGrid islanded operation”, IEEE Transactions on Power System, Vol. 21, No. 2, 916-924, 2006.

[2]. Zeineldin, H. H., El-Saadany, E. F., Salama, M. M. A., “Distributed Generation Micro-Grid Operation: Control and Protection”, Power Systems Conference: Advanced Metering, Protection, Control, Communication, and Distributed Resources, 2006.

[3]. Sao, C. K., Lehn, P. W., “Intentional islanded operation of converter fed microgrid”, PES General Meeting, 2006.

[4]. Laaksonen, H., Saari, P., Komulainen, R., “Voltage and frequency control of inverter based weak LV network microgrid”, International Conference on Future Power Systems, 2005.

[5]. Guerrero, J. M., Berbel, N., Matas, J., Sosa, J. L., de Vicuna, L. G., “Droop Control Method with Virtual Output Impedance for Parallel Operation of Uninterruptible Power Supply Systems in a Microgrid”, Applied Power Electronics Conference, APEC 2007.

[6]. Canadian/American EMTP User Group, “ATP Rule Book”, 1999.

[7]. Tanomura, K., Arai, J., Noro, Y., Takagi, K., Kato, M., “New Control for HVDC System Connected to Large Windfarm”, IEE Japan, Trans. PE, Vol. 126, No. 6, 619-626, 2006.

[8]. Nikkhajoei, H., Lasseter, R.H., “Microgrid Protection”, PES General Meeting, 2007.

[9]. Sumita, J., Nishioka, K., Noro, Y., Shinohara, H., Ito, Y., Kawakami, N., “A study of Isolated Operation of a Microgrid Configured with New Energy Generators”, IEE Japan, Trans. PE, Vol. 127, No. 1, 145-153, 2007.
[10], Funabashi, T., Yokoyama, R., “Microgrid field test experiences in Japan”, PES General Meeting, 2006.

## 7. BIOGRAPHIES

**Junichi Arai** received the BS degree and MS degree in Electrical Engineering from Waseda University in 1970 and in 1972, respectively. He received a doctorate degree in Engineering from Tokyo Metropolitan University in 1995 in Japan. He joined Toshiba Corporation in 1972 and started as a research engineer of power systems. He moved to the Faculty of Engineering at Kogakuin University, Tokyo, in 2006. His research focuses on power system control, equipment maintenance, power electronics applications, micro-grid control, and power quality. He is a member of IEEJ, IEIEJ, C.Eng of IET, and a senior member of IEEE.

**Seiji Fujino** received the B.S. degree in electrical engineering from Kogakuin University, Tokyo, Japan, before obtaining his masters in electrical engineering at Kogakuin University in 2006. He is a student member of the IEE Japan. His research interests are in micro-grid control, computer simulation, and power system control.

**Hideaki Tanaka** received B.S. and M.S. degrees in electrical engineering from Waseda University, Tokyo, Japan in 1974 and 1976, respectively. He joined the Tokyo Electric Power Company in 1976. After beginning his career as a substation engineer, he has primarily dedicated himself to bulk-power system planning and operation. His current interests include asset management on aged transmission facilities and methods for preventing cascading blackouts. He has been teaching power system stability analysis as a part-time lecturer at Waseda University for 17 years. He is a member of the IEE of Japan and IEEE.

**Ryuichi Yokoyama** received the B.S., M.S. and Ph.D. degrees in electrical engineering from Waseda University, Tokyo, Japan in 1968, 1970, and 1974, respectively. Since 1978 he has been working in the Faculty of Engineering of Tokyo Metropolitan University, and is currently a Professor of the Graduate School of Environment and Energy Engineering at Waseda University. His fields of interest include planning, operation control and simulation of large-scale energy and environment systems, as well as risk evaluation and management in competitive energy markets. He is a Senior Member of IEEE and the IEE of Japan, CIGRE, and SICE Japan**.**

Received 11 February 2008
Paper 08GM0744

# 5. Centralized Control of Clustered PV Generations for Loss Minimization and Power Quality

Yosuke Nakanishi (Fuji Electric Systems Company Ltd.),
Hiromitsu Ota (Fuji Electric Systems Co., Ltd.),
Ryuichi Yokoyama (Waseda University),
Kiyoshi Yoshida (The Kansai Electric Power Co., Inc.)
Katsuhiko Kouchi (The Kansai Electric Power Co., Inc.), Japan. Centralized Control of

***Abstract*—** This paper presents new approaches in order to solve problems related to clustered photovoltaic systems and evaluates the performance of the developed method. To cope with inappropriate phenomena caused by malfunctions of islanding detector and over voltages by reverse power flows from PV systems, we have developed a new islanding detector and two types of voltage control systems, and conducted experiments to verify the function of the developed systems. The test results obtained by this demonstrative implementation show that the proposed control system is able to maintain voltages within the regulated level and to equalize the efficiency in a PV system and also that the new method enables us to make total PV generation efficiency higher.

***Index Terms*—**Islanding, over voltage, Photovoltaics, Dispersed power source, clustered PV condition

## 1. INTRODUCTION

When dispersed power sources, such as clustered Photovoltaic (hereafter “PV”) systems, are connected to a distribution line, problems arise in regard to ensuring the detection of islanding. Dispersed power sources could deteriorate power quality, through voltage rise exceeding an appropriate range and mutual interference between active signals, making the detection of islanding difficult.

This demonstrative research aimed to assess the above-mentioned problem of clustered grid-connected dispersed power sources in operation and to develop countermeasures for resolving these issues.

To achieve the above-mentioned objectives, we planned to connect a PV system (total generation capacity is approximately 140kW) to a large-scale power grid in the urban area of Thailand, develop methods and systems that suppress voltage rises caused by reverse power flow from PV systems, develop a new method that deters islanding, and perform assessments of these systems.

## 2. CONFIGURATION OF DEMONSTRATION SITE

We refer to Cho Heng Rice Vermicelli Factory Co., Ltd. (hereafter "Cho Heng Fty"), a rice-processing plant, and its surroundings as the “Cho Heng Fty site.” Figure 1 shows the system concept for this site.

The objectives of this research are to identify problems anticipated when multiple PV systems are connected to a power grid, and to find methods to solve those problems. However, we built a type of dummy distribution system, because it was difficult to install a large-scale PV system that could actually cause such problems within an actual power grid simply for research purposes, we built a type of dummy distribution system. At this site, multiple PV systems (seven for this research) were actually connected to create conditions similar to those of a clustered

grid-connected operation. Various types of experiments on anticipated problems were carried out on these systems to identify the problems and to identify solutions. Specifically, we measured a wide variety of data derived from the dummy demonstration systems with limited installed capacities and quantities, and drew conclusions by using a variety of simulation methods.

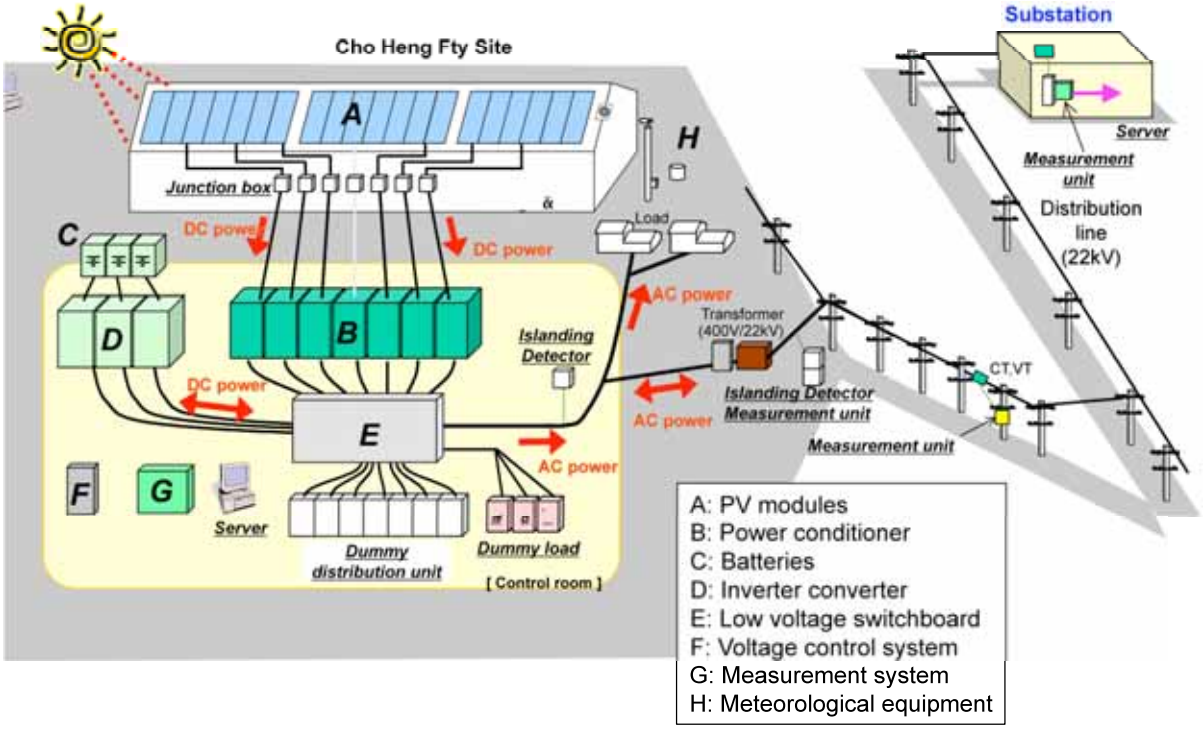


Fig. 1. System Concept for Cho Heng Fty Site

Seven PV arrays were connected to seven 20kW-power conditioners and connected to a commercial power grid via a low voltage switchboard. The power conditioners that have two types of active islanding detection functions were installed to evaluate the possibility of mutual interference among islanding detection functions (reactive power variation type and slip mode frequency shifting type).

Three 20kVA-battery systems were also connected to that power grid. The battery systems consisted of inverters-converters and batteries, which were used for a power source for finely regulating power so that islanding conditions, can be simulated, power storage for the newly developed voltage control system, and active and reactive power controller to imitate PQ-controllable power conditioners for a new voltage control method for integrated PV system monitoring and control.

We installed dummy distribution lines being switch able to impedance values corresponding to the lengths of the distribution lines (0m, 40m, 60m and 100m), which were designed based on the data of the Provincial Electricity Authority (hereafter "PEA"). These lines were used for building dummy power distribution line systems.

Three types of dummy loads, resistance, induction and capacity, were prepared to stabilize loads when islanding was simulated. Figure 2 shows PV arrays put on the warehouse rooftop, and Figure 3 shows power conditioners that are installed in the control room in Cho Heng Fty.

Fig. 2. PV arrays on rooftop of warehouse

Fig. 3. Inside of Control Room

## 3. MAKE DEVELOPMENTS AND DEMONSTRATIVE EXPERIMENTS

### *3.1 Confirmation of the possibility of mutual interference between multiple active islanding detectors*

3.1.1 Mutual interference between reactive power variation islanding detectors (QV)

Reactive power variation systems used in power conditioners installed for this project produced slightly varied reactive power at a constant interval. The reactive power that was absorbed into the power grid when case the power conditioner was connected to the utility's grid, flowed into the load in case islanding occurred, producing frequency fluctuations. By identifying such variations in frequencies, islanding can be detected.

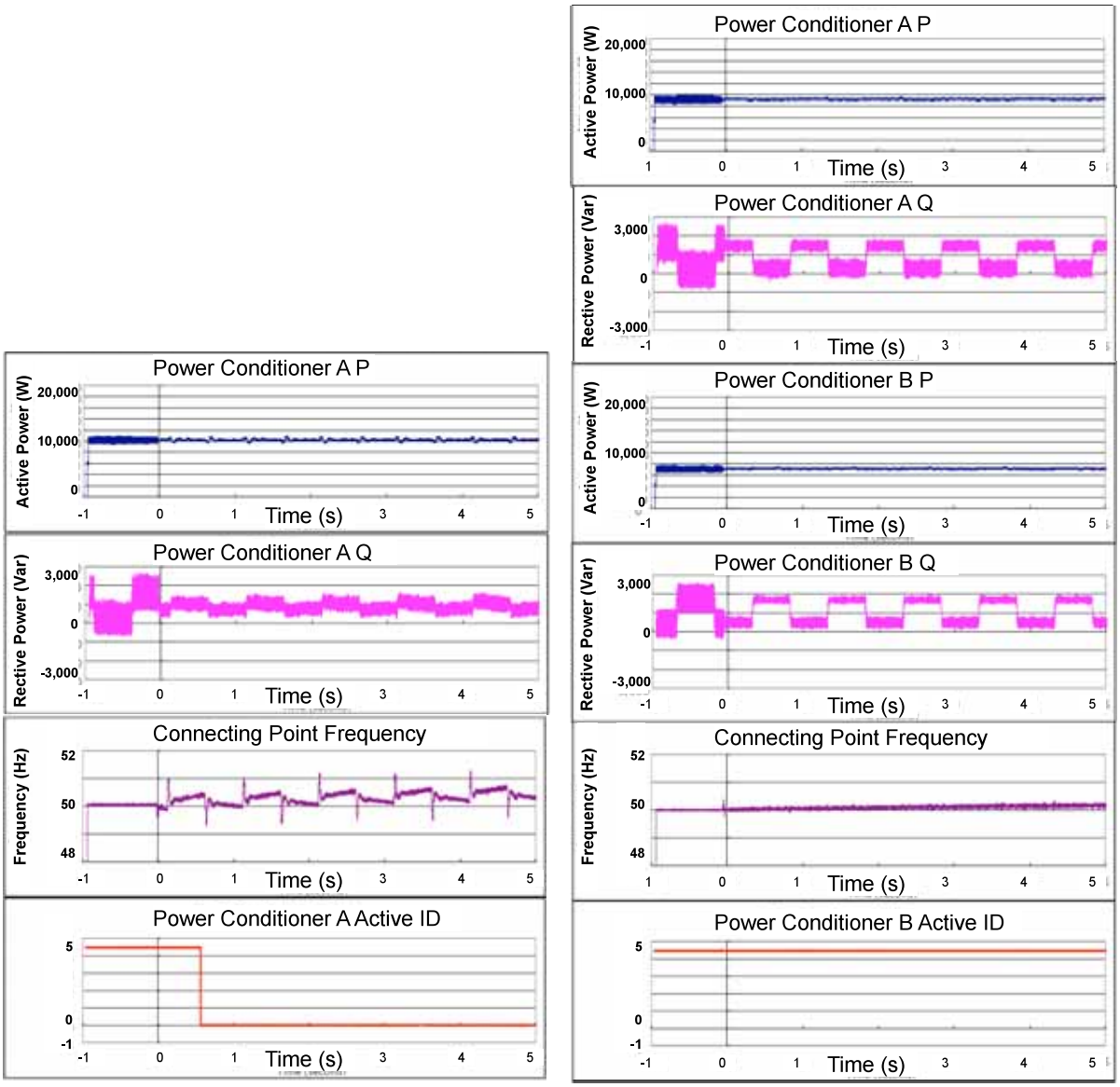


Fig. 4. Waveforms Resulting from Islanding Tests of One QV (left) and Two QVs at 180° Phase Difference (right)

The left figure in Figure 4 illustrates the waveforms during islanding test. The top waveform and the second waveform show active power and reactive power outputs from PV power conditioner with reactive power variation islanding detector, respectively. In the second figure, cyclic variation of reactive power output can be seen. A circuit breaker open signal at a receiving point is set to a starting point (zero seconds). When a system islands under this condition, the frequency of the system varies, as shown in the third waveform. After detecting this frequency fluctuation, the active islanding detector detects islanding as shown in the bottom figure.

The right figure in Figure 4, two reactive power variation signals were in opposite phases (phase difference: 180°) in second and fourth waveforms. In this case, the two reactive power variation signals counteract the other over all the time periods. So, there is nothing that disturbs the system inside the islanding grid. Since the system frequency barely varies, the active islanding detector cannot detect islanding as shown in the fifth waveform. (We cannot see islanding detection signals in the bottom figure.)

This phenomenon is called “mutual interference” of the active signals among active islanding detectors.

### 3.1.2 Malfunction phenomena by the slip mode frequency shifting islanding detector (SM)

A PV power conditioner controls the output power factor at almost 1 by using the system voltage as the synchronous voltage. A slip mode frequency shifting islanding detector uses system voltage, passed through a bimodal BPF (band pass filter), as synchronous voltage in order to prevent islanding. A BPF has the frequency characteristics described in the red solid line in Figure 5.

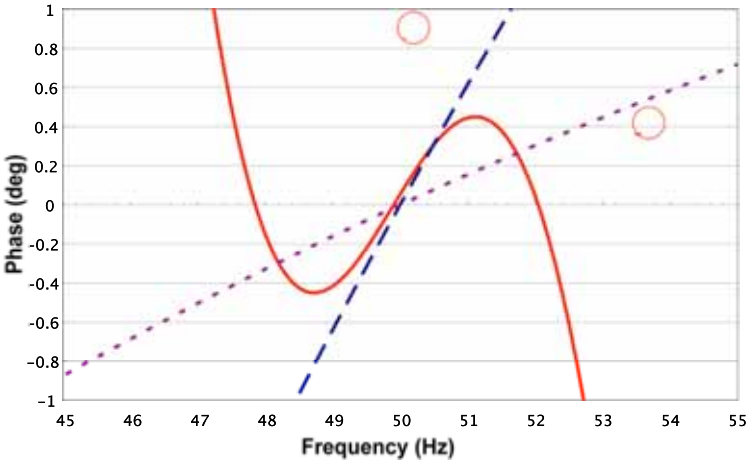


Fig. 5. Frequency Characteristics of Two Types of Loads and Frequency Characteristics of SM

Two blue dotted lines in Figure 5 indicate frequency characteristics of two types of load inside islanding grid. Curve (2) indicates the steep frequency characteristic load which can easily change the phase of electric current depending on the system frequency, while curve (1) is the gently frequency characteristic load which changes the phase of current slightly against frequency change.

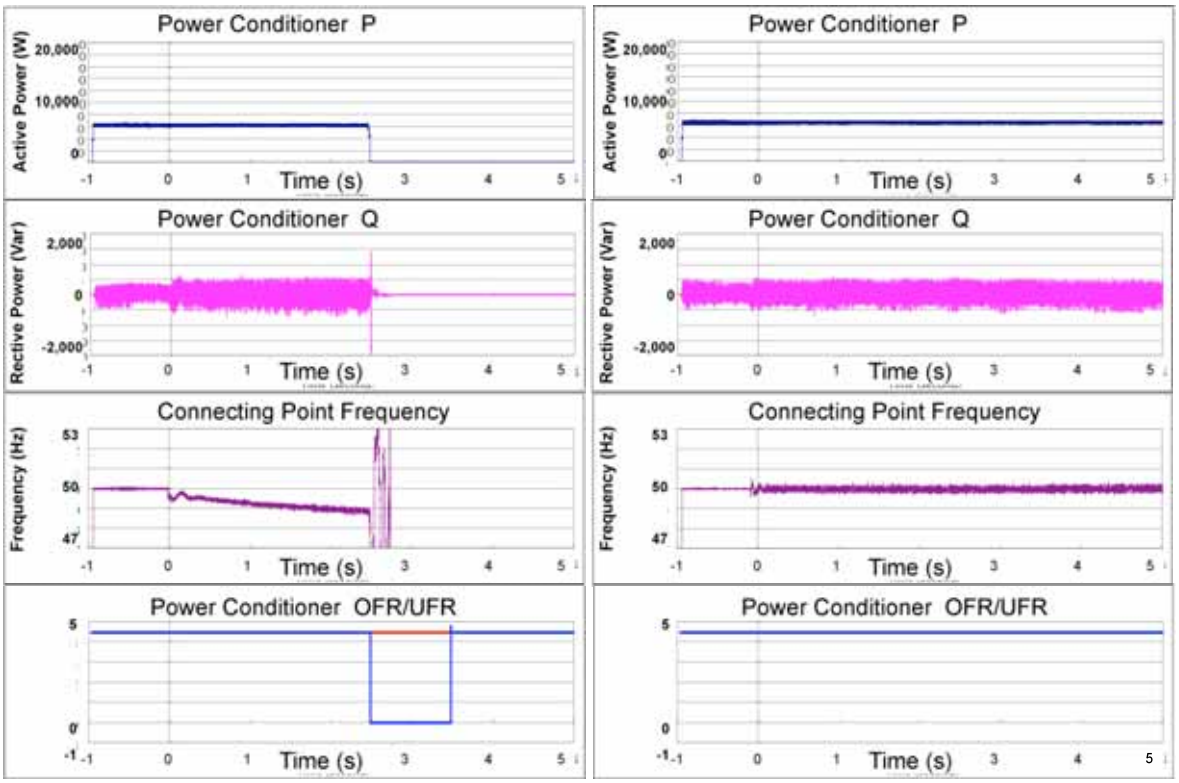


Fig. 6. Waveforms from Islanding Tests for SM with Frequency Characteristics Exceeding Loads (left) and Less Than Loads (right)

The left figure in Figure 6 shows waveforms obtained in islanding grid including PV power conditioner with slip mode frequency shifting islanding detector and load whose frequency characteristic describes curve (1) in Figure 5. The right side in Figure 6 shows the same waveforms, but its load's frequency characteristic is curve (2) in Figure 5.

Accordingly, in the left side of Figure 6, the frequency, in the third waveform, began to fluctuate greatly after falling in islanding and decreased in the end. Concurrently, UFR relay was actuated about 2.5 seconds after the formation of islanding to shut down the operation of the power conditioners, as shown in the bottom waveform.

Meanwhile, in the right of Figure 6, the frequency of the power grid did not indicate a significant variation or shifting after islanding began. As a result, since neither OFR nor UFR was actuated, the power conditioners were not shut down. This allowed the islanding to last longer than five seconds.

### *3.2 Development of a new islanding detector*

Harmonic admittance, seen from a receiving point, has unique characteristics due to the fact that power grids comprise transmission lines, transformers, generators, loads, etc. When islanding occurs, the admittance changes dramatically. The newly developed islanding detector detects islanding by calculating harmonic admittance that is measured and analyzed using Wavelet Conversion. Figure 7 shows that image of the demonstration device to verify the ability of this islanding detection method.

Fig. 7. Image of the Newly Developed Islanding Detector (Device for Demonstration Tests)

Figure 8 indicates the result of a demonstration experiment. The top figure in Figure 8 shows the harmonic admittance being measured. We can see substantial change of admittance values during the course of islanding. The second figure shows the change rate of the above admittance value. We can see the large negative number exceeding threshold value, which has been set previously as -0.3 at the time of islanding. The bottom figure shows the activation signal, which indicates that the newly developed islanding detector detects islanding based on the excess of admittance change rate over threshold value.

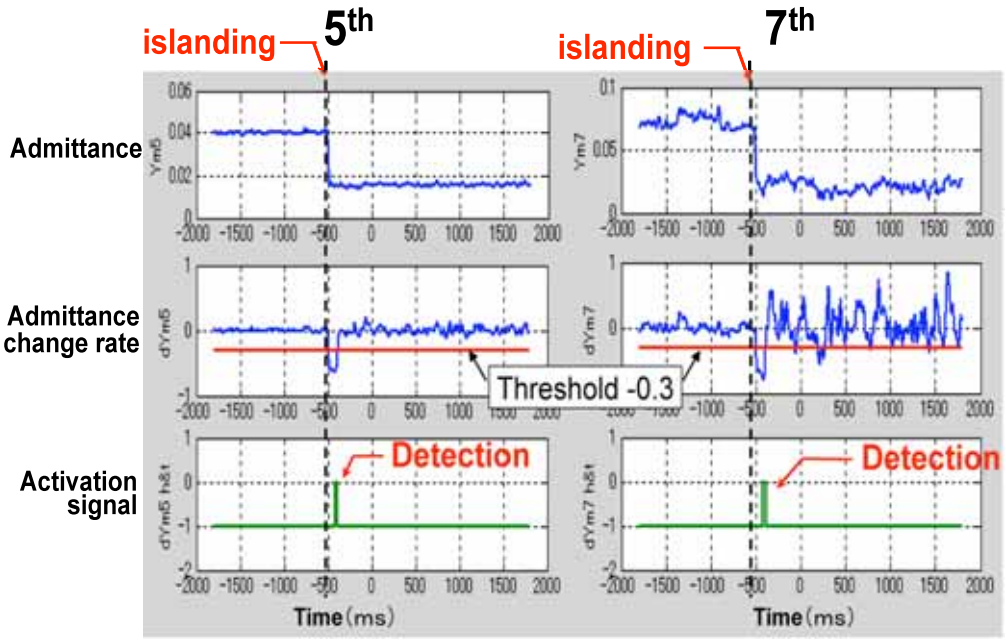


Fig. 8. Waveform of newly developed ID

(Above mentioned calculation is done for each order of harmonics, the left side of Figure 8 indicate the result of 5th harmonics, while the right figures indicate 7th harmonics.)

The results of our demonstration tests revealed that the newly developed islanding detector can detect islanding without fail by setting an appropriately determined threshold value, and that this islanding detector can not unnecessarily actuate even when the power grid experienced non-islanding disturbances.

This islanding detector would be applicable to other power grids if appropriate settings were made.

### *3.3 Evaluation of the problem of over voltage under clustered PV conditions*

Figure 10 shows the voltage profiles in the dummy distribution system at a certain time period. The horizontal axis denotes the points on the dummy distribution system at which the individual PV systems are connected, shown in Figure 9.

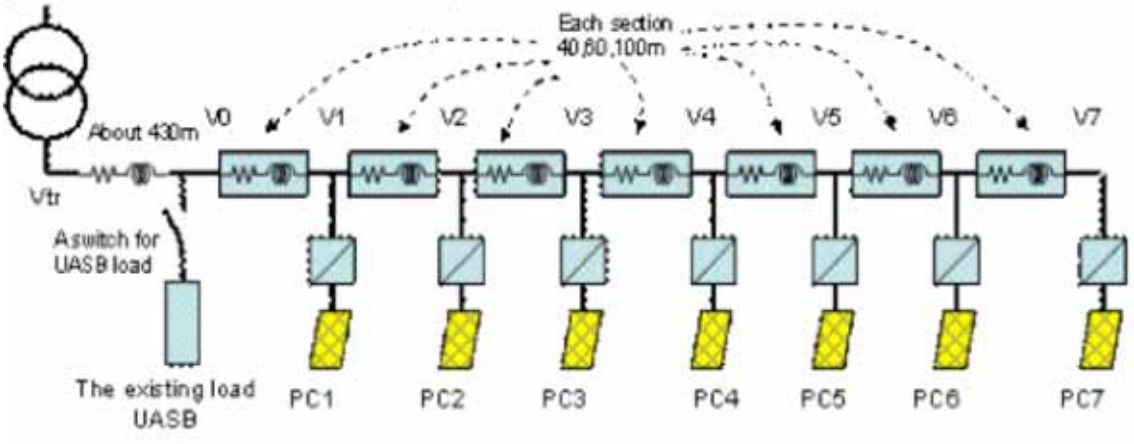


Fig. 9. Dummy Distribution System

In this figure, three curved lines are formed from the respective test cases in which the length of the dummy distribution line of each section was changed to 100m, 60m and 40m, which are denoted as I, II, and III, respectively. The three curved lines are all upwardly convex. They

indicate the voltage steady rise as the measured points approach the end of the distribution system.

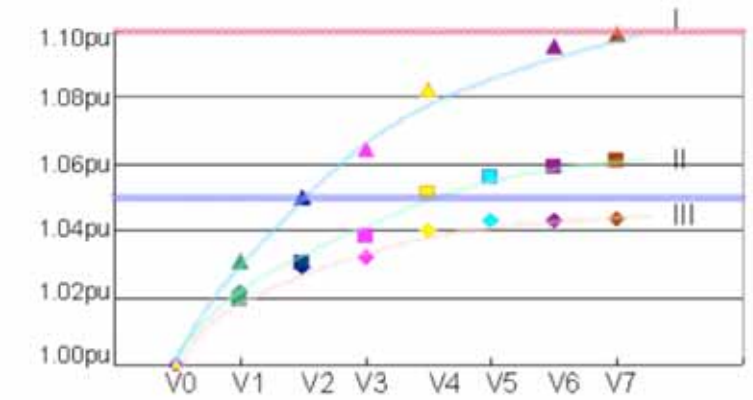


Fig. 10. Voltage profiles in the dummy distribution system for a certain time period

According to the voltage profile I, the voltage at the end of the distribution system, *V7*, is nearly 1.1pu. The upper limit of the voltage regulation for low-voltage (400V) power grids in Thailand is set to a standard value +10%. Thus, the voltage profile I is at the upper limit. This means that for a 400V low-voltage distribution system in Thailand to be controlled within the regulated voltage range, a maximum of seven 7kW PV systems can be connected at 100m intervals. In other words, PV with the total output capacity of approximately 50kW (7kW × the 7 PV systems) can be connected along a 700m (100m × 7 sections) long distribution system.

In the same manner, the total capacity of approximately 2.5MW (350kW×7 PV systems) can be connected along a 14km distribution system, in 22kV high-voltage system.

### *3.4 Development of a new voltage control system using a storage battery*

We attempted to develop a new voltage control system with a battery so as to minimize energy loss. Both functions of conventional automatic voltage regulator furnished with PV power conditioner and the newly developed voltage control system using storage battery, monitor the voltage at the grid connection point and act to suppress voltage rises. While the automatic voltage regulator reduces the PV output, the newly developed voltage control system leaves the PV output as it is, but controls the charging or discharging of the battery installed with PV.

Figure 11 indicates, from the top, the active power outputs of the PV power conditioners, the system voltages, the active power outputs and the reactive power outputs of the battery-inverter-converters. Seven curves indicate data of seven PV systems connecting one distribution line in series (as Figure 9).

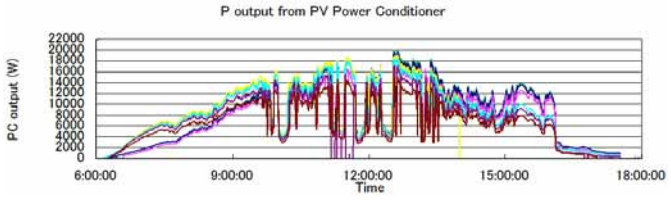

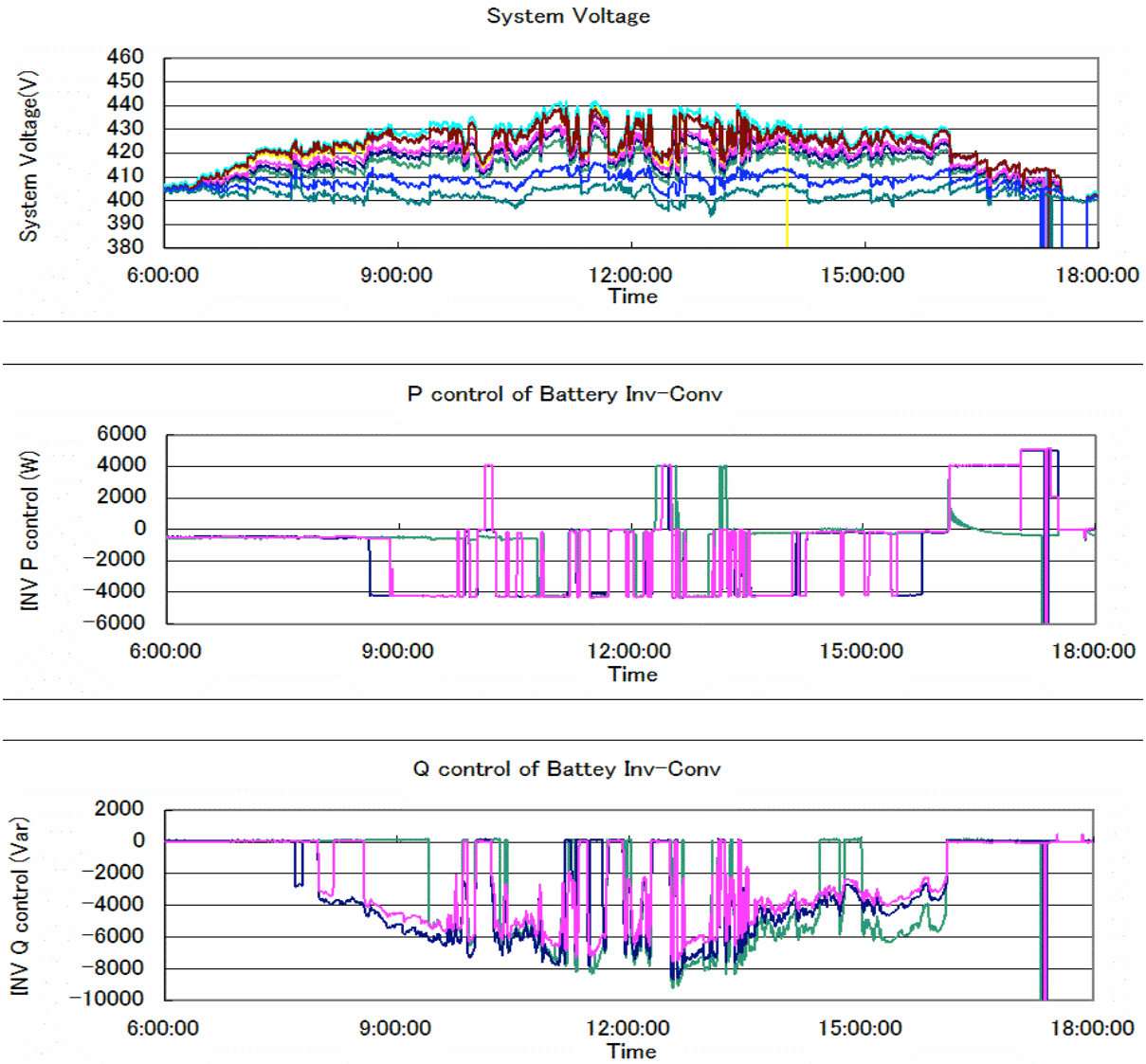


Fig. 11. Dummy Distribution System Data Obtained from 10:00 to 12:00 on May 29, 2006

During the daytime, when the PV output was greater and the system voltage was higher, the battery was charged to reduce the amount of active power flowing to the power grid. As a result, a rise in voltage was suppressed and controlled under 440V. In the morning and the evening, when PV output was smaller and system voltage was lower, the battery discharged the electricity charged during the daytime and outputted active power to the power grid. This allowed the solar energy to be used effectively.

In Figure 12, we can compare the output variation (shown by the pink curved lines) when the power conditioner with an automatic voltage regulator is used with the output variation (shown by the blue curved lines) when the newly developed voltage control system is used. The gap between the blue curved lines and the pink curved lines, which we can see in the evening, indicates the difference in energy output when the newly developed voltage control system is used versus when the conventional automatic voltage regulator is used. Naturally, the former system is able to utilize the solar energy effectively.

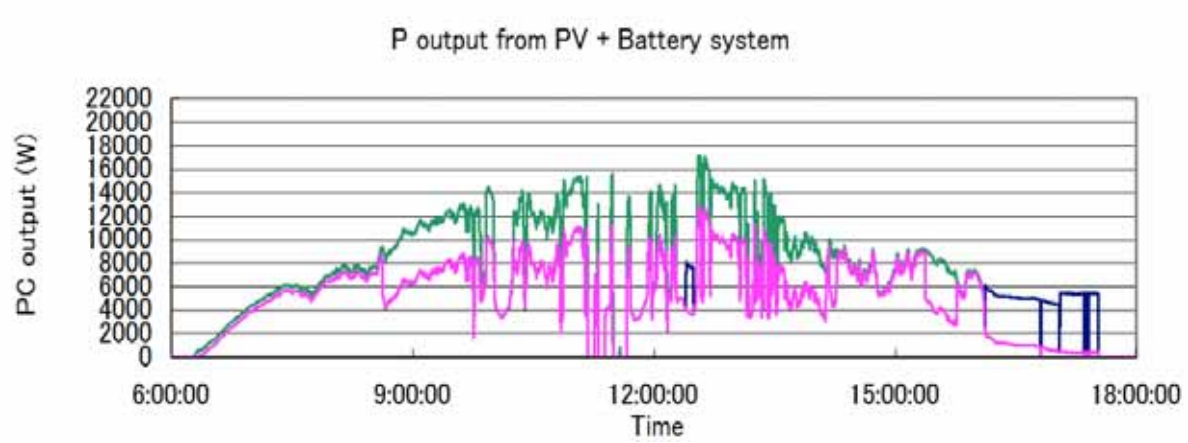


Fig. 12. Waveforms of PV+Battery System Output on May 29

A comparison between two output energies over one day of the pink curved line and the blue curved line can tell us that newly developed PV + Battery voltage control system can output larger energy by about 8kWh/day than PV applied the automatic voltage regulator.

### *3.5 Development of a new voltage control method for integrated PV system monitoring and control*

As shown in the previous chapter C, the range of the voltage rises differs, depending on the point at which it is connected to the distribution line. This will result in differences in the generation efficiency even when PV systems with the same specifications are installed. Figure 13 shows an unfairness problem in a conceptual image.

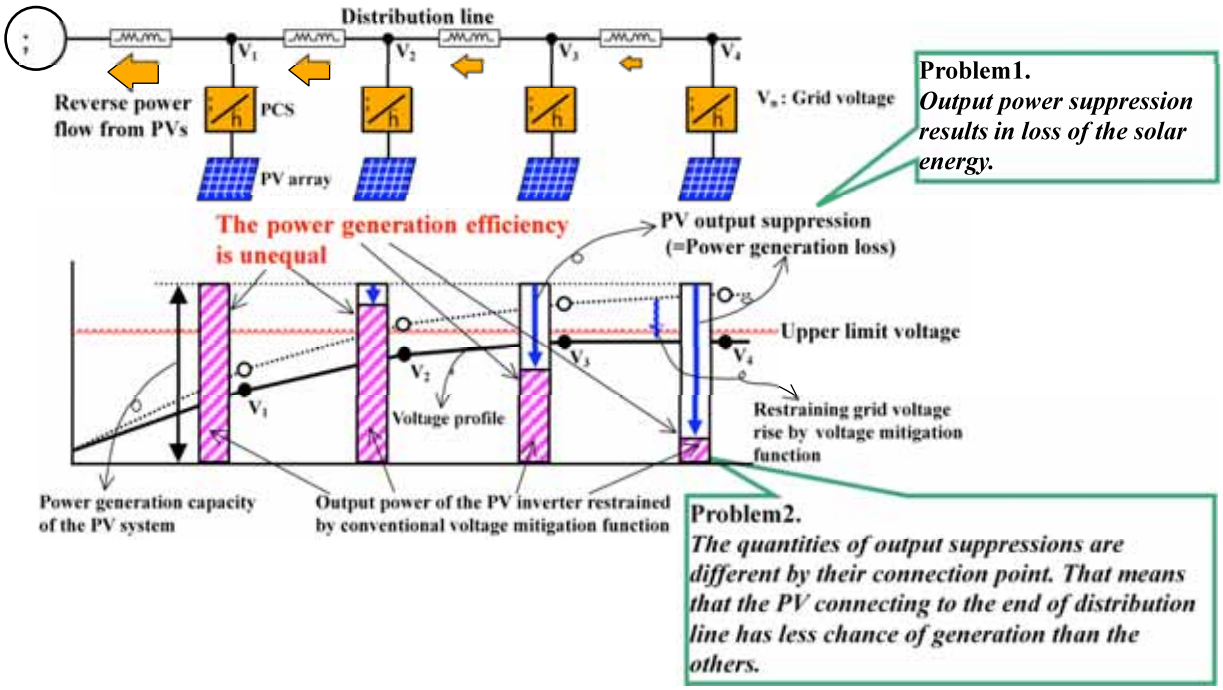


Fig. 13. Conceptual Image described unfairness problem

To solve the problems mentioned above, we developed and demonstrated a voltage suppression system that can centrally control multiple PV systems.

Figure 14 shows a function of the voltage suppression system that we have proposed. Based on the operating data collected, the central control system regularly calculates the output

commands for the optimal power output and transmits the commands to the individual power conditioners. The distribution line data are shown in Figure 15.

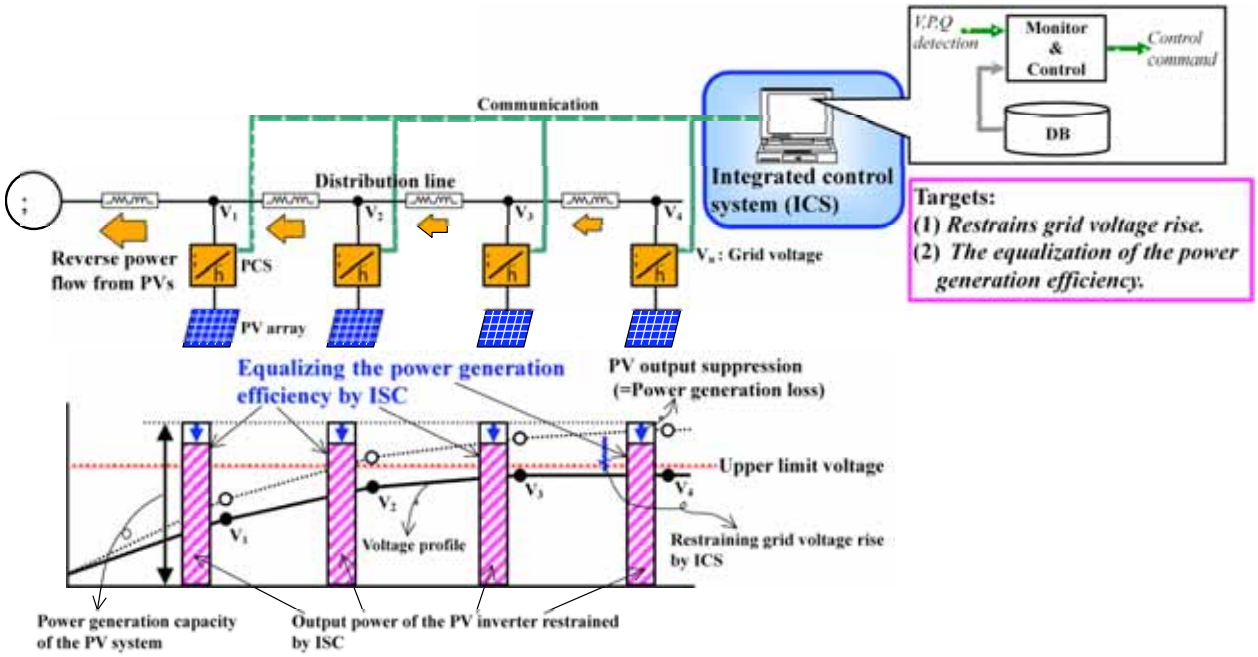


Fig. 14. Function of the proposed voltage suppression system

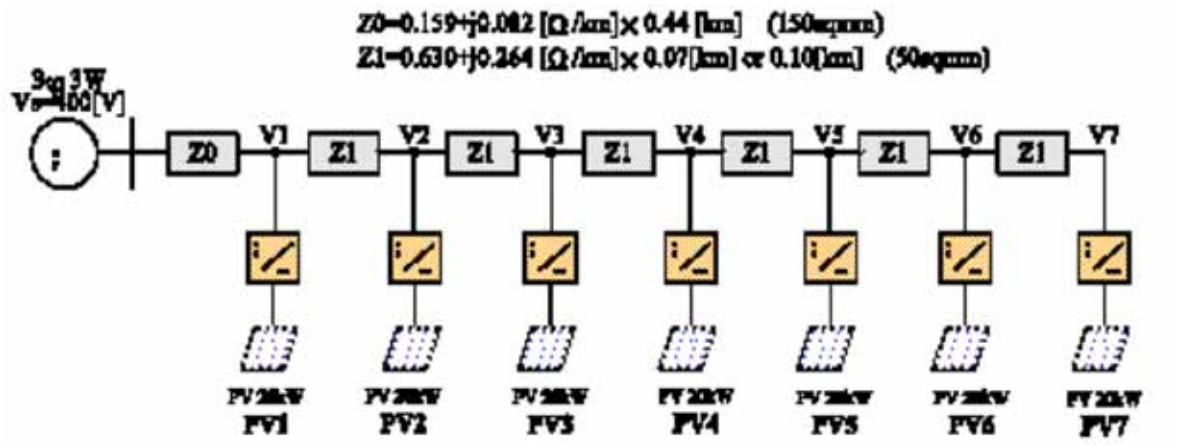


Fig. 15. Distribution line data (A power grid model)

For generally understanding the effect of this system, the results of simulation study describe in Figures 16 and 17. Figure 16 shows the generated output per day from the individual PV systems under the individual control. The vertical axis in the figure denotes the electric energy that could be produced relative to the amount of available solar irradiation presuming 100% power generation can be attained.

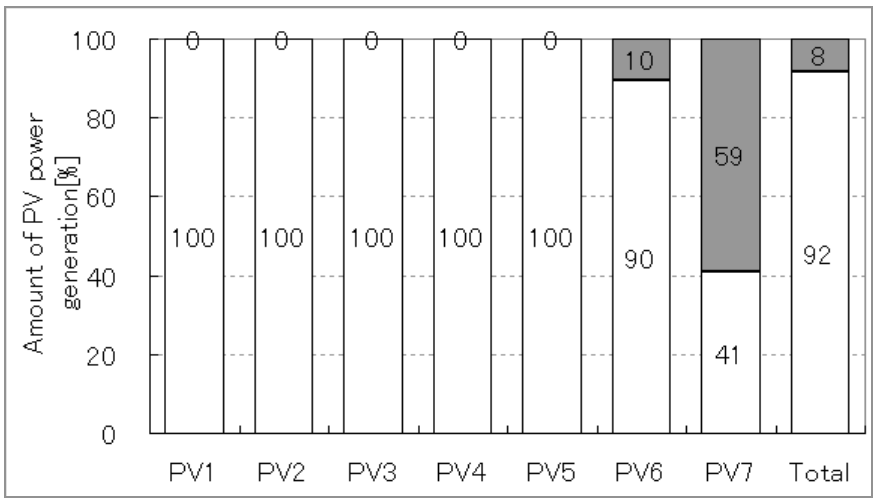


Fig. 16. The result of application (individual control)

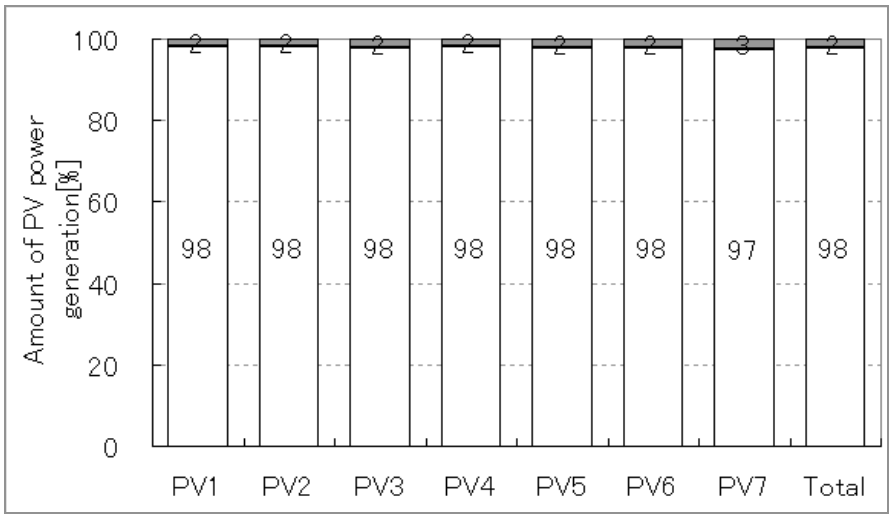


Fig. 17. The result of application (centralized control)

The shaded area represents the portion of electric energy loss caused by the voltage rise. According to the result, the generated output at PV 7 is 41%, less than half the power generated at PV 1. This indicates that even when PV systems with the same performance specifications are installed, there can be a large difference in their generating efficiencies, depending on the connection point.

On the other hand, Figure 17 shows the generated output per day from the individual PV systems under the centralized control. The centrally controlled system equally suppressed the power output of the PV systems when their voltage sensitivity exceeded a given level to eliminate the difference in the generation efficiencies caused when the voltage rises. Comparing this with the individual control method in Figure 16 clearly indicates the difference in generation efficiency. Specifically, the electric energy loss due to the rise in voltage was just 2%. The total generation efficiency also improved, compared with the existing individual control method.

## 4. CONCLUSIONS

1. We demonstrated the possibility that some existing active islanding methods may malfunction due to a phase difference between multiple active signals or load characteristics.

2. We developed a new islanding detector that caused no mutual interference by adopting wavelet transformation. We also conducted demonstrative experiments with the detector and concluded that it was a reliable islanding detection method.
3. We clarified over voltage of the grid line due to reverse power flow from PV systems and confirmed the effects attributable to distribution line length and the number of PV generators.
4. We developed a new voltage control system using a storage battery and confirmed that the new system could make better use of output power from PV systems at the same time keeping voltages within a permissible range in a grid line.
5. We developed a new voltage control method that integrates PV system monitoring and control. We then succeeded in maintaining a regulated voltage level and equalizing the efficiency in a PV system and also found that the new method could make total PV generation efficiency higher.

## 5. ACKNOWLEDGMENT

This project had funded by New Energy and Industrial Technology Development Organization (NEDO). Department of Industrial Works of Ministry of Industry, PEA and many other organizations in Thailand are greatly appreciated for their strong cooperation on this project.

## 6. REFERENCES

[1] IEA PVPS TASK-V: "Evaluation of islanding detection methods for photovoltaic utility-interactive power systems", Report IEA-PVPS T5-09, pp.22-25 (2002)
[2] Ishikawa, Kurokawa, Okada, and Takigawa: "Evaluation of operation characteristics when multiple PV systems connect to a power grid. –Study of voltage rise suppression function-", Japan Solar Energy Society, (2000).

## 7. BIOGRAPHY

**Kiyoshi Yoshida** has received the degree of B.S. and M.S. in Electrical Engineering from Kyoto University in 1982 and 1984 respectively. He joined the Kansai Electric Power Co., Inc in 1984 and has over 18 years experience in system planning, protection scheme designing and system stability analysis including deriving models and field testing in Japan and overseas. He has also been engaged in investigation of the trends in the deregulated power industries in Europe and the United States. Currently, he is working as a general manager, Office of Financing and Accounting of the company.

**Katsuhiko Kouchi** has received the degree of B.S. in Electrical Engineering from Keio University, Tokyo, Japan in 1981. He joined the Kansai Electric Power Co., Inc in 1981 and is currently working as a Project Manager of Power Engineering R&D Center. He is engaged in research of power quality and power system analysis.

**Yosuke Nakanishi** has received the degree of B.S. and M.S. in Electrical Engineering from Waseda University and Ph.D. from Tokyo Metropolitan University in 1978, 1980, and 1996 respectively. He joined Fuji Electric Co. in 1980 and is currently working as a general manager of Power System Analysis Gr., R&D Management Office, Fuji Electric Systems Co., Ltd.. He is a lecturer of Waseda University. His research interests include simulation and analysis of power systems and distribution power systems. He received a Prize Paper Award from IEEE Power Engineering Education committee 1991. He is a senior member of the IEE of Japan and a member of IEEE.

**Hiromitsu OTA** has received the degree of B.S. in Electrical Engineering from Tokyo Science University of Tokyo in 1991. He joined Fuji Electric Co., Ltd. in 1991 and is currently working as an engineer of photovoltaic generation system in Fuji Electric Systems Co., Ltd.

**Ryuichi Yokoyama** has received the degrees of B.S., M.S., and Ph.D. in electrical engineering from Waseda University, Tokyo, Japan, in 1968, 1970, and 1974 respectively. After working in Mitsubishi Research Institute, since 1978 he has been a professor in the Faculty of Technology of Tokyo Metropolitan University. Since 2007, he is a professor of the Graduate School of Environment and Energy Engineering in Waseda University. His fields of interests include planning, operation, control and optimization of large-scale systems and economic analysis and risk management of deregulated power markets. He is a senior member of IEEE and IEE of Japan, and a member of the Society of Instrument and Control Engineers (SICE) of Japan, and CIGRE.

Paper 08GM0037
Received February 1 2008

# 6. Energy Loss Minimization of Electricity Networks with Renewable Generation using FACTS

Xiao-Ping Zhang, Professor and Director, Institute for Energy Research and Policy, The University of Birmingham, UK.

*Abstract* - The UK Government is working towards a target of providing 10 % of UK electricity from renewable sources by 2010 with the aspiration that this will rise to 20% by 2020. However, the connection of any wind farm to the grid must comply with the Grid Code connection requirements. One of the requirements is that the wind farm must have the capabilities to operate within certain reactive power and voltage operating control range. This paper discusses the issue of energy loss minimization of electricity networks with large renewable wind generation. The impact of the special operating arrangements of large wind generation on energy loss of electricity networks is investigated. An optimal power flow (OPF) approach is proposed to minimize the energy loss of electricity network with reactive power and FACTS control, while satisfying the network operating voltage and thermal limits.

***Index Terms*--Reactive power compensation, Voltage control, Optimal power flow, Large on-shore wind farms, Large off-shore wind farms, Distributed generation, Renewable generation, Grid Code.**

## 1. INTRODUCTION

THE UK Government is working towards an ambitious target of providing 10 % of UK electricity from renewable sources by 2010, and 15% of UK electricity from renewable energy by 2015 with the aspiration that this will rise to 20% by 2020. A large part of this electricity will come from offshore wind farms. There are plans for around 6-7GW of electricity representing nearly 10 per cent of current generating capacity to be developed in the sea around the UK where most of such a development is focused on offshore wind farms. It is anticipated that in the future, other technologies such as wave and tidal power generation may also be developed.

The connection of any wind farm to the grid must comply with the UK Grid Code connection requirements. Large-scale on-shore and offshore wind farms are connected directly with the British transmission system. For the connection, one of the requirements is that the wind farm must have the capabilities to operate within certain reactive power and voltage operating control range. In this situation, new computational tool is required to evaluate the reactive power flow and voltage security and their impact on the transmission grid, to which the wind farm is connected.

This paper reviews the current practice of the grid code for large wind farm connections in the UK. Then analysis of the impact of the grid code arrangements on the reactive power and voltage security control is presented, and hence the consequence to energy losses of electricity transmission networks with large scale integration of on-shore and off-shore wind farms is evaluated. This paper proposes an optimal power flow (OPF) approach to minimize the electricity transmission network losses with large wind farms and investigate how to use FACTS devices to minimize network losses while satisfying the grid code connection requirement for reactive power control and the network operating voltage and thermal limits. The case studies are carried out on a 30-bus test network, and results are provided to show the effectiveness of the OPF approach for electricity network planning, design, operation and connection with FACTS technologies while satisfying the connection requirements for reactive power control and the voltage & current operating limits.

## 2. REVIEW OF REACTIVE POWER CONTROL REQUIREMENT FOR WIND FARM CONNECTION

Basically, the Grid Code provides specifications of procedures for both planning and operational purposes and covers both normal and exceptional circumstances. For a wind farm to be connected to the transmission/distribution network, it must comply with the Grid Code, including the requirements of reactive power range, voltage range and control, fault ride through capability, frequency range and frequency control, etc. Among those mentioned above, the voltage and reactive power control requirements are of great importance.

### *2.1 Reactive Power Ranges*

Current Grid Code requirements state that any Medium or Large Wind Farms must provide a reactive power capability of 0.95 lead / lag at its Grid Entry Point [1]. According to the current grid code in the UK, wind farms must control the reactive power at the connection point. For instance, for a large on-shore connected with the transmission network, the grid may require that over the normal active power operating range of the on-shore wind farm, a reactive power capability of 0.95 power factor lagging to 0.95 power factor leading (based on full output power) should be available at the connection point. Such a requirement is also extended to the requirement with the connection of offshore wind farms [1].

According to the Grid Code, each Offshore Power Park Module should be required to be capable of maintaining [1]:

1) unity power factor for LV connections
2) a power factor equivalent to unity at the LV for HV connections at the Offshore Grid Entry Point. A tolerance of ± 5% of Rated MW in MVAr would be allowed either side of the specified power factor. The Offshore Generator will have the option to provide a greater reactive capability than the minimum specified under the Grid Code.

### *2.2 Voltage Ranges and Control*

Wind farms must remain connected to the transmission system when the voltage at the connection point is within the normal and exceptional voltage ranges, for example +/- 5% of nominal value for normal condition and +/-10% for abnormal condition. While the reactive power output from the wind farm should be fully available within the voltage operating ranges.

### *2.3 Reactive Power Control for Wind Farm Connection*

It is known that most wind farms have installed either the fixed speed induction generator (FSIG) or the Doubly Fed induction generator (DFIG), and normally they are operated at the unity power factor. Normally their ability of the voltage and reactive power controls at the connection points may be very limited, and installation of additional VARs devices is required to fulfill the Grid Code requirement for wind farms.

VARs devices such as mechanically switched capacitors/reactors, SVCs and STATCOM. The VARs devices can be either installed at an individual wind turbine level or at a substation level, depending on economic, technical and environmental constraints.

It has been recognized that in order to meet the connection requirements in terms of the control of both reactive power/power factor and voltage operation ranges at the connection point, there is a requirement of optimal planning and allocation of the reactive power compensation for reactive power and voltage control within the wind farm network (and the off-shore transmission network for the case of off-shore wind farm.). It is assumed in this paper that the reactive power control resources are available to control the

reactive power in such a way that the power factor at the connection point or Grid Entry point with the transmission network can be satisfied.

For a power network, the reactive power and voltage controls can be achieved through the control of the following variables

- Power transformer tap changer
- Wind turbine generator power factor
- Reactive power compensation devices such as SVC and STATCOM.

## 3. REPRESENTATION OF LARGE WIND FARMS IN ENERGY LOSS ANALYSIS OF ELECTRICITY TRANSMISSION NETWORK

In the light of the grid code requirement for large wind farms connected with the electricity transmission network, there are three particular situations to be studied for energy loss analysis of the electricity transmission network where the wind farm at the Grid Entry point is represented by a virtual power plant who can provide a reactive power capability of 0.95 lead / lag while the voltage at the Grid Entry point should be within the operating limits. In order to simply the analysis, such a virtual power plant model of the wind farm is discussed in three different situations.

### *3.1 Unity Power Factor Control at the Grid Entry Point*

For this control scheme, the power factor at the Grid Entry point is controlled to zero. In other words, in this control scheme, the reactive power exchange between the wind farm and transmission network at the Grid Entry point is zero while the voltage at the connection point is within the permissible limits.

### *3.2 Lagging Power Factor Control at the Grid Entry Point*

For this control scheme, the power injection at the Grid Entry point has a lagging power factor. In addition to this requirement, the voltage at the Grid Entry point is constrained to the permissible limits.

### *3.3 Leading Power Factor Control at the Grid Entry Point*

For this control scheme, the power injection at the connection point has a leading power factor. In addition to this requirement, the voltage at the Grid Entry point is within the permissible limits.

## 4. ENERGY LOSS MINIMIZATION OF ELECTRICITY TRANSMISSION NETWORK WITHOUT/WITH LARGE WIND FARMS

### *4.1 Energy Loss Minimization of Electricity Transmission Network without Large Wind Farms*

The objective of an optimal reactive power and voltage control for the minimization of energy losses of the electricity transmission network with conventional power plants is to minimize the total active power losses through the optimization of generator active powers, generator reactive powers, transformer tap ratios while subjecting to various power flow constraints, operating constraints. The optimal reactive power and voltage control for energy loss minimization may be given by

Objective: $Min\,(P_{loss})$ (1)

Subject to:

*Power flow constraints:*

$$Pg_i - Pd_i - P_i(V,\theta,T) = DP_i(x) = 0 \quad (2)$$

$$Qg_i - Qd_i - Q_i(V,\theta,T) = DQ_i(x) = 0 \quad (3)$$

*i = 1,2,…, N*

*Operating and control constraints:*

$$h_j^{\min} \le h_j(x) \le h_j^{\max} \qquad \text{j = 1, 2,…,Nh} \quad (4)$$

where

$x = [V,\theta,T,Qg]^T$

*Pg* bus active generation
*Qg* bus reactive generation
*Pd* bus active load
*Qd* bus reactive load
*V* bus voltage magnitude vector
$\theta$ bus angle vector
*T* tap ratio vector of transformers
$DP_i$, bus active power mismatch
$DQ_i$ bus reactive power mismatch
$h(x)$ include reactive powers of generators, transmission line power flows, tap ratios of transformers
$h^{\min}$ and $h^{\max}$ are lower bound vector and upper bound vector, respectively, for inequality constraints including reactive generation limits, transmission line thermal limits, transformer tap ratio limits and bus voltage limits, etc.
*Ng* the total number of generators
*N* the total number of buses
*Nh* the total number of double-side inequality constraints

### *4.2 Energy Loss Minimization of Electricity Transmission Network with Large Wind Farms*

With the incorporation of wind farms in the energy loss minimization of electricity transmission network, the power flow equations in (2) and (3) should be augmented to reflect the power injections from wind farms:

$$Pg_i + Pwind_i - Pd_i - P_i(V,\theta,T) = DP_i(x) = 0 \quad (5)$$

$$Qg_i + Qwind_i - Qd_i - Q_i(V,\theta,T) = DQ_i(x) = 0 \quad (6)$$

where $Pwind_i$ and $Qwind_i$ are active and reactive power injections from the Wind Farm connected at the Grid Entry point of bus *i*, respectively.

### *4.3 Energy Loss Minimization of Electricity Transmission Network with Large Wind Farms using FACTS Controls*

The objective of an optimal reactive power compensation and voltage control problem may be the minimization of the total active power losses plus reactive power compensation costs through the optimization of generator reactive power outputs, FACTS devices, transformer tap ratios while subjecting to various power flow constraints, operating constraints. Such an optimal problem may be given by

Objective: $Min(P_{loss})$ (7)

Subject to:

Power flow constraints:

$$Pg_i + Pwind_i - Pd_i - P_i(V,\theta,V_{FACTS},\theta_{FACTS},T) = DP_i(x) = 0 \quad (8)$$

$$
\begin{aligned}
& Qg_i + Qwind_i - Qd_i \\
& + Qc_i(V,\theta,V_{FACTS},\theta_{FACTS}) \\
& - Qr_i(V,\theta,V_{FACTS},\theta_{FACTS}) \\
& - Q_i(V,\theta,V_{FACTS},\theta_{FACTS},T) = DQ_i(x) = 0
\end{aligned} \tag{9}
$$

$i = 1,2,\ldots, N$

Operating and control constraints:

$$h_j^{\min} \le h_j(x) \le h_j^{\max} \qquad j = 1, 2,\ldots,Nh \tag{10}$$

where

$x = [V,\theta,V_{FACTS},\theta_{FACTS},T,Qg,Qr,Qc]^T$

*Pg* bus active generation

*Qg* bus reactive generation

$Pwind_i$ active and reactive power injectionfrom the Wind Farm connected at the Grid Entry point of bus *i*.

$Qwind_i$ reactive power injection from the Wind Farm connected at the Grid Entry point of bus *i*

*Pd* bus active load

*Qd* bus reactive load

*V* bus voltage magnitude vector

$\theta$ bus angle vector

*T* tap ratio vector of transformers

$DP_i$, bus active power mismatch

$DQ_i$ bus reactive power mismatch

$h(x)$ active and reactive powers of generators, transmission line power flows, tap ratios oftransformers

$h^{\min}, h^{\max}$ lower bound vector and upper bound vector, respectively, for inequality constraints including active and reactive generation limits, transmission line thermal limits, transformer tap ratio limits and bus voltage limits, etc.

*Ng* the total number of generators

*N* the total number of buses

*Nh* the total number of double-side inequality constraints

## 5. SOLUTION OF ENERGY LOSS MINIMIZATION OF ELECTRICITY TRANSMISSION NETWORK

### *5.1 Nonlinear Interior Point Methods*

According to the nonlinear interior point methods proposed in [2], the above problems in Section IV can be solved by the following sets of linearized Newton equations

$$
\begin{bmatrix}
-\Pi l^{-1} Sl & 0 & -\nabla h & 0 \\
0 & \Pi u^{-1} Su & -\nabla h & 0 \\
-\nabla h^T & -\nabla h^T & H & -J^T \\
0 & 0 & -J & 0
\end{bmatrix}
\begin{bmatrix}
\Delta \pi l \\ \Delta \pi u \\ \Delta x \\ \Delta \lambda
\end{bmatrix}
= \begin{bmatrix}
-\nabla_{\pi l} L_\mu - \Pi l^{-1} \nabla_{Sl} L_\mu \\
-\nabla_{\pi u} L_\mu - \Pi u^{-1} \nabla_{Su} L_\mu \\
-\nabla_x L_\mu \\
-\nabla_\lambda L_\mu
\end{bmatrix} \tag{11}
$$

$$
\Delta sl = \Pi l^{-1}(\nabla_{sl} L_\mu - Sl \Delta \pi l) \tag{12}
$$

$$\Delta su = \Pi u^{-1}(-\nabla_{su} L_{\mu} - Su\Delta \pi u) \tag{13}$$

where $sl$ and $su$ are slack variables for inequalities. $\pi l$ and $\pi u$ are dual variables for inequalities. $\lambda$ are dual variables for equalities.

$$H(x,\lambda,\pi l,\pi u) = \nabla^2 f(x) - \lambda \nabla^2 g(x) - (\pi l + \pi u)\nabla^2 h(x) ,$$

$$J(x) = \left[\frac{\partial \Delta P(x)}{\partial x}, \frac{\partial \Delta Q(x)}{\partial x}\right], g(x) = \begin{bmatrix}\Delta P(x) \\ \Delta Q(x)\end{bmatrix}, \lambda = \begin{bmatrix}\lambda_p \\ \lambda_q\end{bmatrix}, Sl = diag(sl_j), Su = diag(su_j), \Pi l = diag(\pi l_j), \Pi u = diag(\pi u_j)$$

### *5.2 General Procedure of the Solution*

Step 0: Select possible locations for FACTS
Step 1: Get system data for transmission lines, transformers, generators, Wind Farms
Step 2: Solve the problems in Section IV by the nonlinear interior point method in (11) - (13).
Step 3: Output

(a) Optimal transformer tap settings
(b) Minimized power losses
(c) Optimal VAR location and requirement
(d) Voltage profile of the system
(e) Power flow distribution of the system

## 6. NUMERICAL EXAMPLES

### *6.1 Test Systems*

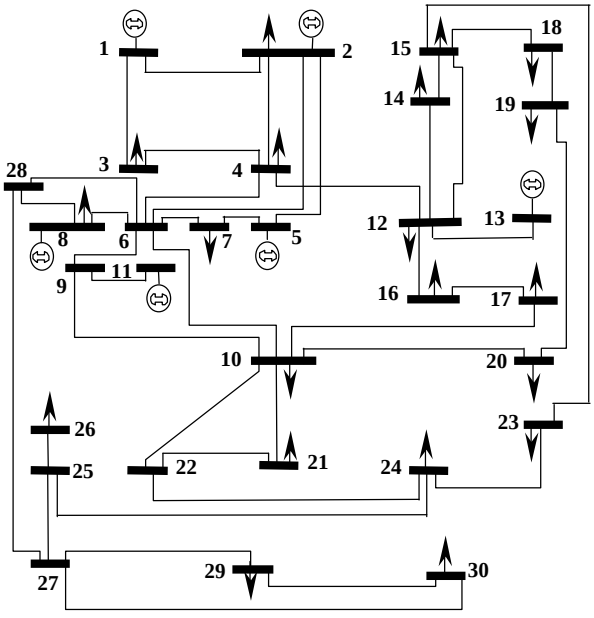


Fig. 1. Single-line circuit diagram of the IEEE 30-bus system.

Test cases in this paper are carried out on the IEEE 30-bus system. The IEEE 30-bus system as shown in Fig. 1 has 6 generators, 4 OLTC transformers and 37 transmission lines. For all cases in this paper, the convergence tolerances are 5.0e-4 for complementary gap and 1.0e-4 (0.01MW/Mvar) for maximal absolute bus power mismatch, respectively. It is assumed that the total active power generation of the

generator at bus 2 is 600 MW; the total active power generation at buses 8, 11 and 13 is equal to 100 MW while the generator at bus 1 balances the rest of the demand.

Based on the IEEE 30-bus system, energy loss analysis will be carried out over there different scenarios: (a) energy losses of the electricity transmission network without optimal reactive control; (b) energy losses of the electricity transmission network with optimal reactive power control; (c) the electricity transmission network with optimal reactive power control and FACTS control. In the following, energy loss analysis on these three scenarios will be presented.

### *6.2 Energy Losses of the Electricity Transmission Network with Optimal Reactive Power Control*

**In this scenario, there are four cases to be investigated:**

*Case 1:* This is a base case of the electricity network with conventional power plants where all the power plants can maintain the terminal voltages to their settings of 1.0 p.u.

*Case 2:* This is a case of the electricity network with conventional power plants where all the power plants can maintain the terminal voltages to their voltage limits using reactive power and transformer controls.

*Case 3:* This is similar to case 2 except that the generator at bus 2 is replaced by an offshore wind farm where the power factor at the Grid Entry point is 0.95 leading.

*Case 4:* This is similar to case 2 except that a unity power factor is maintained at the Grid Entry point.

*Case 5:* This is similar to case 2 except that the power factor at the Grid Entry point is 0.95 lagging.

For Cases 2-5, power losses are minimized through reactive power control by generators and tap ratio settings of transformers. For Cases 3-5, the total power generation from the wind farm connected at bus 2 represents around 20% of the total generation.

TABLE I
ENERGY LOSS RESULTS OF CASES 1-5 WITHOUT/WITH OPTIMAL REACTIVE POWER CONTROL

| Cases | Case 1 (Base Case) | Case 2 | Case 3 | Case 4 | Case 5 |
|---|---|---|---|---|---|
| Power Losses (MW) | 14.35 | 12.38 | 12.38 | 12.48 | 12.65 |
| Power Loss Reduction with respect to Base Case without Optimal Control | - | 13.73% | 13.73% | 13.03% | 11.85% |

The energy loss results of Cases 1-5 are presented in Table I. From Table I, it can be seen that with the coordinated optimal control of reactive powers of generators and tap ratios of transformers, power losses can be reduced significantly by over 10% with respect to that of base case without optimal control. Furthermore, in comparison of Cases 3-5 to Case 2, with the connection of the large-scale wind farm into electricity network, it is likely that power losses will be increased due to the Grid Code requirement.

### *6.3 Energy Losses of the Electricity Transmission Network with Coordinated Control of Reactive Power Generation, Transformers and FACTS*

Based on Cases 2-5, it has been found that there are the largest sensitivities at buses 23, 24, 26, 30. Cases 6-9 are carried out with FACTS control, which are corresponding to Cases 2-5, respectively where FACTS devices - STATCOMs or SVCs are placed at buses 23, 24, 26, 30. The results are presented in Table II.

TABLE II
ENERGY LOSS RESULTS OF CASES 6-9 WITH OPTIMAL REACTIVE POWER AND FACTS CONTROL

| | Case 6 | Case 7 | Case 8 | Case 9 |
|---|---|---|---|---|
| FACTS locations | Buses 23, 24, 26, 30 | Buses 23, 24, 26, 30 | Buses 23, 24, 26, 30 | Buses 23, 24, 26, 30 |
| Power Losses (MW) | 12.13 | 12.13 | 12.22 | 12.39 |
| Power Loss Reduction with respect to that without FACTS | 2.0% | 2.0% | 2.1% | 2.1% |

From Table II, it can be seen clearly that the reactive compensation by shunt FACTS devices is useful in the power loss minimization. Comparing the results of Table II with that of Table I, it is obvious that the reactive power control of generators plays a very important role in power loss minimization where such a control is very effective. However, the reactive power control for power loss minimization with generators in deregulated environments becomes difficult. It is now at a stage for power engineers to re-think the role of reactive power control by generators in power loss minimization, as CO2 reduction becomes a worldwide concern. In light of this, the reactive control for power loss minimization should be reflected in electricity market design and hence market efficiency.

In comparison of Cases 6-9, with the connection of the large-scale wind farm into electricity network, it is likely that power losses will be increased due to the Grid Code requirement. Due to the fact that large offshore wind farms are equipped with advanced FACTS devices for reactive control and wind turbines have also reactive control capability, it is possible that in the future a large offshore wind farm can be operated very much like a conventional power plant with integrated advanced communication and control technologies.

## 7. CONCLUSIONS

This paper has reviewed the current practice of the grid code for large wind farm connection in the UK. Then analysis of the impact of the grid code arrangements on the reactive power and voltage security control has been presented. This paper has proposed an optimal power flow (OPF) approach to minimize the electricity transmission network losses with large wind farms and investigate how to use FACTS devices to minimize network losses while satisfying the grid code connection requirement for reactive power control and the network operating voltage and thermal limits. The consequence to energy losses of electricity transmission networks with large-scale integration of large wind farms has been evaluated. The case studies have been carried out on a 30-bus test network, and results have been provided to show the effectiveness of the OPF approach for electricity network operation with FACTS technologies while satisfying the connection requirements for reactive power control and the voltage & current operating limits. With the connection of large-scale wind farms into electricity network in the replacement of conventional power plants, it is likely that power losses will be increased due to the Grid Code requirement. However, with the advance in communication and control technologies, it is possible to operate a large wind farm like a conventional power plant.

## 8. REFERENCES

[1]. OFGEM Grid Code Subgroup, "Recommendations for the application of Grid Code technical requirements to offshore electricity transmission networks," OFGEM, London, UK. 7th Nov. 2007.

[2]. X.-P. Zhang, E. Handschin, and M. M. Yao, “Modeling of the generalized unified power flow controller (GUPFC) in a nonlinear interior point OPF,” *IEEE Trans. on Power Systems*, vol. 16, no. 3, pp.367-373, Aug. 2001

## 9. BIOGRAPHIES

**Xiao-Ping Zhang** (M’95, SM’06) received the BEng., MSc. and PhD degrees in electrical engineering from Southeast University in 1988, 1990, 1993, respectively. He worked at NARI, Ministry of Electric Power, China on EMS/DMS advanced application software research and development between 1993 and 1998. He was visiting UMIST from 1998 to 1999. He was an Alexander-von-Humboldt Research Fellow with the University of Dortmund, Germany from 1999 to 2000. He was a lecturer, senior lecturer and then an associate professor at the University of Warwick, UK till early 2007. Currently he is a Reader at the University of Birmingham, England, UK. He is also Director of the Institute for Energy Research and Policy. He is a coauthor of the monograph "Flexible AC Transmission Systems: Modeling and Control" published in 2006. He is a senior member of the IEEE and a member of CIGRE.

Received 1 February 2008
Paper 08GM0402

# 7. Loss Reduction From Use of New SVC Model

Jizhong Zhu, Davis Hwang, and Ali Sadjadpour, AREVA T&D Inc., Redmond, WA, USA.

***Abstract*--** This paper presents an application of a flexible AC transmission system (FACTS) device as additional control in reactive power (VAR) optimization problem and analyzes the impact on system loss minimization. The adopted FACTS device is a new static VAR compensator (SVC). The general SVC consists of internal devices, and local devices, and the operation mode of the general SVC model is voltage control mode only. The new SVC model controls local, remote, internal and external devices simultaneously. It has two modes of operation: (1) Voltage control mode; and (2) Q control mode. This paper analyzes the functions of the new SVC, and implements them in the practical power systems. The impact of VAR optimization with new SVC model on loss minimization is also discussed by comparing it with VAR optimization with general SVC model as well as VAR optimization without SVC model.

***Index Terms***—Power systems, loss minimization, VAR optimization, flexible AC transmission system (FACTS), static VAR compensators (SVC), performance index, power system control

## 1. INTRODUCTION

The purpose of reactive power (VAR) optimization is mainly to improve the voltage profile in the system and to minimize the real power transmission loss while satisfying the unit and system constraints. This goal is achieved by proper adjustment of reactive power control variables like generator bus voltage magnitudes, transformer tap settings, reactive power generation of the devices such as capacitor, reactor, synchronous condensers and the static VAR compensators (SVC), etc [1-2].

To solve the VAR optimization problem, a number of optimization techniques [1-14] have been proposed, which include the Gradient method, Non-linear Programming (NLP), Quadratic Programming (QP), Linear programming (LP), Interior point (IP) method, and Genetic Algorithm (GA).

This paper doesn't focus on the optimization algorithm to implement VAR optimization. It considers a new SVC model in VAR optimization formulation and analyzes the impact on system loss minimization.

As power transfer grows, the power system can become increasingly more difficult to operate, and the system becomes more insecure with unscheduled power flows and higher losses. The rapid development of self-commutated semiconductor devices, have made it possible to design power electronic equipments. These equipments are well known as Flexible AC Transmission systems (FACTS) devices [1-2]. The FACTS controllers, such as Static VAR Compensator (SVC), Thyristor Controlled Series Compensator (TCSC) and Static Synchronous Compensator (STATCOM) can increase or reduce reactive power according to the demand of reactive power in the network to improve the stability, reduces system loss and also improves the load ability of the system.

The existing SVC model only consists of internal devices, which are part of the SVC, and local devices, which are installed at the same substation as the SVC. The general operation mode of the existing SVC is voltage control mode. The presented new SVC model controls local, remote, internal and external devices simultaneously. It has two modes of operation: (1) Voltage control mode; and (2) Q control mode.

This paper analyzes the functions of the new SVC, and implements them in the practical power systems. The impact of VAR optimization with new SVC model on loss minimization is

also discussed by comparing it with VAR optimization with general SVC model as well as VAR optimization without SVC model.

## 2. VAR OPTIMIZATION WITH SVC CONTROL

The formulation of VAR optimization with SVC control can be expressed as follow.

### *2.1 Objective function*

The objective function of the VAR optimization is loss minimization.

$$MinF = P_L \tag{1}$$

### *2.2 Constraints*

The linear and nonlinear constraints that include voltage, flows, real generation, reactive sources and transformer taps are considered as follows.

$$P_{Gi} - P_{Di} = V_i \sum_{j=1}^{NB} V_j \left( G_{ij} \cos\theta_{ij} + B_{ij} \sin\theta_{ij} \right) \quad i = 1,2,..., N_B - 1 \tag{2}$$

$$Q_{Gi} + Q_{SVCi} - Q_{Di} = V_i \sum_{j=1}^{NB} V_j \left( G_{ij} \sin\theta_{ij} - B_{ij} \cos\theta_{ij} \right) \quad i = 1,2,..., N_B - 1 \tag{3}$$

$$P_{Gi\min} \le P_{Gi} \le P_{Gi\max}, \qquad i \in NG \tag{4}$$

$$Q_{Gi\min} \le Q_{Gi} \le Q_{Gi\max}, \qquad i \in NG \tag{5}$$

$$Q_{SVCw\min} \le Q_{SVCw} \le Q_{SVCw\max}, \; w \in NSVC \tag{6}$$

$$V_{Gi\min} \le V_{Gi} \le V_{Gi\max}, \qquad i \in NG \tag{7}$$

$$V_{Dk\min} \le V_{Dk} \le V_{Dk\max}, \qquad k \in ND \tag{8}$$

$$T_{j\min} \le T_j \le T_{j\max}, \qquad j \in NT \tag{9}$$

$$P_{ij\min} \le P_{ij} \le P_{ij\max}, \qquad ij \in NL \tag{10}$$

where

$P_{Gi}$: real power generation of generator i;
$P_{Di}$: real power load at load bus i;
$Q_{Di}$: reactive power load at load bus i;
$V_{Gi}$: the voltage magnitude at generator bus i;
$V_{Dk}$: voltage magnitude at load bus k;
$Q_{Gi}$: VAR generation of generator i;
$Q_{SVCw}$: VAR output of the SVC w;
$P_{ij}$: real power flow through the transmission line ij;
$T$: transformer tap position;
$\theta$: voltage angle;
$P_L$: system real power loss;
$NG$: set of generation buses;
$NT$: set of transformer branches;
$NL$: set of transmission branches;

*ND*: set of load buses;
*NB:* set of total network buses;
*NSVC:* set of total SVCs;

The subscripts "*min*" and "*max*" stand for the lower and upper bounds of a constraint, respectively.

## 3. NEW SVC MODEL

### *3.1 Control Devices of New SVC*

Generally, SVC is a shunt connected static VAR generator/load whose output is adjusted to exchange capacitive or inductive current so as to maintain or control specific power system variable. Typically, the power system control variable is the terminal bus voltage. There are two popular configurations of SVC. One is a fixed capacitor (FC) and thyristor controlled reactor (TCR) configuration and the other one is a thyristor switched capacitor (TSC) and TCR configuration.

The new SVC model controls local, remote, internal and external devices simultaneously.

The definitions of internal, external, local and remote devices are as follows.

*Internal device* is part of the SVC (at the same voltage level under the same station as the SVC) and consists of any combination of thyristor controlled reactor, fixed shunt capacitor or breaker switched shunt capacitor

*External device* is a device outside of the SVC that could be installed either at the local substation or a remote substation. These devices are breaker switched and could be shunt capacitors or shunt reactors.

*Local device* is a device installed at the same substation as the SVC.

*Remote device* is a device installed at a different substation from the SVC.

Figure 1 shows these devices in the new SVC model.

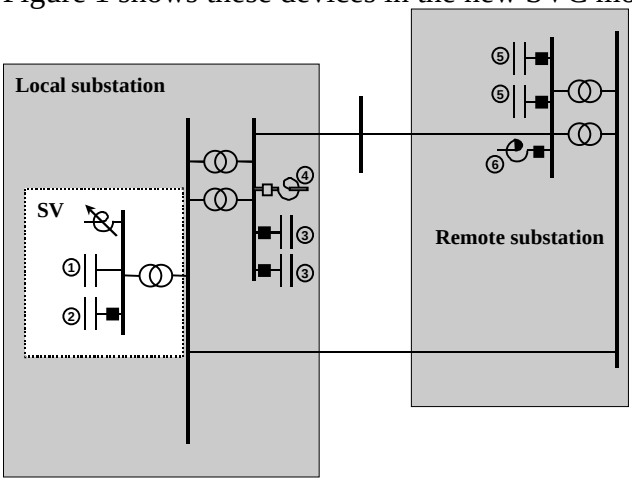


Figure 1. Internal, External, Local and Remote Control Devices of SVC

As shown in Figure 1, the number labels (1-6) represent respectively the following SVC contro devices:

1. Internal fixed capacitor.
2. Internal switched capacitor
3. Local, external breaker switched capacitors

4. Local, external breaker switched reactor
5. Remote, external breaker switched capacitors
6. Remote, external breaker switched reactor

### *3.2 Characteristic of New SVC*

When switching external devices, the SVC uses a reactive power threshold or voltage threshold that is within the SVC maximum and minimum limits. The following Figure 2 illustrates this.

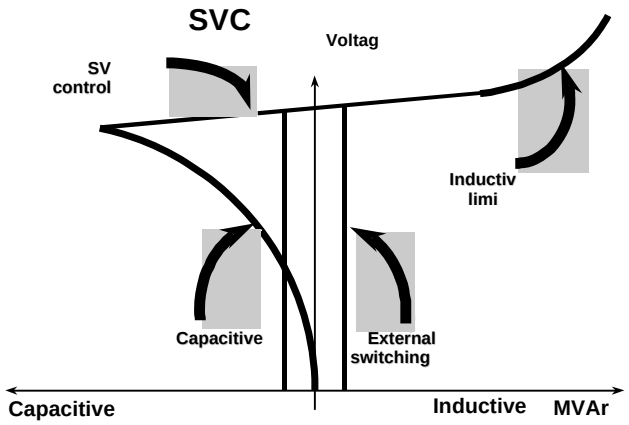


Figure 2. SVC Characteristics

The reason for the external device switching is to preserve reactive reserve at the SVC in order to keep the SVC within its control range. In other words, a SVC may be required to absorb or produce reactive power following a contingency and it is desirable to keep it at a small MVAr output to cater for a number of contingency possibilities. This can be achieved by switching external (or internal) devices when the SVC exceeds a given amount of MVAr inductive or capacitive.

Assuming that the device that is switched does not cause the SVC output change by more than 80 MVAr, then the SVC will remain within the MVAr thresholds and will retain voltage control with sufficient reactive reserve. In this example, the actual SVC limits are 250 MVAr inductive and 250 MVAr capacitive. If all external and internal devices have been switched and the SVC reaches its actual limit, it will lose voltage control and become a fixed admittance.

### *3.3 Operation Mode of the SVC*

The existing SVC model has only voltage control mode, but the new SVC has two modes of operation:

1. Voltage control mode. The SVC monitors a voltage and adjusts the reactive power output to maintain a voltage set point by switching external devices.
2. Q control mode. The SVC maintains a constant reactive power output according to a Q set point as long as the regulated voltage remains within a predefined voltage range. If the regulated voltage goes outside the predefined range, then the SVC automatically switches to voltage control mode and controls the regulated voltage using the maximum or minimum threshold limit of the voltage range as a voltage set point.

If one substation has two new SVCs installed, we use the concept of master and follower to deal with In this case, the extra coordination between master and follower will be needed. A follower of TEMSE SVC will share MVAr output with its master proportionally according to the SVC size and will not contro reactive devices. If its master is out of service, then the follower will take over as the master and contro the reactive devices.

Regarding the mode coordination, the follower will follow its master if the automatic mode change from Q to voltage control mode happens in its master. The voltage set point from the master is always used under the voltage control mode though its follower may have different voltage set point. However, the Q set point will be separate and can be different between the master and its follower.

## 4. EVALUATION OF NEW SVC

The installation of SVC will not only improve the system voltage profile, but also reduce system losses. In order to evaluate the effect of SVC to system, the following two indices are introduced. They are called as voltage benefit factors (VBF) and loss benefit factors (LBF).

$$LBF_i = \frac{(P_{L0} - P_L(Q_{si}))}{Q_{si}} \times 100\% \qquad i \in ND \quad (11)$$

$$VBF_i = \left| \frac{\sum_i (V_i(Q_{si}) - V_{i0})}{Q_{si}} \right| \times 100\% \quad i \in ND \quad (12)$$

where,

$Q_{si}$: the amount of the SVC VAR support at the load bus i.

$LBF_i$: the loss benefit factor from the SVC VAR compensation $Q_{si}$ ,
$VBF_i$: the voltage benefit factor from the SVC VAR compensation $Q_{si}$ ,
$P_{L0}$ : the power transmission losses in the system without installation of SVC.
$P_L(Q_{si})$: the power transmission losses in the system with installation of SVC for compensation $Q_{si}$.
$V_{i0}$: the voltage magnitude at load bus i without installation of SVC.
$V_i(Q_{si})$: the voltage magnitude at load bus i with installation of SVC for compensation $Q_{si}$.
ND: the number of load buses that have either low or high voltage.

If $LBF_i$ is negative, it means network losses will increase after SVC is installed in site i, i.e., there is no loss benefit for installing SVC at this location. Thus, set $LBF_i = 0$ for this situation.

The reason that we use the absolute value in equation (12) is that the voltage may be very low or high. It is necessary to improve the voltage profile for both cases. That is to bring the abnormal voltage into the permitted voltage regions. If the local voltage is too low, it needs to raise the voltage through the VAR support. Thus

$$V_i(Q_{si}) - V_{i0} > 0 \qquad i \in ND \quad (13)$$

If the local voltage is too high, it needs to reduce the voltage through the VAR support. Thus

$$V_i(Q_{si}) - V_{i0} < 0 \qquad i \in ND \quad (14)$$

Since system real power loss reduction is major concern in this paper, we mainly analyze the impact on loss by use of new SVC model. The following performance index will be used to asses the effectiveness of new SVC model comparing with the general SVC model.

$$PI_{Li} = \frac{(P_L(SVC) - P_L(New\_SVC))}{P_L(SVC)} \times 100\% \qquad i \in ND \qquad (15)$$

where,

$PI_{Li}$: the performance index for assessing loss minimization.
$P_L$(SVC): the power losses in the system with installation of the general SVC.
$P_L$(NEW_SVC): the power losses in the system with installation of new SVC.

## 5. TEST EXAMPLE

In order to show the effectiveness of the new SVC, all kinds of cases are tested. The test system consists of 568 buses, and 920 branches including lines and transformers. According to the analysis, two new SVCs are installed, operating with one as a master and another as a follower. The regulated bus is at 400KV and the monitoring bus voltage will be at Bus 376, Bus 379, and Bus 380. The SVCs Control 7 devices: 3 shunt reactors, which are external devices and 4 internal shunt capacitors, which are internal devices. They are RX_1, RX_2, RX_3, C1_CX2, C1_CX3, C2_CX2, and C2_CX3, respectively.

(1) Test scenario 1: Voltage control mode. The total system loads are 29816.45MW.

Case 1: Without any SVC control in system. The system power loss and the voltage values of the monitoring buses are shown in Table I.

Table I
RESULTS WITHOUT SVC FOR CASE 1

| Power loss (MW) | V376 (p.u.) | V379 (p.u.) | V380 (p.u.) |
|---|---|---|---|
| 900.31 | 0.947 | 0.940 | 0.940 |

Case 2: Install two general SVCs (not new SVCs). The capacities of two SVCs are:

$$-337 \le Q_{svc1} \le 0$$
$$-332 \le Q_{svc2} \le 0$$

The corresponding results of power loss and the voltage values of the monitoring buses are shown in Table II.

TABLE II
RESULTS WITH GENERAL SVC FOR CASE 2

| Power loss (MW) | V376 (p.u.) | V379 (p.u.) | V380 (p.u.) |
|---|---|---|---|
| 875.44 | 0.973 | 0.977 | 0.977 |

Case 3: With 2 new SVC installed. The capacities of two SVCs are the same as in case 2. The corresponding results of power loss and the voltage values of the monitoring buses are shown in Table III, where all reactors of SVC are switched out, and the capacitors SVC1_CX_2, SVC1_CX_3, SVC2_CX_2 in operation.

The calculation results and comparison for case 1 – case 3 are shown in Figures 3 and 4. The performance index of using the new SVC comparing with general SVC is 3.61%. The PI of using the new SVC will be 6.27% if comparing with case 1 without SVC control.

TABLE III
RESULTS WITH NEW SVC FOR CASE 3

| Power loss (MW) | V376 (p.u.) | V379 (p.u.) | V380 (p.u.) |
|---|---|---|---|
| 843.86 | 1.020 | 1.027 | 1.027 |

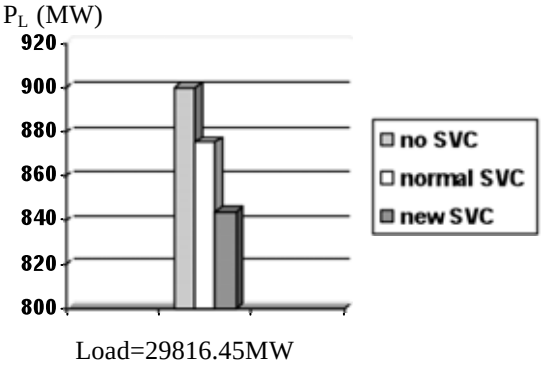


Figure 3. Power loss reduction with SVC

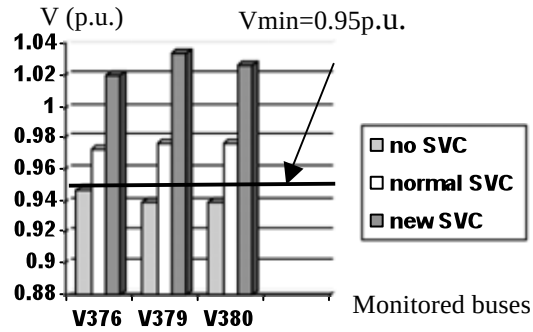


Figure 4. Voltage change with / without SVC

From test scenario 1, no matter which kind of SVC is used, the loss reduction is obvious. So we focus on the comparison between the general SVC and the new SVC in the following scenarios.

(2) Test scenario 2: Voltage control mode. The total system loads are 28855.40MW (Case 4). The other data and parameters are the same as test scenario 1.

The corresponding calculation results with the general SVC or new SVC are shown in Table IV – V.

The performance index of using the new SVC comparing with general SVC is 1.00%.

Table IV
RESULTS WITH GENERAL SVC FOR CASE 4

| Power loss (MW) | V376 (p.u.) | V379 (p.u.) | V380 (p.u.) |
|---|---|---|---|
| 776.87 | 1.002 | 1.006 | 1.006 |

TABLE V
RESULTS WITH NEW SVC FOR CASE 4

| Power loss (MW) | V376 (p.u.) | V379 (p.u.) | V380 (p.u.) |
|---|---|---|---|
| 769.09 | 1.020 | 1.030 | 1.023 |

(3) Test scenario 3: Voltage control mode. The total system loads are 27894.38MW (Case 5). The other data and parameters are the same as test scenario 1.

The corresponding calculation results with the general SVC or new SVC are shown in Table VI – VII.

The performance index of using the new SVC comparing with general SVC is 0.75%.

It is noted from the case 1 to case 5 that the performance index of loss reduction will be decreased as the system load level declines. It means that there is much more loss reduction for using new SVC model compared with the use of the general SVC model under the heavy load level. The benefit of using the new SVC model is very notable.

Table VI
RESULTS WITH GENERAL SVC FOR CASE 5

| Power loss (MW) | V376 (p.u.) | V379 (p.u.) | V380 (p.u.) |
|---|---|---|---|
| 707.93 | 1.006 | 1.010 | 1.010 |

TABLE VII
RESULTS WITH NEW SVC FOR CASE 5

| Power loss (MW) | V376 (p.u.) | V379 (p.u.) | V380 (p.u.) |
|---|---|---|---|
| 702.64 | 1.020 | 1.026 | 1.019 |

(4) Test scenario 4: Q control mode. The total system loads are 29816.45MW.

Since the general SVC doesn't have this control mode, the test is performed for the new SVC only. The calculation results are shown in Table VIII and Figure 5.

Table VIII
LOSS REDUCTION AS Q-SETTING CHANGE
(Fix Q control and Voltage range 0.95-1.05)

| Q-setting | V376 | V379 | V380 | System loss |
|---|---|---|---|---|
| -50 MVAr | 0.964 | 0.963 | 0.963 | 883.91MW |
| -60 MVAr | 0.962 | 0.961 | 0.961 | 885.77MW |
| -70 MVAr | 0.960 | 0.958 | 0.958 | 887.63MW |
| -80 MVAr | 0.958 | 0.955 | 0.955 | 889.54MW |
| -90 MVAr | 0.956 | 0.953 | 0.953 | 891.51MW |
| -100MVAr | 0.954 | 0.950 | 0.950 | 893.50MW |

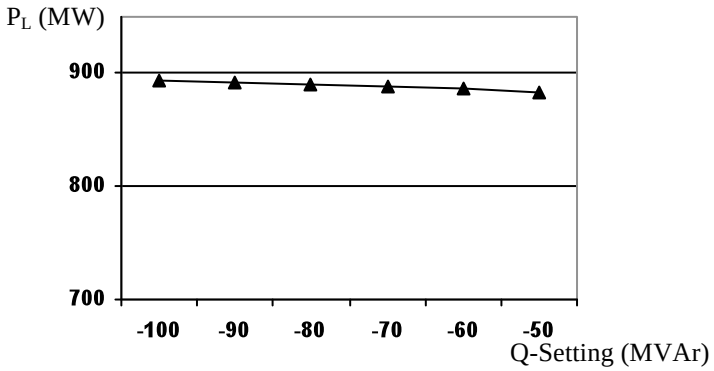


Figure 5. Loss change as Q setting change

It can be observed from Figure 5 that the system power loss will reduce as the increase of the reactive power setting value on the Q setting mode while the system voltages are still within the required range.

## 6. CONCLUSION

This paper reports an application of a new static VAR compensator (SVC) as additional control in reactive power (VAR) optimization problem and analyzes the impact on system loss minimization. Unlike the general SVC, the new SVC model controls local, remote, internal and external devices simultaneously. It has two modes of operation: (1) Voltage control mode; and (2) Q control mode. This paper analyzes the functions of the new SVC, and implements them in the practical power systems. A performance index for evaluating the impact of VAR optimization with new SVC model on loss minimization is also proposed. The proposed VAR optimization problem with new SVC model is tested on a system with 568 buses and 920 branches. All kinds of cases are simulated and discussed in the paper. The new SVC model has notable benefit through comparing it with VAR optimization with general SVC model as well as VAR optimization without SVC model.

## 7. REFERENCES

[1] L.L. Lai (Editor), "Power System Restructuring and Deregulation: Trading, Performance and Information Technology," John Wiley & Sons, UK, Sept 2001, pp258-284.

[2] P. Subburaj, N. Sudha, K. Rajeswari, K. Ramar, and L. Ganesan, "Optimum Reactive Power Dispatch Using Genetic Algorithm," Academic Open Internet Journal, Vol.21, 2007, p6

[3] O. Alsac and B. Sttot, "Optimal Power Flow with Steady-State Security," IEEE Trans., PAS, Vol.93, 1974, pp745-751

[4] Y.J. Yuryevich and K.P. Wong, "Evolutionary programming based optimal power flow algorithm," IEEE Trans. on Power Systems, Vol. 14, No. 4, Nov. 1999, pp.1245-1250

[5] J.Z. Zhu and M.R. Irving, "Combined Active and Reactive Dispatch with Multiple Objectives using an Analytic Hierarchical Process," IEE Proc. C, Vol.143, No.4, 1996, pp344-352

[6] H.W. Dommel and W.F. Tinney, "Optimal Power Flow Solutions," IEEE trans., PAS, Vol.87, No.10, 1968, pp1866-1876

[7] M.R. Irving, and M.J.H. Sterling, "Efficient Newton-Raphson Algorithm for Load Flow Calculation in Transmission and Distribution Networks," IEE Proc. C, Vol.134, 1987

[8] J.Z. Zhu and X.F. Xiong, "VAR optimization and pricing in multi-areas power system," 2003 IEEE General Meeting, Toronto, July 13-18, 2003

[9] J.Z. Zhu and X.F. Xiong, “Optimal Reactive Power Control using Modified Interior Point Method”, Electric Power Systems Research, Volume 66, 2003, Pages 187-192
[10] M.O. Mansour, and T.M. Abdel-Rahman, “Non-linear VAR Optimization Using Decomposition and Coordination,” IEEE Trans. PAS, Vol. 103, 1984, pp. 246-255.
[11] N.H. Dandachi, M.J. Rawlins, O. Alsac, and B. Stott, “OPF for Reactive Pricing Studies on the NGC System,” IEEE Power Industry Computer Applications Conference, PICA’95, Utah, May 1995, pp. 11-17.
[12] J.A. Momoh and J.Z. Zhu, “Improved Interior Point Method for OPF Problems,” IEEE Transactions on Power Systems, Vol.14, No.3, Aug. 1999, pp1114-1120
[13] K. Iba, “Reactive Power Optimization by Genetic Algorithm,” IEEE Trans. Power Systems, Vol. 9, No.2, pp. 685-692, May 1994.
[14] I. P. Abril, J. A. González, “VAR Compensation by Sequential Quadratic Programming,” IEEE Trans. Power Systems, Vol. 18, No.1 , February 2003, pp 36-41

## 8. BIOGRAPHIES

**Jizhong Zhu** (SM’98) received the Ph.D. from Chongqing University, P.R. China, in Feb. 1990. Dr. Zhu was a professor in Chongqing University. His work experience includes Chongqing University in China, Brunel University in UK, National University of Singapore, Howard University in USA, and AREVA T&D Inc. (since 2000). His research interest is in the analysis, operation, planning and control of power systems.

**Davis Hwang** received his Ph.D. degree in Electrical and Computer Engineering at the University of Texas, Austin in 1985. Since then he has been with AREVA T&D Inc. (used to be ESCA) and involved in Network Analysis Applications for many EMS projects and more re

**Ali Sadjadpour** received his BS and MS degrees in Electrical Engineering from Iowa State University, Ames, Iowa in 1981 and 1983. Since then he has been with Harris Corporation (Power Systems Applications), Central and South West Corporation (Systems Operations), and AREVA T&D Inc. (since 1997).